# Identification of *trans*-acting factors that control the non-Mendelian drive of the rye B chromosome

Dissertation
zur Erlangung des akademischen Grades
doctor rerum naturalium (Dr. rer. nat.)

vorgelegt der
Naturwissenschaftlichen Fakultät III
Agrar- und Ernährungswissenschaften,
Geowissenschaften und Informatik
der Martin-Luther-Universität Halle-Wittenberg

vorgelegt von Herr Jianyong Chen

Gutachter:
1. Prof. Dr. Andreas Houben
2. Prof. Dr. Jaroslav Doležel
Tag der öffentlichen Verteidigung: 17. März 2025, Halle (Saale)

# Acknowledgments

This is a wonderful journey. I would like to express my sincere gratitude to my supervisor, Prof. Andreas Houben, for letting me board this ship to explore the mystery of the B chromosome. His unwavering support, invaluable guidance, and constant encouragement were throughout this journey. I am deeply grateful for his dedicated efforts in reviewing and refining this work.

I would like to thank Dr. Jörg Fuchs for his support as my mentor, as my colleague, and as my friend. Special thanks go to Katrin Kumke and Oda Weiss for their excellent technical support and kind help which made my life easier. I would like to thank Saravanakumar Somasundaram for his patience and kindness in helping me with my cloning work. I would like to thank Taoran Liu for her courage in taking up the torch of rye B chromosome research.

I would like to thank our CSF group members Anna Voigt, Dr. Solmaz Khosravi, Dr. Yi-Tzu Kuo, Dr. Veit Schubert, Dr. Anastassia Boudichevskaia, Bhanu Prakash Potlapalli, Sylvia Swetik, and Gihwan Kim. It is a great pleasure to work with such a great team.

Many thanks to Suriya Amutha, Jana Lorenz, and my mentor Dr. Stefan Heckmann for their help with my virus experiment. Special thanks to Prof. Takashi Ryu Endo for providing us with the invaluable seeds. I would like to thank Dr. Jan Bartos and Dr. Mark Timothy Rabanus-Wallace for their kind assistance with the genome assembly.

A big thank you to Bianka Jacobi for supporting me through life's challenges over the years. This work was funded by the China Scholarship Council (CSC) scholarship and the Leibniz Institute of Plant Genetics and Crop Plant Research (IPK).

我由衷感谢我的父母，我大哥大嫂以及我两个可爱的小侄女，谢谢他们一直以来对我的支持。

最后，谨以此论文献给我的妻子周文会，虽然她可能无法理解其中的内容，但她可以用它来垫桌脚或者拍打蟑螂。同时也谢谢小狗周瓜波和小猫周瓜米在我不在的日子对周文会的陪伴。

# Contents

# Abbreviations

| | |
|---|---|
| 3D-SIM | Super-resolution spatial structured illumination microscopy |
| 5-TAMRA | 5-Carboxytetramethylrhodamine |
| Ab10 | abnormal A chromosome 10 |
| ABD2 | actin binding domain 2 |
| B | B chromosome |
| BSMV | Barley stripe mosaic virus |
| BUSCO | Benchmarking Universal Single-Copy Orthologs |
| CFP | cyan fluorescent protein |
| chrB | B-pseudomolecule |
| D locus | distorter locus |
| DAPI | 6-diamidino-2-phenylindole |
| DCR | drive control region |
| defB | drive control region-deficient B chromosome |
| DEs | differentially expressed genes |
| EYFP | enhanced yellow fluorescent protein |
| FISH | fluorescence *in situ* hybridization |
| FITC | fluorescein isothiocyanate |
| GFA | Graphical Fragment Assembly |
| HMW | High-molecular-weight |
| *Kindr* | kinesin-14 motor |
| MBD | microtubule binding domain |
| MI | the first meiosis |
| MII | the second meiosis |

| | |
|---|---|
| *mtrm*$^{126}$ | *matrimony* |
| NaOH | Sodium hydroxide |
| OGM | Optical genome mapping |
| PANTHER | Protein Analysis Through Evolutionary Relationships |
| PMC | pollen mother cell |
| PMI | the first pollen mitosis |
| PMII | the second pollen mitosis |
| PSR | Paternal Sex Ratio chromosome |
| rDNA | ribosomal DNA |
| RT | room temperature |
| RT-PCR | Reverse transcription polymerase chain reaction |
| sgRNA | single guide RNA |
| TPM | transcripts per million |
| *Trkin* | TR-1 kinesin |
| UTRs | 5’ untranslated regions |
| VIGE | Virus-induced genome editing |

# 1 Introduction

The accessory B chromosome represents a masterwork of evolution since they are not required for the normal growth and development of organisms but they exist in all eukaryotic phyla (Kimura and Kayano 1961; Jones 1991; Burt and Trivers 2006). The B chromosome was named as its distinctiveness from the A chromosomes, which are the standard chromosomes in eukaryotes. Different B chromosomes may vary in behavior, and DNA/chromatin composition properties [reviewed in e.g. (Douglas and Birchler 2017; Camacho et al. 2000; Houben et al. 2013; Jones 1995)]. Generally, it is assumed that B chromosomes are derived from A chromosomes, either from the same or from a related species [for related studies see e.g. rye (Martis et al. 2012), *Aegilops speltoides* (Ruban et al. 2020) and maize (Blavet et al. 2021)], but follow their own evolutionary pathway (Camacho et al. 2000; Beukeboom 1994). Until 2023, B chromosomes are known for 2951 species across the tree of life (Garcia and Nualart 2023).

Jones and Rees (1982) used two criteria to distinguish B chromosomes from the A chromosomes and other special chromosomes: B chromosomes are dispensable and do not pair with any member of the standard chromosome complement. During the 5$^{th}$ B Chromosome Conference in Petnica, Serbia (14-17 October 2023), a group of scientists worldwide working on B chromosomes revisited the early definitions (Ferree et al. 2024): While many characteristics vary among different B chromosomes, such as their evolutionary origins, size, segregation behaviors, gene content, and function, there is one defining trait of all B chromosomes: they are non-essential for the organism. An A chromosome is a chromosome that is necessary for viability or fertility. On the other hand, the loss of a B chromosome would not affect the viability or fertility of the host organism. Most B chromosomes do not confer obvious advantages under standard growth conditions on the host organisms and have no or slight effects on the host when their numbers are low. But exceptions exist, e.g. studies of the plant pathogen *Zymoseptoria tritici* demonstrate that some B chromosomes influence the fitness of the fungus during host infection in a cultivar-dependent manner (Habig et al. 2017). In rye, the B chromosome may contribute to heat tolerance during meiosis (Pereira et al. 2017). In *Allium schoenoprasum,* the germination rate and survival of B-containing individuals

increased under drought conditions (Plowman and Bougourd 1994). Regarding the second criterion proposed by Jones and Rees (1982), B chromosomes do not pair with the standard A chromosomes during meiosis. However, in a few cases, B chromosomes have been observed to pair with certain A chromosomes during meiosis e.g. Chen et al. (1993) observed a copy of the B chromosome of *Agropyron cristatum* paired at its distal end with an A chromosome, while the other two B copies paired together.

In contrast to Gregor Mendel's first and second laws (the law of segregation and the law of independent assortment), the transmission of B chromosomes in many species is greater than 0.5. However, some B chromosomes can't drive. According to the transmission data of B chromosomes from about 70 species, only about 60% of B chromosomes can drive (Jones 1995). B chromosomes without drive may persist through generations due to stable mitotic and meiotic segregation, with slight benefits conveyed to the organism. Alternatively, these B chromosomes may drive, but in a subtle manner that is difficult to detect. The maximum number of B chromosomes tolerated varies between species (e.g. maize and rye could possess up to 20, and 6 B chromosomes, respectively) and likely depends on the balance between drive efficiency and adverse effects like reduced fertility and vigor caused by the B chromosome.

## *1.1 The non-Mendelian behavior of B chromosomes in plants*

Knowledge of the drive mechanism at the cellular level is limited to a few cereals, even though the drive is one of the most important features of many B chromosomes. Depending on the species, the drive mechanisms act pre-meiotically, meiotically, and/or post-meiotically (Figure 1, Supplementary Table 1). Usually, B chromosomes from the same or closely related genus often show the same or similar drive behavior, but exceptions exist. For instance, in the genus *Phleum*, the *P. phleoides* B chromosome shows drive during the first pollen division (Bosemark 1956) but no drive of the *P. nodosum* B chromosome was observed in pollen (Bosemark 1957; Fröst 1969). In contrast, the *P. nodosum* B chromosome shows female drive (Bosemark 1957).

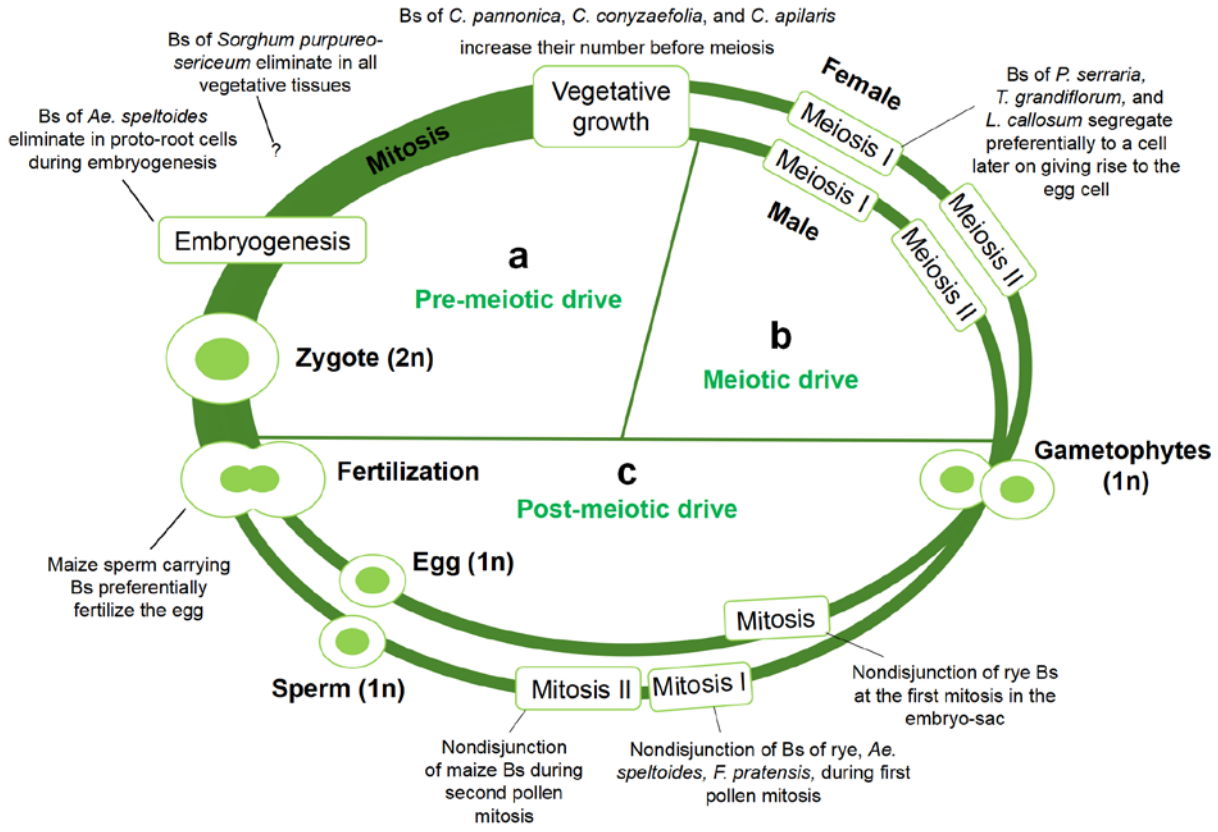


Figure 1 The non-Mendelian behavior of B chromosomes (Bs) of different species during the live cycle of plants, modified from Chen et al. (2022). The chromosome drive mechanism acts (**a**) pre-meiotically, (**b**) meiotically, and/or (**c**) post-meiotically. Controlled elimination of B chromosomes occurs during early embryogenesis. "?" indicates unknown timing of the elimination of the Bs of *Sorghum purpureo-sericeum.*

## *1.2 Pre-meiotic and meiotic drive of B chromosomes*

Pre-meiotic accumulation of B chromosomes has only been reported in few plant species and is more common in animals (Austin et al. 2009). In *Crepis pannonica, C. conyzaefolia,* and *C. capillaris*, a higher number of B chromosomes in pollen mother cells (PMCs) were found compared with their number in root meristems (Fröst 1964; Fröst and Östergren 1959; Rutishauser and Rothlisberger 1966). Nondisjunction of B sister chromatids occurs

during inflorescence development in a genotype-dependent manner (Figure 1a), as evidenced by the presence of varying numbers of B chromosomes in the PMCs of *C. capillaris* (Parker et al. 1989; Rutishauser and Rothlisberger 1966).

Female meiosis is an optimal stage for B chromosome drive, as it is asymmetric in most plants and vertebrates. This asymmetry results in only one product of meiosis becoming an egg nucleus, while the other nuclei do not transmit to the next generation. This setting provides the foundation for mechanisms that cause chromosomes to preferentially end up in the egg nucleus, as opposed to the other products of meiosis. In *Plantago serraria, Trillium grandiflorum*, and *Lilium callosum*, B chromosomes segregate preferentially to a cell later on, giving rise to the egg cell during meiosis (Figure 1b) (Fröst 1959; Kayano 1957; Rutishauser 1956). During meiosis I (MI), the majority of the B chromosomes were seen lying outside the MI plate and on the micropylar side, the side that would give rise to the egg cell (Kayano 1957). No mechanism of numerical increase of B chromosomes to the next generation was found on the male side in the same species.

Different from female meiosis, male meiosis produces four spores (tetrads) which have equal opportunity to fertilize the egg cell. And B chromosome univalents are often lost due to their irregular behavior at MI. To reduce its meiotic loss, rye B could increase its ability to form B bivalents at the metaphase of MI in 2B plants (Jiménez et al. 1997). However, unlike the drive, rye B chromosomes moderate their polymorphic transmission rates to reach the gain/loss balance since too many B chromosomes would affect the fitness of the host plants (Puertas et al. 1998). Another case is the suppression of the meiotic loss of maize B chromosomes. The loss of the B univalent in a low transmission line is due to the misorientation of the B chromosomes during metaphase-anaphase I; in contrast, the B univalent in the high transmission line is always correctly oriented (González-Sánchez et al. 2007).

## *1.3 Post-meiotic drive of B chromosomes*

The post-meiotic accumulation of B chromosomes is the best-analyzed drive process. It is frequent in plants, where the formation of mature pollen involves two post-meiotic divisions that result in sperm and vegetative nuclei (Figure 1c). In rye, *Aegilops speltoides*, and *Festuca pratensis*, B chromosomes undergo nondisjunction during the first pollen mitosis and then they will be included in the generative nucleus or remain lagging so that most vegetative nuclei receive A chromosomes only (Figure 2a) (Banaei-Moghaddam et al. 2012; Ebrahimzadegan et al. 2023; Wu et al. 2019). A quantitative flow cytometric approach was employed to investigate the accumulation of B chromosomes in generative nuclei of *Ae. speltoides* plants and it demonstrated that, irrespective of the number of B chromosomes present in the mother plant, B chromosomes accumulate in the generative nuclei to >93% (Wu et al. 2019). Similarly, in rye, the nondisjunction of B chromosomes is a highly efficient process in all kinds of populations, including those from Turkey (93%), Iran (92%), Korea (93%), Japan (96%), China (88%) and Pakistan (95%, weedy rye, *S. segetale*) (Niwa and Sakamoto 1995; Niwa and Sakamoto 1996). At the second pollen mitosis, B sister chromatids normally divide like standard chromosomes, and each sperm nucleus contains the same number of B chromosomes (Figure 2a).

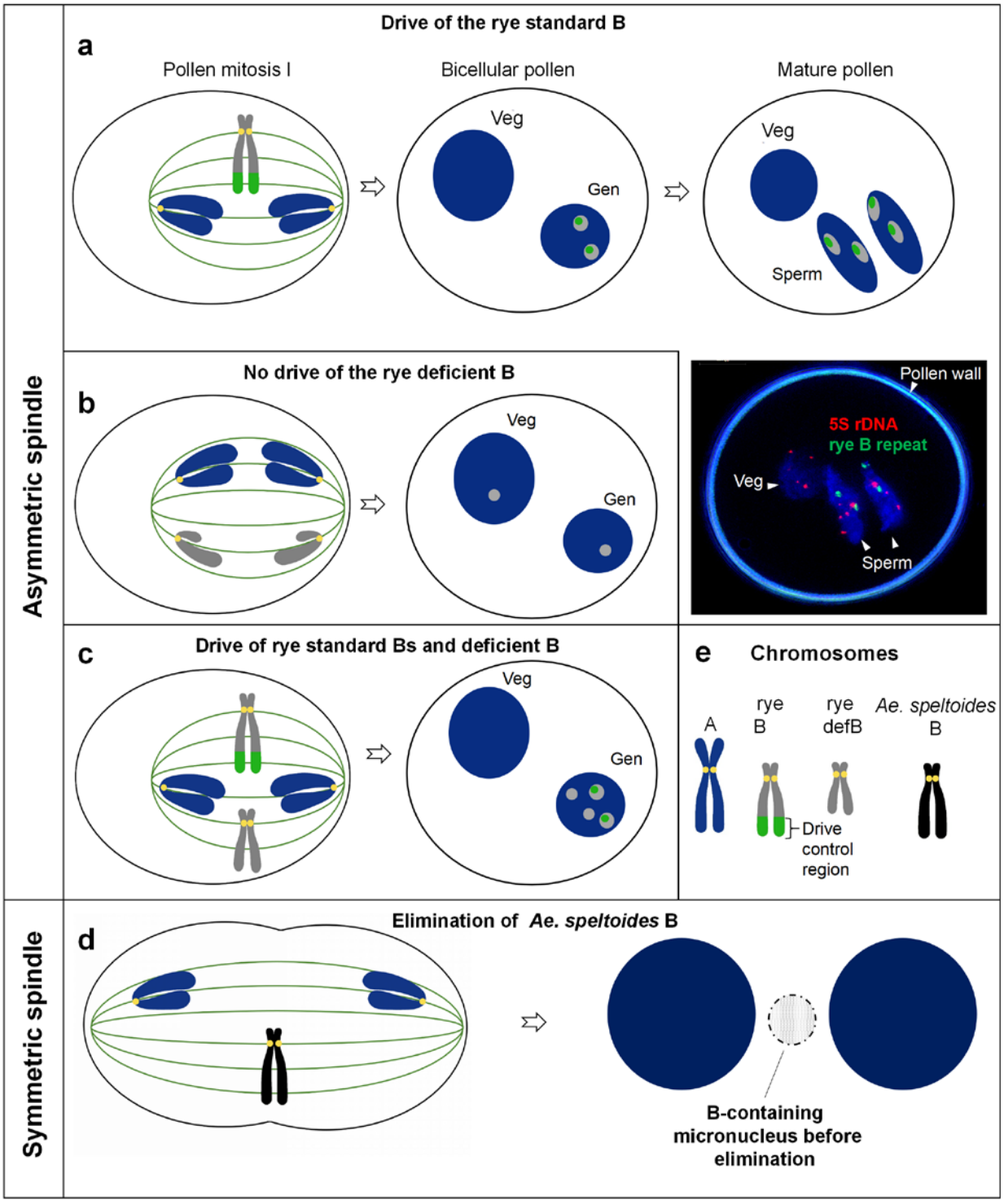


Figure 2 The segregation behavior of rye and *Ae. speltodies* B chromosomes (Bs), modified from Chen et al. (2022). (**a-c**) Drive of the rye B occurs during the first pollen grain mitosis. Veg: vegetative nucleus, Gen: generative nucleus. (**a**) Standard B behavior during pollen development. Mature pollen of rye with Bs after FISH with B-repeat (in green) and A chromosome-specific 5S rDNA (in

red). Bs accumulate in sperm nuclei due to nondisjunction and asymmetric spindle formation. (**b**) No drive occurs if the drive control region of the B is missing. (**c**) Standard B with a complete drive control region and deficient B variants. Drive of both B variants occurs (Endo et al. 2008). The genetic element in the drive control region acts *in trans*. (**d**) Nondisjunction of the *Ae. speltoides* B in proto-root cells during early embryogenesis results in micronucleation and complete elimination. In contrast to B chromosome drive, a symmetrical cell division occurs as part of the chromosome elimination process. (**e**) Different types of chromosomes. The rye B's drive control region is shown in green.

The nondisjunction of sister chromatids is likely a key component of the B chromosome drive in many species. It happens when the sister chromatids are held together by DNA-DNA topological entanglement and the cohesion complex after replication. Proteins that are responsible for removing DNA catenation (e.g. topoisomerase II, condensin) or sister chromatid cohesion (e.g. separase) are likely to be involved in the process of nondisjunction. Lagging chromosomes are also known to arise from error-prone kinetochore-microtubule interactions as reviewed by (Kamenz and Hauf 2017). While nondisjunction of A chromosomes frequently results in cell death or genetic instability, controlled nondisjunction of B chromosomes at a defined developmental stage, such as the first pollen grain mitosis, results in the accumulation of B chromosomes in the generative nuclei. Notably, despite this lagging of B chromosomes, the cell cycle progresses and no cell death occurs. The mechanisms underlying this phenomenon remain unclear. It is uncertain whether the intrinsic mitotic spindle assembly checkpoint is impaired or whether B chromosomes can evade checkpoint control.

Nondisjunction is not common on the female side in those plants whose B chromosomes exhibit nondisjunction in pollen grains. For example, the crossing results indicated no drive or nondisjunction of B chromosomes of *Anthoxanthum aristutum* (Östergren 1947), *F. pratensis* (Bosemark 1954), *P. phleoides* (Bosemark 1956), and *Ae. speltoides* (Mendelson and Zohary 1972) happened on the female side. Only a few cases, such as the rye B chromosome, have been observed to drive in female gametophytes, as demonstrated by its nondisjunction at the first mitosis in the embryo sac (Håkansson 1948).

The drive of the rye B works equally well when the B was introduced as an additional chromosome into *Secale vavilovii* (Puertas et al. 1985), hexaploid wheat (Endo et al. 2008;

Lindström 1965; Müntzing 1970; Niwa et al. 1997), or hypo-pentaploid *Triticale* (Kishikawa and Suzuki 1982). Thus, the rye B chromosome controls the nondisjunction process by itself (Matthews and Jones 1983; Romera et al. 1991). The heterochromatic end of the long B arm plays a role in the regulation of nondisjunction. B chromosomes lacking the drive control region undergo normal disjunction at the first pollen mitosis (Figure 2b). This region acts *in trans* because nondisjunction occurs for the drive control region-deficient B (defB) if a standard B (Lima-de-Faria 1962) or the drive control region of the long arm of the B (Endo et al. 2008) is present in the same cell (Figure 2c). Thus, defB carries the *cis*-acting element(s) responsible for nondisjunction.

The Giemsa-banding positive drive control region is enriched with at least eight different satellite repeats and replicates later than the rest of the entire genome (Blunden et al. 1993; Carchilan et al. 2007; Klemme et al. 2013; Lima-de-Faria 1963). The distinctive feature of the drive control region is that, in contrast to the Giemsa-positive subtelomeric heterochromatic regions of A chromosomes, this domain is simultaneously marked by trimethylated histone H3K4 and trimethylated H3K27 (Carchilan et al. 2007), an unusual combination of apparently conflicting post-translational histone modifications. The question of whether non-repressive (H3K4me) and repressive (H3K27me) histone modifications coexist within the same nucleosome or occupy alternate nucleosomes remains unanswered.

Why does nondisjunction of the B chromosomes occur, and does a dysfunctional centromere lead to nondisjunction? In rye and *Ae. speltoides,* no major differences in the CENH3 signal size were found between A and B centromeres, and interaction between B centromeres and tubulin fibers was observed (Banaei-Moghaddam et al. 2012; Wu et al. 2019). Thus, a different centromere activity of B chromosomes might be excluded. An important hint regarding the mechanism of chromosome drive comes from the finding that the microtubule spindle of both species is asymmetrical during the first pollen mitosis, in accordance with previous studies in other species (Borg et al. 2009; Banaei-Moghaddam et al. 2012; Wu et al. 2019). It seems probable that the incorporation of lagging B chromosomes into the generative nucleus is attributable to the fact that the equatorial plate is situated in closer proximity to the generative pole. Spindle asymmetry as a

component of the drive process has also been suggested for the B chromosomes of the lily *L. callosum* (Kimura and Kayano 1961), the Asteraceae *C. capillaris* (Rutishauser and Rothlisberger 1966), and the grasshopper *Myrmeleotettix maculatus* (Robinson and Hewitt 1976). Standard meiotic mouse A chromosomes with a stronger centromere also harness the spindle asymmetry to drive (Akera et al. 2017). It is noteworthy that the targeted loss of B chromosomes is also caused by nondisjunction. However, in contrast to drive, a symmetrical cell division occurs as part of the chromosome elimination process. In *Ae. speltoides,* the unresolved cohesion of B chromosomes leads to micronucleation and subsequent elimination during early embryogenesis of proto-root cells (Ruban et al. 2020) (Figure 2d). Not only in plants but also in animals, nondisjunction of specific chromosomes leads to programmed DNA elimination. Extended cohesion between sister chromatids at the distal end at anaphase results in a partial loss of the sea lamprey (*Petromyzon marinus*) genome during early embryogenesis (Timoshevskiy et al. 2016; Modahl et al. 2020). A programmed chromosome elimination process also occurs in the *Sciara* species. During embryonic development, paternal X chromosomes undergo elimination since nondisjunction of them at the distal ends gives rise to their retardation after anaphase segregation (Escribá and Goday 2013).

It is possible that in *Ae. speltoides* and rye, the cohesion between B sister chromatids during first pollen mitosis is stronger than the microtubule traction force required to divide chromatids. But why does the cohesion differ between A and B chromatids? A specific composition of (peri)centromere sequences was observed in the B chromosomes of rye (Banaei-Moghaddam et al. 2012), *Ae. speltoides* (Wu et al. 2019), maize (Jin et al. 2005), *F. pratensis* (Ebrahimzadegan et al. 2019), the daisy *Brachycome dichromosomatica* (Leach et al. 1995), and the grasshopper *Xyleus discoideus angulatus* (Bernardino et al. 2017). It seems probable that the B-specific (peri)centromere sequence composition plays a functional role in the drive of B chromosomes. Furthermore, heterochromatin, checkpoint, cohesion, or other as yet unidentified proteins may exhibit differential expression between A and B chromosomes, which could result in disparate segregation dynamics of B chromosomes.

## *1.4 Nondisjunction of the maize B chromosome at the second pollen mitosis and preferential fertilization*

Maize, which belongs to the subfamily *Panicoideae*, has evolved a distinct B drive mechanism that involves two distinct stages: nondisjunction and preferential fertilization. During the second pollen division, the B chromosomes of maize undergo nondisjunction which results in one sperm nucleus containing duplicate B chromosomes and a sperm nucleus without B chromosomes (Roman 1947). Next, during double fertilization, the sperm with B chromosomes fertilize the egg at a higher frequency than the polar nuclei (Roman 1948). In addition, the nondisjunction of maize B chromosomes occurs during the first pollen division, but its frequency is very low (Rusche et al. 1997). It is noteworthy that certain lines of maize exhibit a reversal of preferential fertilization, whereby the B-containing sperm are more likely to join with the polar nuclei than with the egg (Carlson 1969). The property of preferential fertilization is under the control of the female parent (Carlson 1969).

A B-deficiency chromosome mini B#20 undergoes nondisjunction when supplied with the *trans*-acting factors in a full-sized B chromosome (Kato et al. 2005). Genome assembly of the maize B chromosome and short-read mapping revealed that B chromosome-specific ZmB repeats function as the *cis*-factor that mediates nondisjunction since it is the only sequence unique to the mini B#20 chromosome (Blavet et al. 2021). ZmB locates in and around the centromere and has a segment with homology to heterochromatic knobs as well as degenerate telomere repeat arrays (Alfenito and Birchler 1993; Blavet et al. 2021; Hsu et al. 2003; Jin et al. 2005). In a maize line from Native American collections, the presence of B chromosomes will cause the knobs in the A chromosome to remain adhered at the second pollen mitosis—the same mitosis at which the B centromere nondisjoins (Rhoades and Dempsey 1972; Rhoades et al. 1967). ZmB and knobs are both late replicating in S-phase, which could potentially explain the failure of the sister chromatids of the B chromosome to separate at the second pollen mitosis (Blavet et al. 2021).

The *trans*-acting factors are located elsewhere on the B chromosome (Auger and Birchler 2002; Lin 1978; Roman 1947; Ward 1973). One of them is located in the region near the

very distal tip of the long arm and 34 predicted protein-encoding genes are within this region (Blavet et al., 2021).

## *1.5 Other chromosome drive in nature*

Drive systems are generally classified as either 'killer' or 'true' based on their mechanism of action (Bravo Núñez et al. 2018). Selfish genetic elements can either ‘kill’ other gametes or actively promote their inclusion in the final haploid product to inherit themselves over Mendel's law. As the drive of the B chromosome belongs to the latter, I will only introduce the 'true' drive in nature.

Centromere drive: Centromeres are typically composed of repetitive DNA which is packaged by a specific histone H3 variant, CENP-A or CENH3. The kinetochore is recruited on the epigenetically determined centromeric chromatin and binds the spindle microtubules directly. Chromosome segregation depends on the force from kinetochore-microtubules attachment to spindle poles. Thus, the expansion of the centromere-associated satellite might recruit more kinetochore proteins to produce a stronger force to distort Mendel’s law during female meiosis. In the cross between yellow monkeyflowers *Mimulus guttatus* and *M. nasutus*, a “distorter locus” (D) locus of *M. guttatus* showed a 98:2 segregation bias (Fishman et al. 2001). The D locus is related to an expansion of the centromere-associated Cent278 satellite on chromosome 11, which results in centromere drive during female meiosis (Fishman and Saunders 2008). In the western house mouse (*Mus musculus domesticus*), the centromeres of Robertsonian fusions that are stronger, as manifested by increased kinetochore protein levels and altered interactions with spindle microtubules, are preferentially retained in the egg. On the other hand, the weaker centromeres of Robertsonian fusions preferentially segregate to the polar body (Chmátal et al. 2014).

Ab10 in maize: A well-studied mechanism of meiotic drive represents the abnormal A chromosome 10 (Ab10) of maize (Longley 1945). With the aid of a kinesin-14 motor (*Kindr*) and a knob repeat, Ab10 moves faster than A chromosomes to the micropylar direction at the anaphase of MI and Meiosis II (MII), leading Ab10 to be included in the

lower cell, which will go on to form an egg (Dawe et al. 2018). The drive of B chromosomes and Ab10 occurs at different life cycle stages, one in meiosis (Ab10) and the other at the second pollen mitosis, so the drive mechanisms are different. Furthermore, a second kinesin-14 gene, TR-1 kinesin (*Trkin*), which exhibits significant sequence divergence from *Kindr*, is also involved in driving Ab10 (Swentowsky et al. 2020): *Trkin* is located in a 4-Mb region of Ab10 that is not syntenic with any other region of the maize genome and mobilizes neocentromeres composed of the minor tandem repeat TR-1. The TRKIN/TR-1 system is likely to facilitate the meiotic drive of the *Kindr*/knob180 system.

*R2d2* in mouse: *R2d2* is a repetitive DNA of a 127 kb-long monomer found on mouse chromosome 2 and experiences transmission rates above 95% from heterozygous female mice (Didion et al. 2016). The inherent asymmetry in female meiosis is also exploited by *R2d2*. In heterozygous females, the *R2d2*-containing chromosome lags during anaphase and preferentially remains in the egg rather than the polar body (Clark et al. 2024). It happens in both meiosis I and II and is likely caused by the interaction with the spindle or different cellular structure (Clark et al. 2024).

B chromosome drive in *Drosophila:* Many examples of the meiotic drive were found in the model species *Drosophila*, e.g. B, X, and Y chromosomes. Here, I will focus on the B chromosome of *Drosophila*, which was discovered very recently in a single laboratory stock of *D. melanogaster* (Bauerly et al. 2014). This B chromosome is gene-poor and present in multiple, identical copies ranging from 3 to 14 (Bauerly et al. 2014). The B chromosome of *D. melanogaster* can't drive in the wild-type background and would be lost by repeated outcrossing (Bauerly et al. 2014). However, the original stock contains a nonfunctional gene called *matrimony* (*mtrm*$^{126}$), in which the B chromosome shows female drive (Bauerly et al. 2014; Hanlon and Hawley 2023). Matrimony encodes a female-specific meiotic regulator of Polo kinase, together with the *TM3* balancer chromosome, creating a genotype that promotes the drive of the B chromosomes (Hanlon and Hawley 2023).

The PSR chromosome in jewel wasp: Paternal Sex Ratio chromosome (PSR), is a sex ratio-distorting B chromosome, that was first detected in the jewel wasp, *Nasonia vitripennis* (Werren 1991). During the mitotic division right after fertilization, PSR can

cause the complete elimination of the sperm's essential chromosomes, this process is known as paternal genome elimination (Aldrich et al. 2017). Wasps reproduce through haplodiploidy, in which unfertilized eggs develop into haploid males, while fertilized eggs become diploid females. PSR can distort the sex ratio in a population since it will lead to more haploid males in the fertilized eggs (Dalla Benetta et al. 2020). PSR has characteristics of both 'killer' and 'true' drive systems since it ‘kills’ the host paternal genome and actively promotes its inclusion in the maternal genome. Knock-down of *haploidizer*, a locus on PSR that contains a C4-type zinc finger DNA binding domain, resulted in suppression of sex ratio distortion and paternal genome elimination (Dalla Benetta et al. 2020). Therefore, it is clear that *haploidizer* is necessary for PSR's genome elimination activity. However, it is still unclear how PSR avoids self-elimination. It is possible that PSR's chromatin composition is resistant to genome elimination since PSR's chromatin is largely heterochromatic and devoid of H3K27me1 and H4K20me1 (Lee et al. 2023; Zhang and Ferree 2024).

Nondisjunction of the X chromosomes in fly: During MII in the *Bradysia* (previously called *Sciara*) fly, all the sister chromatids segregate except for the X chromatids that undergo nondisjunction and the daughter cell without X chromosome degenerates, whereas the sperm has two copies of the X (Esteban et al. 1997; Gerbi 2022; Metz 1925). However, the nondisjunction of the X chromosomes leads to three copies of the X chromosome after fertilization. Thus, one or two of the paternally derived X chromosomes will be eliminated to restore the diploid state during an early cleavage division (reviewed in (Gerbi 2022)). Nondisjunction of the X chromosomes might be related to under-phosphorylated histone H3 status on its centromeric region. During meiosis II, the centromeric region of the X chromosome of *Bradysia* fly does not become phosphorylated at the four histone H3 sites (H3 phosphorylation at Ser10, Ser28, Thr3, and Thr11), which differs from the rest of the chromosomes (Escribá et al. 2011). No kinetochore formation was observed on the centromeres of X chromosomes and they failed to align on the metaphase plate at MII (de Saint Phalle et al. 2021).

## *1.6 Aims of this study*

In my Ph.D. dissertation, I used rye as a model to decipher the non-Mendelian drive of the rye B chromosome. I addressed the following questions:

1. Can we narrow down the region that controls the drive of the rye B chromosome?
2. Can we identify candidate genes located in the control region that controls the drive?
3. What are the functions of these candidate genes?

# 2 Materials and Methods

## *2.1 Plant materials*

Cultivated rye (*Secale cereale* L. subsp. *cereale*) of the Japanese JNK strain without and with additional standard or drive deficient rye B chromosome (defB) which lost the ability to drive due to the loss of the drive control region (Ribeiro et al. 2004) and weedy rye containing B chromosomes collected from Pakistan (*Secale cereale* L. subsp. *segetale*, no. 34) (Niwa and Sakamoto 1996) and Afghanistan (*Secale cereale* L. subsp. *afghanicum,* (Niwa and Sakamoto 1995) were grown under long-day conditions of 16 h light at 18 °C and 8 h dark at 15 °C, 50% relative humidity, and 100 to 120 µmol $m^{-2}$ $s^{-1}$ light intensity. They were vernalized at 4 °C for two months at the third leaf stage and then moved back to the greenhouse.

Wheat (*Triticum aestivum* L., cv. Chinese Spring) without and with different variants of rye B chromosome ($B^s$, $B^s$-8, $B^k$, $B^k$-1, $B^k$-2 (Endo et al. 2008), and $B^k$-3) were grown under greenhouse conditions with a 16 h photoperiod (21 °C day/ 17 °C night, 50% relative humidity, 100 to 120 µmol $m^{-2}$ $s^{-1}$, light intensity). The $B^s$ chromosome of the wheat-rye B addition line was initially introduced into a Nepalese strain of wheat from a spring rye variety from Transbaikal, Siberia (Lindström 1965) and then transferred into the wheat genotype 'Chinese Spring' by (Endo et al. 2008). The $B^k$ chromosome was derived from cultivated rye in Korea, and it was introduced into wheat cv. 'Chinese Spring' by (Niwa et al. 1997). The B chromosome variants $B^s$-8, $B^k$-1, and $B^k$-2 were created by the application of a gametocidal system, which resulted in the generation of deficient B chromosomes, like, terminal deletions and translocations with wheat chromosomes (Endo et al. 2008). The $B^k$-3 was identified when we screened the selfing progenies of wheat with $B^k$-2 by FISH.

Wheat cv. Bobwhite with high levels of Cas9 expression (high-Cas9 line 707) (Wang et al. 2022), together with wheat cv. Chinese Spring with $2B^s$, was grown in the field (Gatersleben, Germany). Wheat cv. Chinese Spring with $2B^s$ was pollinated by high-Cas9 line 707 to create Cas9-expressing wheat with rye $B^s$. Cas9-positive F1 plants were selected by PCR using the primer pair zCas9-F and zCas9seq1 (Wang et al. 2022).

Wild type and transgenic *Nicotiana benthamiana* expressing the reporter construct CaMV35S:: cyan fluorescent protein (CFP)-histone H2B (Martin et al. 2009) were grown under greenhouse conditions with a 16 h photoperiod (22 °C day/ 18 °C night, 50% relative humidity, 100 to 120 µmol $m^{-2}$ $s^{-1}$, light intensity).

## *2.2 Preparation of chromosome spreads*

To prepare mitotic chromosomes, seeds were germinated on wet filter paper at room temperature (RT) for 2-3 days. Excised roots were treated with ice-cold water for 24 h for cell cycle synchronization, fixed in ice-cold 90% acetic acid for 10 min on ice or 3:1 ethanol: acetic acid for 1-3 days at RT, and stored in 70% ethanol at -20 °C. Roots were treated with 45% acetic acid for between 10 and 120 minutes before being transferred onto a glass slide. Meristematic cells were then isolated in a droplet of 45% acetic acid under a coverslip. After 2 seconds- of treatment over an alcohol burner, the meristem was squashed between the slide and coverslip. Finally, the coverslip was removed after freezing it in liquid nitrogen, and the slide was kept in 99.8% ethanol at -20 °C until use.

To prepare pachytene chromosomes, spikes of wheat with rye $B^s$ were collected and fixed in 3:1 ethanol: acetic acid for 3 days following the emergence of 2/3 of the flag leaf. Three anthers per sample were then transferred to a 0.2 ml tube containing 10 µl 45% acetic acid and mixed to create a homogeneous cell suspension. Subsequent slide mounting and storage followed to steps for mitotic chromosomes.

## *2.3 Standard fluorescence in situ hybridization (FISH) and probe generation*

The PCR products and plasmids used as FISH probes were fluorescence labeled by nick translation (NT Labeling Kit, Jena Bioscience). The repeats Sc26c38 and Sc9c130 were obtained by PCR using the primers described by (Klemme et al. 2013) (Table 1). The DCR28 gene fragment was obtained by PCR (Table 1). pTZE3900, containing a 3.9 kb long fragment of the repeat E3900 (Blunden et al. 1993), and pUC119-Revolver,

containing an 89 bp long sequence of the rye-genome specific repeat Revolver (Tomita et al. 2008) were used. In addition, four oligonucleotides (30 nt - 40 nt, Oligo-D1100-mix) with fluorescein isothiocyanate (FITC) at their 5'-end were designed according to the sequence of the repeat D1100 (Sandery et al. 1990). The oligo probes 5S ribosomal DNA (rDNA) (Chen et al. 2019) were modified with 5-TAMRA (5-Carboxytetramethylrhodamine) at their 5'-end (Table 2).

Chromosomes were denatured in a Sodium hydroxide (NaOH) - 70% ethanol solution (6 mg/ml) for 5 min at RT, then washed, and dehydrated in a series of increasing ethanol concentrations (70%, 90%, and 99.8%) for 5 min each, and air-dried. For each FISH probe, 1 µl of probes (10 mM for oligo probes; 50-75 ng/µl for probes generated by nick translation) was added to 10 µl hybridization mixture, denatured at 99 °C for 10 min and stored at -20°C immediately until use. The mixture was added to the air-dried slides, sealed with coverslips, and incubated in a moist chamber at 37 °C for 12-24 h (Aliyeva-Schnorr et al. 2015). After hybridization, slides were washed in 2X SSC for 20 m at 58 °C and distilled water at RT for 2 min, and air dried. Finally, 8 µl 4',6-diamidino-2-phenylindole (DAPI) solution (1 µg/ml, DAPI/antifade solution) in antifade was added to each slide and sealed with a coverslip. Microscope images were taken using an Olympus BX61 fluorescence microscope equipped with an ORCA-ER CCD camera (Hamamatsu) and a deconvolution system. Images were analyzed using the cellSens Dimension software (Olympus, v1.11) and Adobe Photoshop (v13.0).

Table 1 Primers of PCR amplification for FISH

| ID | Sequence (5'-3') | Target |
|---|---|---|
| Sc9c130-F1 | GCATGTCATCGGTAGGATAGG | Sc9c130 |
| Sc9c130-R1 | ACCCCTTCCCTTTCGATCTAC | Sc9c130 |
| Sc26c38F | CAAGACATGCTCACGCTCAG | Sc26c38 |
| Sc26c38R | CGCACTTCCGAGTAACCTGT | Sc26c38 |
| DCR28-3F | TGTCTACGCCGTTTACAATGA | DCR28 |
| DCR28-3R | GCTCACGGAATAAAGGGGTCA | DCR28 |

Table 2 The sequences of the modified oligo probes

| ID | Sequence (5'-3') |
|---|---|
| Oligo-D1100-1 | FITC-ACCGCATCTCCCTCACTCACAATTTCGATTCCTCCTT |
| Oligo-D1100-2 | FITC-GGTCTCGTTTCCCGCCCAAAGTTTCGCCCC |
| Oligo-D1100-3 | FITC-GTATAGCAAAAGAGTTTCCCAAATAGGCGGCACGA |
| Oligo-D1100-4 | FITC-CGGGTATGGGAACGTAGCATGGAGTTTGGTGG |
| Grass-5S-1 | TAMRA-TCATACCAGCACTAAAGCACCGGATCCCATCAGAAC |
| Grass-5S-2 | TAMRA-GCGTGCTTGGGCGAGAGTAGTACTAGGATGGGTGAC |

## *2.4 Pollen FISH*

Mature pollen was fixed in ice-cold 90% acetic acid for 20 min and maintained in 70% ethanol at -20 °C. The protocol for suspension pollen-FISH described by (Han et al., 2007; Rusche et al., 1997) was adapted following. After centrifugation (12,000 g for 1 min), the ethanol was removed, and the pollen pellet was rinsed with 1 ml 10 mM HCl three times by vortexing and centrifugation (12,000 g for 1 min) at RT. Pepsin solution (80 µl at 20 mg/ml, dissolved in 10 mM HCl) was added, and the solution was incubated at 37 °C for 30 min. The pollen was rinsed with 2X SSC by vortexing and centrifugation (9500 g for 1 min), and the pollen pellet was denatured in 100 µl NaOH- 70% ethanol solution (6 mg/ml) for 5 min at RT, pollen was rinsed with 2X SSC twice by vortexing and centrifugation (9500 g for 1 min). Oligos were combined and diluted in hybridization mix (10 mM Oligo-D1100-mix; 10 mM Oligo-5S rDNA-mix), denatured at 99 °C for 10 min, and maintained at -20 °C for 10 min (Aliyeva-Schnorr et al., 2015). The hybridization mixture was added to the pollen pellet and incubated in the dark for 20-24 h at 37 °C. Following hybridization, the pollen was washed twice in 2X SSC at RT by vortexing and centrifugation (12,000 g for 1 min), and incubated for 30 min at 45 °C in 2X SSC. The supernatant was discarded, and the pollen pellet was resuspended in 15 µl DAPI solution (1 µg/ml DAPI/antifade solution), dropped onto slides, and sealed with a coverslip. Slides were incubated in darkness at RT overnight and maintained at 4 °C until microscopy. Super-resolution spatial structured illumination microscopy (3D-SIM) using a 63×/1.40 Oil Plan-Apochromat objective from the Elyra PS.1 microscope system (Carl Zeiss GmbH). Image stacks were captured separately for each fluorochrome using the 561, 488, and 405 nm laser lines for excitation and appropriate emission filters. Maximum intensity projections from image stacks were

calculated using ZENBlack software (Carl Zeiss GmbH). SIM image stacks were used to generate spatial animations using the Imaris 9.7 (Bitplane, UK) software.

## *2.5 DNA and RNA isolation, cDNA synthesis, and RNA sequencing*

Leaf segments (1—3 cm) from rye and wheat samples were frozen in tubes by immersion in liquid nitrogen pulverized by bead beating in a vibrating mill (MM400, Retsch). 1.2 ml extraction buffer (1.21 g Tris, 4.09 g NaCl, 1.86 g EDTA, diluted in 100 ml $H_20$) was added to each tube and incubated for 15 min at 65 °C. Tubes were allowed to cool for 1 minute at RT. 600 ml Chloroform: Isoamyl alcohol (24:1) was added, and the solution was manually agitated. The homogenate was pelleted by centrifugation (13,000 g for 2 min), and the supernatant was moved to a fresh tube. The DNA was precipitated in 700 µl isopropanol, pelleted, and washed twice in 70% ethanol by repeated vortexing and centrifugation (13,000 g for 2 min). The pellet was air-dried until all ethanol was evaporated, and the DNA was eluted in 50 µl of $dH_20$. The DNA concentration was determined by spectrophotometry (Thermo Scientific NanoDrop One). RNA from 6 tissues (root apical meristem, PMII (the second pollen mitosis) anthers, leaves, spikes undergoing meiosis, young shoot, and immature seeds 7 days after pollination) of wheat with $2B^s$ were collected (Table 3). For comparative transcriptome analysis, RNA-seq data of PMI (the first pollen mitosis) wheat +0B/ 2B/4B and rye +0B/2B (Boudichevskaia et al. 2022), and of PMI anthers of wheat+ $1B^s$-8/ $1B^k$-1/ $1B^k$-2 and rye +1defB were collected (Table 3) Anthers undergoing different stages of development (meiosis, PMI, and PMII), were stage classified by visual inspection under a light microscope. Anthers (undergoing PMI or PMII) or whole young spikes (undergoing meiosis) were immediately frozen in liquid nitrogen and stored at -80 °C.

Total RNA was extracted using the Spectrum™ Plant Total RNA-Kit (Sigma-Aldrich). RNA samples were treated with DNA-free DNase before cDNA synthesis following the on-column DNA removal protocol (RNase-Free DNase I Kit, Norgen Biotek Corp). RNA was quantified using the Qubit device (RNA HS assay kit, Thermo Fisher Scientific Inc, Waltham, MA, USA). Total RNA quality was verified by determining the RNA Integrity

Number (RIN) using the Agilent Technologies 2100 Bioanalyzer (Agilent, Santa Clara, CA, USA). Sequencing libraries were prepared using the Illumina TruSeq RNA Sample Preparation Kit v2 (Illumina, Inc., San Diego, CA, USA) followed by size selection of the pooled samples by agarose gel electrophoresis (size range: 320-420 bp). Libraries were quantified by qPCR (Mascher et al. 2013) and sequenced on the Illumina HiSeq 2500 device (paired-end, 2 x101 cycles, rapid run mode, onboard clustering; DNA Sequencing Service of the IPK Gatersleben, Germany) according to the manufacturer's directions (Illumina, Inc., San Diego, CA, USA). The raw RNAseq reads were trimmed using Trimmomatic (v 0.38.1) (Bolger et al. 2014), SLIDINGWINDOW:4:20, MINLEN:80). For short-read sequencing, the genomic DNA of wheat +3B$^{k}$-2, wheat +2B$^{k}$-3, and wheat +2B$^{s}$ were sequenced using the DNBSEQ sequencing platform at BGI Genomics (Hong Kong, China). ~36 Gb Paired-end 150 (PE150) data were generated for each sample (ENA accession number PRJEB69479).

Table 3 Information of the RNA-seq samples

| Sample | Group | Tissue |
|---|---|---|
| T1 | wheat | Anther (PMI) |
| T2 | wheat | Anther (PMI) |
| T3 | wheat | Anther (PMI) |
| T4 | wheat | Anther (PMI) |
| W1 | wheat+1B$^{s}$-8 | Anther (PMI) |
| W2 | wheat+1B$^{s}$-8 | Anther (PMI) |
| W3 | wheat+1B$^{s}$-8 | Anther (PMI) |
| W4 | wheat+1B$^{s}$-8 | Anther (PMI) |
| X1 | wheat+2B$^{s}$ | Anther (PMI) |
| X2 | wheat+2B$^{s}$ | Anther (PMI) |
| X3 | wheat+2B$^{s}$ | Anther (PMI) |
| X4 | wheat+2B$^{s}$ | Anther (PMI) |
| Y1 | wheat+4B$^{s}$ | Anther (PMI) |
| Y2 | wheat+4B$^{s}$ | Anther (PMI) |
| Y3 | wheat+4B$^{s}$ | Anther (PMI) |
| Y4 | wheat+4B$^{s}$ | Anther (PMI) |
| U1 | wheat+1B$^{k}$-1 | Anther (PMI) |
| U2 | wheat+1B$^{k}$-1 | Anther (PMI) |
| U3 | wheat+1B$^{k}$-1 | Anther (PMI) |
| U4 | wheat+1B$^{k}$-1 | Anther (PMI) |
| M1 | wheat+1B$^{k}$-2 | Anther (PMI) |

| | | |
|---|---|---|
| M2 | wheat+1B$^{k}$-2 | Anther (PMI) |
| M3 | wheat+1B$^{k}$-2 | Anther (PMI) |
| M4 | wheat+1B$^{k}$-2 | Anther (PMI) |
| B0_1 | Rye | Anther (PMI) |
| B0_2 | Rye | Anther (PMI) |
| B0_3 | Rye | Anther (PMI) |
| Bdef_1 | Rye+1defB | Anther (PMI) |
| Bdef_2 | Rye+1defB | Anther (PMI) |
| Bdef_3 | Rye+1defB | Anther (PMI) |
| Bplus_1 | Rye+2B | Anther (PMI) |
| Bplus_2 | Rye+2B | Anther (PMI) |
| Bplus_3 | Rye+2B | Anther (PMI) |
| TSB01 | wheat+2B$^{s}$ | Shoot apical meristem (2 days after germination) |
| TSB02 | wheat+2B$^{s}$ | Root apical meristem (2 days after germination) |
| TSB03 | wheat+2B$^{s}$ | Young spike (meiosis) |
| TSB04 | wheat+2B$^{s}$ | Anthers (PMII) |
| TSB05 | wheat+2B$^{s}$ | immature seeds (7 days after pollination) |
| TSB06 | wheat+2B$^{s}$ | Young and mature leaves |

## *2.6 PacBio sequencing*

High-molecular-weight (HMW) DNA of wheat cv. Chinese Spring possessing ~6 rye standard B chromosomes (Figure 3) was isolated from leaves using the NucleoBond HMW DNA kit (Macherey Nagel, Germany), and quality was assessed using the Fragment Analyzer device (Agilent Technologies Inc, CA, USA). DNA was quantified using the Qubit dsDNA High Sensitivity assay kit (Thermo Fisher Scientific, MA, USA). HiFi libraries were prepared from 15 µg HMW DNA according to the "Procedure & Checklist - Preparing HiFi SMRTbell® Libraries using SMRTbell Express Template Prep Kit 2.0" manual (PN 101-853-100 Version 03, Pacific Biosciences of California Inc., USA) with an initial DNA fragmentation (speed 32) performed using the Megaruptor 3 device (Diagenode, Belgium) and final library size fractionation by SageELF (Sage Science, USA). The size of the final libraries was measured using the Fragment Analyzer device (Agilent Technologies Inc, CA, USA). Polymerase-bound SMRTbell complexes were formed according to standard protocols (Pacific Biosciences of California Inc., USA). Sequencing (HiFi CCS) was performed using the Pacific Biosciences Sequel IIe device (30 h movie time, loading concentration 45 – 70 pM, 4 h pre-extension time, diffusion loading, mean insert length

according to SMRT link raw data report between 16,4 and 19 kb) following standard manufacturer's protocols (Pacific Biosciences of California Inc., Menlo Park, CA, USA) at IPK Gatersleben and Pacific Biosciences Revio platform at BGI Genomics (Hong Kong, China). The Sequel IIe generated ~92 Gb data and the Revio generated ~166 Gb data. These data are available from the ENA accession number PRJEB69479.

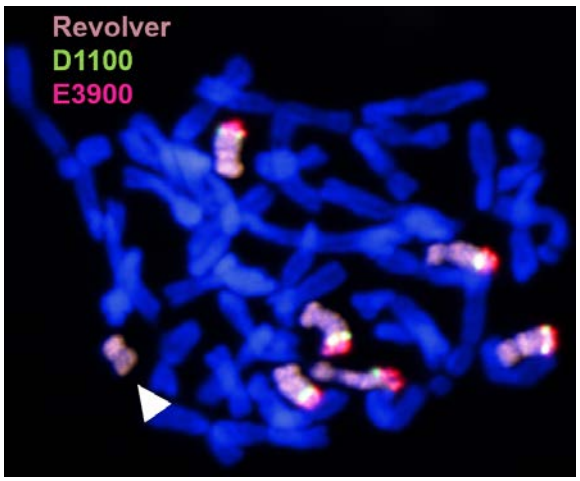


Figure 3 The mitotic cell of wheat cv. Chinese Spring with six rye standard Bs and a truncated B-fragment after FISH using the B-specific repeats D1100 (green) and E3900 (red) and the rye genome-specific repeat Revolver (orange) as probes. The arrow indicates the truncated B chromosome.

## *2.7 Chromosome conformation capture (Hi-C) sequencing*

Hi-C sequencing libraries were generated from leaves of wheat with 2 rye B chromosomes as described by (Padmarasu et al. 2019) using *Dpn*II enzyme, and were sequenced using the NovaSeq6000 device (Illumina Inc., USA) at IPK Gatersleben. ~173 Gb were generated and ~148 Gb clean data were used for scaffolding after filtering. These data are available from the ENA accession number PRJEB69479.

## *2.8 Whole-genome assembly and scaffolding*

PacBio HiFi reads and Nanopore ultra-long reads (provided by Jiri Macas, Ceske Budejovice and Thomas Schmutzer, Halle) of wheat cv. Chinese Spring possessing ~6

rye standard Bs were assembled into contigs with hifiasm (Cheng et al. 2023; Cheng et al. 2021) (v0.19.3-r572; parameters: -l 0 -D 20, Ultra-long ONT integration). The coverage of HiFi reads on each contig was extracted from the Graphical Fragment Assembly (GFA) file output by hifiasm. Contig statistics were calculated with Quast (Gurevich et al. 2013) (v2.3) and gene content completeness was evaluated with Benchmarking Universal Single-Copy Orthologs (BUSCO) (v4.1.2; dataset: Viridiplantae Odb10) (Simão et al. 2015). The Arima Genomics mapping pipeline (https://github.com/ArimaGenomics/mapping_pipeline) was used to process the Hi-C data, including read mapping to the contigs, read filtering, read pairing, and PCR duplicate removal, and scaffolding was performed using YaHS (v1.2a.2) (Zhou et al. 2023). Hi-C contact maps were generated using Juicebox (https://github.com/aidenlab/Juicebox). To evaluate the quality of the assembly and scaffolding, synteny between the 21 largest scaffolds (expected to correspond to the 21 bread wheat chromosomes) and the IWGSC RefSeq v2.1 assembly of wheat cv. Chinese Spring was established by sequence homology. 100-bp sequences spaced 10-kb apart on each scaffold to the IWGSC RefSeq v2.1 assembly via blastn (blast program: megablast, v2.10.1). The results were visualized by dot plot using R (v4.01).

## *2.9 Scaffolding of the rye B chromosome*

Scaffolding based on Hi-C and the Optical genome mapping (OGM, provided by Hana Šimková, Olomouc, CZ) was complemented by a cytogenetics approach. Bilby (GenBank: AF245032.1), CL11 (GenBank: JQ963576.1), Sc55c1 (GenBank: KC243248.1), Sc63c34 (GenBank: KC243249.1), D1100 (GenBank: KC560866.1), Sc26c38 (GenBank: KC243242.1), E3900 (GenBank: AF222021.1), Sc9c130 (GenBank: KC243235.1), and mitochondrial DNA (GenBank: AP008982.1) and chloroplast DNA (GenBank: NC_021761.1) were aligned to the contigs using BLASTn (blast program: megablast, v2.10.1). The abundance of each repeat on the contigs was quantified in 1-Mb windows (Supplementary Table 2). Links from Hi-C data and optical mapping data were used to combine the contigs into super-scaffolds (Supplementary Table 2). Super-scaffolds were assigned to a pseudomolecule (i.e., an assembled chromosome) based on their repeat

content and FISH results (Klemme et al. 2013). A fasta file was generated with agptools (https://warrenlab.github.io/agptools/). The distribution of the repeats on the B-pseudomolecule (chrB) was visualized by pyGenomeTracks (v3.8) (Lopez-Delisle et al. 2021). To determine the DCR, DNBSEQ short-read data of wheat +3B$^{k}$-2, wheat +2B$^{k}$-3, and wheat +2B$^{s}$ were aligned to the reference genome of the 21 wheat large scaffolds, B-pseudomolecule and unassigned rye B-like contigs using bowtie2 (v 2.5.0, default) (Langmead and Salzberg 2012). The alignments on the B-pseudomolecule and unassigned rye B-like contigs were extracted via samtools (v1.9) (Li et al. 2009) and visualized by pyGenomeTracks (v3.8).

## *2.10 Comparing the assembled size of repeats to unassembled short-read data*

To estimate the actual proportion of B-located repeats, 17.2 Gb (representing 1x genome coverage) short-read DNBSEQ sequencing data of wheat with 2B$^{s}$ (single-end, 150-bp) were used. The B pseudomolecule was cut into 150 bp sequences. Both data were aligned to the wheat genome (IWGSC RefSeq v2.1 assembly) using bowtie2 (v 2.5.0, default) and unaligned reads were written to separate files. Organellar DNA was not able to be compared since it also exists in cytoplasm. Sc55c1 was not analyzed as it has similar sequences in the standard wheat genome. Therefore, the unaligned DNBSEQ short reads and unaligned 150-bp pseudomolecule sequences were aligned to the remaining seven repeats Bilby, CL11, Sc63c34, D1100, Sc26c38, E3900, and Sc9c130 using bowtie2 (v 2.5.0, default). The numbers of aligned reads of each repeat were used for calculation. The proportion of the assembled size of each repeat = number of 150-bp pseudomolecule sequences/ number of DNBSEQ short reads.

## *2.11 Transcriptome assembly and differential expression analysis*

Cleaned RNA sequence reads obtained as described previously (Table 3) were mapped to a hybrid reference, including the rye B-like contigs and the genome of wheat cv.

'Chinese Spring' (IWGSC RefSeq v2.1) with HISAT2 (v 2.2.1) (Kim et al. 2019) with default parameters. The alignment was processed to produce a gene feature annotation with StringTie (v 2.1.1, default parameters) (Pertea et al. 2015). A set of non-redundant transcripts was generated using gffread (v 0.12.6) (Pertea and Pertea 2020). TransDecoder (v 5.5.0) was used to annotate coding regions within transcripts (https://github.com/TransDecoder/).

Differential expression analysis of plants with a wheat genetic background was performed against a reference transcriptome featuring the rye B transcripts combined with the annotated transcriptome of wheat cv. 'Chinese Spring' (IWGSC RefSeq 2.1, using both HC and LC genes). The corresponding analysis of plants with a genetic rye background substituted the rye ‘Lo7’ genome for the wheat genome (Rabanus-Wallace et al. 2021). Salmon (v.3.0, default parameters) (Patro et al. 2017) was used to estimate the abundance of each transcript from each tissue: sample combination based on the RNAseq reads acquired as previously described. DESeq2 (v 1.34.0) (Love et al. 2014) was used to compare the expression of each transcript during PMI between genotypes with and without the drive control region of the rye B (P-value < 0.01, foldchange >2). Transcripts showing differential expression in all 11 comparisons were selected as candidate *trans*-acting factor(s) influencing PMI nondisjunction of the rye B.

## *2.12 Analysis of the differentially expressed candidates and PCR-based mapping*

Differentially expressed genes were clustered using CD-HIT-EST (similarity threshold: 0.8, v1.3) (Fu et al. 2012). The PANTHER (Protein Analysis Through Evolutionary Relationships) classification system (http://www.pantherdb.org) was used to infer the likely functional roles of the translated proteins. To find paralogous A chromosome genes, the sequences of the candidates were aligned to the transcriptome of the rye cv. Lo7 (Rabanus-Wallace et al. 2021) (blast program: megablast, v2.10.1). Where PANTHER can not classify the translated proteins, the homology-based functional annotations from rye cv. Lo7 (Rabanus-Wallace et al. 2021) were assigned their homologous B

chromosome-located candidates. B chromosome-specific primers were generated using the WheatOmics PrimerServer tool (Ma et al. 2021; Zhu et al. 2017) compared to wheat IWGSC RefSeq v2.1 assembly and rye 'Lo7' reference genome (IWGSC 2018; Rabanus-Wallace et al. 2021) (Table 4). Genomic DNA of plants with or without drive control region of the rye B chromosome were used as templates. GoTaq DNA Polymerase (Promega) was used for PCR following the protocol recommended by Promega, and the PCR products were checked using 1% agarose gels.

Table 4 Primers used for PCR-based mapping

| primer ID | Left primer (5'-3') | Right primer (5'-3') | Product |
|---|---|---|---|
| Bilby | TTTGCGACAATGACTCAAGC | TGTAGCTCATCGTGGAGTCG | 582 bp |
| DCR145-1 | CGCAGGTCTCGTGGCTTTAT | AATTGGCAATGTTCCGCTGC | 620 bp |
| DCR154-1 | ACAACGGCCAACTCATTCCT | CCTCCCAAGAACTCGTCCAC | 790 bp |
| DCR169-1 | TCCTGGATCCATGGACCACT | GAACACCCCTTGAGCACACT | 239 bp |
| DCR260-1 | AAGAGGGAATACGGTGCCAG | CAGATCTAGAGTGGGCAGCAG | 167 bp |
| DCR28-2 | AGCCGAAAACTCTGCTGGG | GCACGCAAACAAGGTCTCAA | 574 bp |
| DCR398-1 | CAAACATTCGGCACCAAGGG | GGCGTAATCTTCTGGAGCGA | 742 bp |
| DCR399-1 | TGAGATCCTGCCTCCAACCT | CGGGGAAGGACACGTTCTTT | 100 bp |
| DCR400-1 | AGCCTTGTTCCTCACCCAAG | TAAACACAATCCCAGCCCCC | 399 bp |
| DCR83-3 | TGGCCCTGTCTTCCACTTTC | GGTTTGTCGGGGTCATGAGA | 347 bp |

## *2.13 Phylogenetic analysis*

The protein sequence of DCR28 was aligned to PANTHER (http://www.pantherdb.org/) and NCBI (https://www.ncbi.nlm.nih.gov/) to check its phylogeny (Program Selection: blastp). 434 DCR28-like protein sequences from 325 species in NCBI were downloaded. MEGA X (64-bit, v11.0.13) (for Windows) was used to analyze the phylogenic relationship of *DCR28*-like protein: first, multiple alignments were performed using 434 DCR28-like protein sequences and DCR28 via CLUSTALW; second, the phylogenic tree was constructed using result from multiple alignment (method: Maximum likelihood)

## *2.14 Transient expression of genes of interest in the mitotic system of tobacco leaf*

*Cloning of reporter constructs*:

The enhanced yellow fluorescent protein (EYFP) and mCherry fluorescent tags were fused to the gene of interest using the Golden Gate assembly method (Engler et al. 2008). Phusion High-Fidelity DNA Polymerase (New England Biolabs, NEB) was used for PCR following the protocol recommended by NEB. DCR28 was amplified from the cDNA of anthers of wheat+2B$^{s}$ undergoing the first pollen mitosis using primers spanning both 3' and 5' untranslated regions (UTRs). The primers (DCR28_5_UTR, DCR28_3_UTR; Table 5) were designed as previously described. The PCR products were purified using the Monarch PCR & DNA Cleanup Kit (NEB). Subsequently, a second round of PCR was performed using a pair of primers (NT-DCR28F and NT-DCR28R; Table 5), which included overhangs containing a BsaI site, to amplify the purified product from the start codon to the stop codon of DCR28. The second PCR product was purified and used for Golden Gate assembly.

The coding sequence of DCR28-like rye was obtained from two combined DNA fragments. Fragment DCR28A2 (primer: EYFP28A2F and EYFP28A2R; Table 5) was amplified and purified as previously described using cDNA of the rye root meristem as a template. PCR amplification of the fragment DCR28A1 failed due to its high GC content. Therefore, DCR28A1 was codon optimized (https://eu.idtdna.com/pages/tools/codon-optimization-tool) and synthesized by Eurofins Genomics GeneStrands (DCR28A1_opt, Table 5). For Golden Gate assembly, the reaction contained 1.5 µl T4 ligase buffer, 0.5 µl T4 DNA ligase, and 1 µl *Eco*31I (FastDigest) from Thermo Fisher Scientific. The assembly included 100 ng of each component: destination vector PICH86966, pICH41295:35Sprom (35S promotor), pICH41258-mCherry-6xGly or pICH41258-EYFP-6xGly, purified PCR product(s), pAGM9121-rbcSE9ter (terminator) (Table 6). Finally, dd$H_2O$ was used to fill up the reaction to 15 µl. The reaction was mixed and cycled between 37°C (3 min) and 16°C (5 min) for 20 cycles, and then subjected to a final inactivation for 5 minutes at 80°C and kept at 10 °C. 15 µl of the assembled mixture is transformed into the *E. coli* TOP10

competent cells by heat shock. Sanger sequencing was used to verify the accuracy of the vectors.

Table 5 Sequences of the primers and synthesized DNA fragment used in cloning

| Primer | Sequence (5'-3') |
|---|---|
| DCR28_5-UTR | GTCCGCTCCTCCATCTCTTG |
| DCR28_3-UTR | GTCTGGTACTGGCTCACAAGA |
| NT-DCR28F | TTGGTCTCTAGGTATGGATCCCCGCCCCACC |
| NT-DCR28R | AAGGTCTCACGAATTAGTCAACTGTATTTGTTGTTGT |
| EYFP28A2F | TTGGTCTCTCCGCAGAAACCCCGTTCTTTAGCG |
| EYFP28A2R | AAGGTCTCTCGAACATCTCATCAATGGCATCATCC |

Synthesized DNA fragment DCR28A1_opt (677 bp):

TTGGTCTCTAGGTATGGACCCTCATCCAACCCCGTTCAGGGCCAAGAGGAAGTCCGTCGCAGCAC
CCGCCAAAACCCCTGCTCCGAAGCCCAAGAGCGTGACCACAGCCAGAGGCAAGATGACGACTTC
GGCCACTACCTCAGCAGTGTCTGCCGGAGCTGCTCCGCAACCTCGGCTTCGCAGGGCGTTTGGG
ACGGTTCGCTCCTCGAACCCATTGGCTGAGAAGCCAGCGCCTCCTCCACCTCAAAAGCACTCCAA
GCTGTCACCGCCACCGCCGCAAAAGCCGCTCAAAGTGAGCCCTCCAAAGCTCCAGAAACCCGCA
GCCAAAGTCTCTAGTCCGCCGCCACAAAAGCCAGCGAAGGTCAGCCCACCACCACAGCAGAAGC
CCTCTAAGCTCTCCCCACCAATTCCCGCCAAAGCCGCAAGACCCAGTCGTCCAGCCGAAAAGCCG
CTCCTGAAGAAGGCGTGCCCTGGTCCCGATTTGGCGGCAAAAGCGAAGAAGAAGTCGCAACGCG
TCAGCTTCCAGGACGACGTAGCTGCCCTAGCGGCTCCACGGTCAGGCGAGAAGGTCAAGGCCAG
CATCGAGGAATCCGCCGGCAGGACACCCCTTGTTCCGGTGAAAGCCCTGGA
GAAGAAGCCCGCGAAGGTGGTTGCCGCAGA GACCCCGTTCTTTAGCG

*Transient protein expression in N. benthamiana*:

The cell cycle dynamic of DCR28 was characterized in a *Nicotiana benthamiana* cell division-enabled leaf system described by (Xu et al. 2020). *N. benthamiana* with transgenic CFP-histone H2B (Martin et al. 2009) was used to visualize the dynamics of the chromosome and determine the stages of mitosis. First, each vector was transformed into agrobacteria GV3101 separately and grown in a YEB liquid medium (5 g/l beef extract,1 g/l yeast extract, 5 g/l peptone, 5 g/l sucrose, 0.5 g/l MgCl2) supplemented with rifampicin [50 ng/l], gentamycin [30 ng/l], and vector-specific antibiotics. After 48 h incubation, the agrobacteria were collected by centrifugation (4,000 rpm for 20 min) and resuspended in the infiltration buffer (10 mM MES (2-morpholinoethanesulphonic acid, pH 5.6) supplemented with 10 mM $MgCl_2$). The spectrophotometer was used to measure the concentration of each suspension using $OD_{600}$. For co-infiltration, each agrobacterial suspension was diluted to a final $OD_{600}$ of 0.4 except CycD3 (Table 6), which was 0.6.

After they were mixed in equal volumes and incubated at RT for 3 h to 24 h. For the mixtures that were used to study cell division, CycD3 is required (Xu et al. 2020). To inject the agrobacterial suspension into the leaves of 4-week-old plants, a blunt-tipped Soft-Ject® syringe was used. After infiltration, the plants were further grown in a 25°C growth chamber for 36-48 h. A confocal laser scanning microscope (LSM 780, Carl Zeiss GmbH) was used for microscopic analysis. Images were taken with a 40x (C-Apochromat 40x/1.20 W Korr FCS M27) water immersion objective and the "ZEN 2012 SP5 FP3" software version 14.0 (Carl Zeiss GmbH). Raw images were processed with Fiji version 2.3.051. Multichannel images and stacks were split by color, and their brightness and contrast were adjusted individually for each channel. Stacks were merged into one image by maximum intensity projection if a single image from the stack was not representative.

Table 6 Vectors used in this study

| Name | Backbone vector | Description | Selection |
|---|---|---|---|
| pICH86966[a] | / | empty vector | Kan |
| pAGM1287-EYFP | pAGM1287 | EYFP | Spec |
| pAGM9121-rbcSE9ter | pAGM9121 | terminator | Spec |
| pICH41258-EYFP-6xGly | pICH41258 | N-terminal EYFP tag | Spec |
| pICH41258-mCherry-6xGly | pICH41258 | N-terminal mCherry tag | Spec |
| pICH41295:35Sprom | pICH41295 | 35S promotor | Spec |
| #1940[b] | pEXPpJOG349_nptII | 35S::mCherry-MBD | Spec |
| #1939[b] | pJOG394 | 35S::mCherry-ABD2 | Spec |
| CycD3[c] | pGWB2 | 35S::AtCYCD3;1 | Kan |
| pICH86966-35SProm-EYFP | pICH86966 | 35S::EYFP | Kan |
| pICH86966-35SProm-EYFP-DCR28 | pICH86966 | 35S::EYFP-DCR28 | Kan |
| pICH86966-35SProm-mCherry-DCR28 | pICH86966 | 35S:: mCherry-DCR28 | Kan |
| pICH86966-35SProm-EYFP-DCR28A | pICH86966 | 35S::EYFP-DCR28A | Kan |
| pICH86966-35SProm-mCherry-DCR28A | pICH86966 | 35S::mCherry-DCR28A | Kan |

**a**: plasmid from addgene (https://www.addgene.org/); **b**: plasmids friendly provided by Dr. Katharina Bürstenbinder (IPB, Halle); **c**: plasmid from Xu, Lee, and Liu (2019), kindly provided by Dr. Katharina Bürstenbinder (IPB, Halle); Spec = Spectinomycin, Kan = Kanamycin

## *2.15 Virus-induced genome editing (VIGE)*

Barley stripe mosaic virus (BSMV) was used to deliver single guide RNA (sgRNA) into the Cas9-expressing wheat with single rye $B^S$.

*gRNA design and cloning*: A sgRNA (5'-CAGGTGATGGATCGAGACAG-3'), named gE3900-6, was designed to target the B chromosome repeat E3900 following the design guidelines from (Schindele et al. 2020). gE3900-6 was cloned into the generic guide RNA expression vector BSMV-γ-sg (Tamilselvan-Nattar-Amutha et al. 2023).

*In vitro transcription of BSMV-sgRNA constructs* followed (Wang et al. 2022). ~3 - 4 kb DNA fragments of BSMV α, β and γ were amplified using T7 primers designed by Suriya Tamilselvan-Nattar-Amutha (IPK, Germany) (Table 7) and ExTaq polymerase (Takara Bio). The PCR products were purified using the Monarch PCR & DNA Cleanup Kit (NEB) and transcribed *in vitro* to α, β and γ virus chains using HiScribe™ T7 High Yield RNA synthesis kit (New England BioLabs, catalog number E2050S) following the Capped RNA Synthesis protocol provided by the manufacturer. The m7G(5′)ppp(5′)G RNA Cap (New England BioLabs, catalog number S1404L) was used as Cap Analog with 4:1 of Cap Analog: GTP ratio. The quality and concentration of RNA transcripts (usually within 2–2.5 µg/µl range) were assessed on the agarose gel.

*Plant inoculation*: The second leaf of wheat seedlings at the two-leaf stage was inoculated using the mixture of 60 µl phosphate buffer and transcription products of BSMV α, β, and γ chains (2.5 µl each). The phosphate buffer (10 mM) (pH=7.0) containing 0.5% of each celite 545 (Roth) and silicon carbide (400 mesh particle size, Sigma-Aldrich). The inoculation was performed by hand-rubbing the second leaf from the base to the tip while wearing clean nitrile gloves. The procedure was repeated three times for each plant, each time applying 20 µl of the mixture. After inoculation, the plants were kept in darkness overnight. The virus infection symptoms were usually observed 7-10 days after inoculation. After harvesting the seeds from the infected plants, a pair of primers Bnuf2-1 (Table 7) targeting the kinetochore protein nuf2 gene on the B chromosome was used to confirm the presence of the rye B chromosome in the progenies. The work was performed in a S2 laboratory.

Table 7 Primers used for RNA synthesis and detection of B chromosomes in the progeny

| Primer | Sequences (5'-3') |
|---|---|
| BSMValpha_T7_F | TAATACGACTCACTATAGTATGTAAGTTGCCTTTGGG |
| BSMVbeta_T7_F | TAATACGACTCACTATAGTAAAAGAAAAGGAACAACC |
| BSMVgamma_T7_F | TAATACGACTCACTATAGTATAGCTTGAGCATTACCG |
| BSMVcommon_R | TGGTCTTCCCTTGGGGGACC |
| Bnuf2-1F | TGGTTCCTCTCGCTTGTTCC |
| Bnuf2-1R | GGCGAGTGTGAAGTCCTTGA |

Note: amplification of α, β, and γ are using their corresponding left primers and the common right primer BSMVcommon_R.

# 3 Results

## *3.1 Reducing the size of the trans-active B chromosome region that regulates B chromosome drive*

Rye B chromosome variants with and without drive behavior (drive: $B^s$, $B^k$, and $B^k$-2; non-drive: $B^s$-8 and $B^k$-1) were established in the background of wheat (Endo et al. 2008). $B^s$ and $B^k$ represent standard B chromosomes identified in different rye genotypes. The variants $B^k$-1 and $B^k$-2 are rye B/wheat A translocation chromosomes with contracted subtelomeric regions of the long B arm (Endo et al. 2008). A previously-undocumented deficient B variant named $B^k$-3 was identified when we screened the progeny of wheat with $B^k$-2.

Drive status was assayed based on relative accumulation levels of Bs in the pollen sperm versus vegetative nuclei. We performed fluorescence *in situ* hybridization (FISH) on mature pollen using probes targeting the B-specific D1100 satellite repeat and 5S ribosomal (rDNA), as an A-specific control probe. Drive is evident if sperm nuclei show D1100 signals, but not the vegetative nucleus (Figure 4 a). On the other hand, no B chromosome drive occurs if both types of nuclei exhibit D1100 signals (Figure 4 b). Pollen FISH revealed that 89 – 91% of pollen showed sperm-specific accumulation of the B variants $B^s$, $B^k$ and $B^k$-2, while there was no sperm-specific accumulation of $B^k$-1 and $B^k$-3 (Table 8). Thus, $B^s$, $B^{k,}$ and $B^k$-2 can efficiently drive in wheat, comparable to the frequency of standard B chromosomes in the background of different rye genotypes (Niwa and Sakamoto 1995; Niwa and Sakamoto 1996).

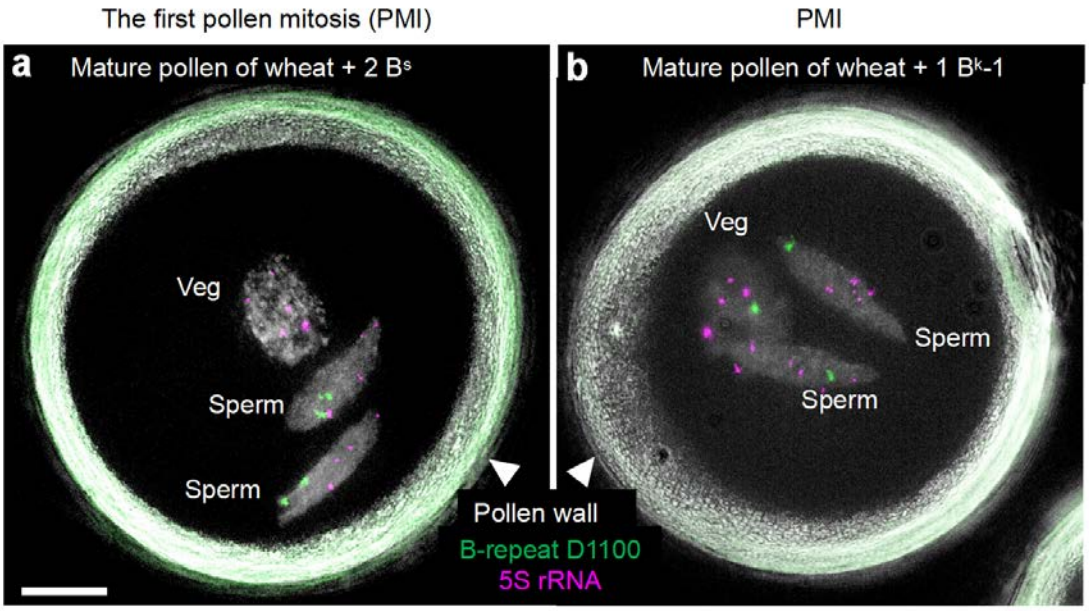


Figure 4 Pollen-FISH combined with super-resolution microscopy (3D SIM) was used to determine the position of B chromosome in mature pollen of wheat (**a**) with two rye drive-positive $B^s$ and (**b**) with a drive-negative, deficient $B^k$-1 chromosome variant in intact pollen. Repeat D1100 (green) indicates the B chromosome and 5S rDNA (magenta) is A chromosome-specific marker used as a positive FISH control. Bar = 10 µm. Veg: vegetative nucleus, Gen: generative nucleus.

To cytogenetically identify the drive control region, we used FISH to compare the composition of the long arm for all 6 B variants ($B^s$, $B^k$, $B^s$-8, $B^k$-1, $B^k$-2, $B^k$-3) using probes targeting the rye genome-specific repeat Revolver, and the B-specific repeats D1100, Sc9c130, E3900, and Sc26c38 (Figure 5). Sc26c38, E3900, and Sc9c130 positive chromosome regions are adjacent to each other in linear order, and E3900 and D1100 repeats intermingle (Figure 5b) (Klemme et al. 2013). FISH revealed that the rye B/wheat A translocation chromosomes $B^k$-1 and $B^k$-2 possess translocation breakpoints in the terminal region of the long B arm. All drive-positive B variants ($B^s$, $B^k$, $B^k$-2) showed D1100 and E3900 signals, but E3900 signals were absent in all drive-negative variants ($B^s$-8, $B^k$-1, $B^k$-3). Drive-negative $B^s$-8 also lost the D1100-signals completely, and drive-negative $B^k$-1 and $B^k$-3 showed a truncated D1100 region. In addition, a small gap almost in the middle of the D1100 region is present in drive-negative $B^k$-3 but not in $B^k$-1 (Figure 5a). We conclude, therefore, that $B^k$-3 is the largest B variant among the drive-negative B

variants. Sc26c38 is found not only in the drive-positive variants $B^s$, $B^{k,}$ and $B^k$-2, but also in the drive-negative $B^k$-1 and $B^k$-3 (Figure 5). The B-specific subtelomeric repeat Sc9c130 is absent in all drive-negative variants as well as in $B^k$-2 (Supplementary Figure 1c), indicating that the distal region of the long B arm is not required for drive. Thus, the DCR corresponds to the E3900, Sc26c38, and D1100 repeat-containing chromosome region between the breakpoints of $B^k$-3 and $B^k$-2 (Figure 5b).

Table 8 Quantitative analysis of the rye B chromosome drive.

| Variant | Total | Number of pollens with B-specific signals | B-signals only in vegetative nucleus[a] | B-signals only in sperm nuclei[b] | B-signals in all nuclei[c] | Drive frequency |
|---|---|---|---|---|---|---|
| $1B^k$-1 | 195 | 103 | 0 | 0 | 92 | 0 % |
| $2B^k$-2 | 77 | 15 | 3 | 55 | 4 | 88.7 % |
| $2B^k$-3 | 101 | 20 | 0 | 0 | 81 | 0 % |
| $2B^s$ | 112 | 11 | 6 | 91 | 4 | 90.1 % |
| $2B^k$ | 122 | 21 | 6 | 92 | 3 | 91.1 % |

Wheat lines with different B variants were analyzed by pollen-FISH using the B-specific probe D1100. Figure 4 shows representative examples of pollen with and without B chromosome drive; **Variant**: Wheat cv. Chinese Spring possessing different rye B chromosome variants; **a**: B-signals only in vegetative nucleus; **b**: B-signals only in sperm nuclei; **c**: B-signals in all nuclei; **Frequency** of B-specific signals accumulate in sperm nuclei: Frequency of pollen with B chromosome variants = b/(a+b+c)

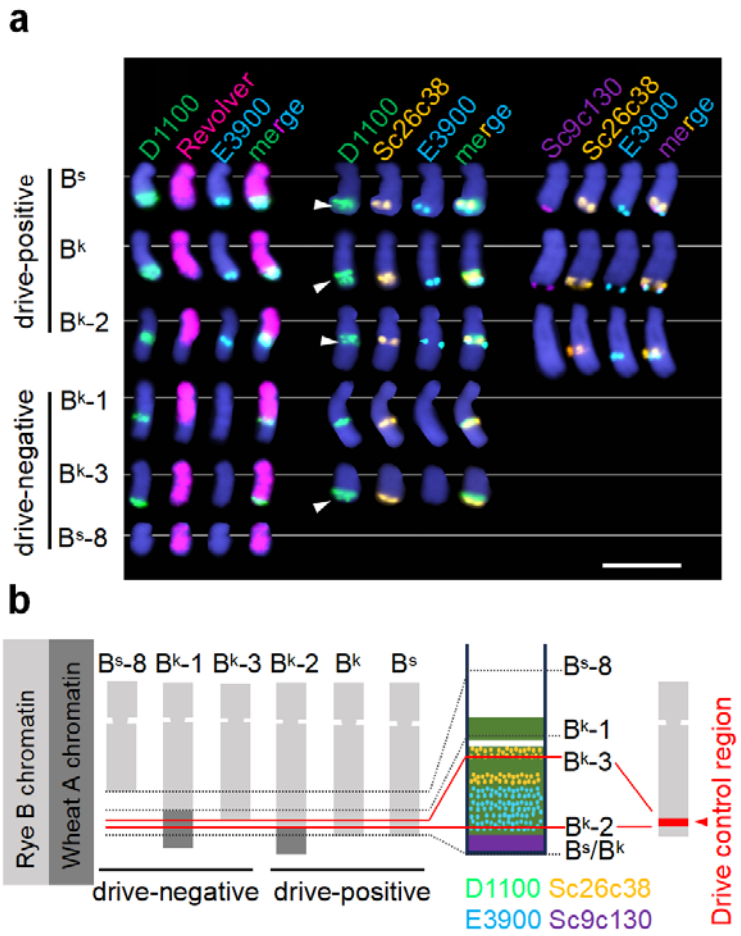


Figure 5 The subtelomeric region of the rye B chromosome long arm controls the B chromosome drive.

(**a**) The repeat composition of the terminal region of the long B chromosome arm of the drive-positive B variants $B^s$, $B^k$, $B^k$-2 and the drive-negative B variants $B^s$-8, $B^k$-1, $B^k$-3 were analyzed by FISH using the rye genome-specific repeat Revolver (magenta), and the B-specific repeats D1100 (green), E3900 (sky blue), Sc9c130 (violet), and Sc26c38 (orange) were used as probes to determine the drive control region. White arrowheads indicate the signal gap in the D1100-positive region. Chromosomes are counterstained with DAPI (blue). Bar=10 μm. The original figures are in Supplementary Figure 1. (**b**) Schemata of the different rye B chromosome variants showing based on (a), the distribution of the B-specific repeats D1100 (green), E3900 (sky blue), Sc9c130 (violet), and Sc26c38 (orange). Light grey and diagonal stripes depict rye and wheat chromatin, respectively. The continuous long black lines represent the ends of $B^k$-8, $B^s$, and $B^k$. The blue dotted lines indicate the ends of $B^k$-1, $B^k$-3 and $B^k$-2. On the right, the chromosomal position of the drive control region is shown as a read region of a drive-positive B chromosome.

## *3.2 Assembly of the rye B chromosome reveals its complex sequence composition*

B chromosomes are notoriously difficult to sequence and assemble owing to their complex repeat structure and high similarity with the A chromosome sequence of the same species. To avoid confounding by the A chromosomes of rye, we sequenced the rye B chromosome in the background of wheat (cv. Chinese Spring); sequence similarity between the A chromosomes of wheat and the rye B chromosome is significantly less than between the A and B encoded sequences of rye, making it easier to differentiate between wheat A and rye B-derived sequence. A rye B addition line was screened by FISH to select plants possessing six standard rye $B^s$ copies, in addition to 21 pairs of wheat A chromosomes. Several plants contained an additional truncated rye B (Figure 3).

An initial 15-Gb primary assembly was constructed from highly accurate PacBio HiFi and ultra-long Oxford Nanopore reads (provided by Jiri Macas, Ceske Budejovice and Thomas Schmutzer, Halle) using the assembly tool hifiasm and achieved a BUSCO completeness of 96.0% based on 2147 contigs with an N50 length of 43.6 Mb (L50=85; Table 9). The logic that the multiplicity of B chromosomes per cell outnumbered that of any given wheat chromosome threefold is confirmed by the clear bimodal distribution of mean HiFi read coverage levels per contig and the approximate 1:3 ratio of wheat A (~14x):rye B (~44x) coverage level (Figure 6a). Hi-C scaffolding resulted in 21 long scaffolds (>500 Mb) (Figure 7) and their alignments to the reference genome of wheat cv. Chinese Spring (IWGSC RefSeq v2.1 assembly) revealed their 1 to 1 syntenic correspondence to near-complete wheat chromosomes (Figure 8). Contigs accounting for ~452 Mbp were assigned to the rye B based on HiFi read coverage (B ~ coverage > 23x) as none of the wheat pseudomolecules were found to comprise any of the contigs ~ coverage > 23x (Figure 6b; Table 2).

Table 9 Statistics of the assembly by QUAST and BUSCO

| | | |
|---|---|---|
| **QUAST** | Number of contigs | 2147 |
| | Largest contig | 369,738,579 |
| | Total length | 150,83,438,686 |
| | N50 | 43,653,268 |
| | N75 | 19,499,721 |
| | L50 | 85 |
| | L75 | 216 |
| | GC (%) | 46.13 |
| | Mismatches # N's | 0 |
| **BUSCO** | Total BUSCO groups searched | 3236 |
| | Complete BUSCOs | 3108 (96%) |
| | Complete and single-copy BUSCOs | 182 (5.6%) |
| | Complete and duplicated BUSCOs | 2926 (90.4%) |
| | Fragmented BUSCOs | 106 (3.3%) |
| | Missing BUSCOs | 22 (0.7%) |

The B-assigned contigs were arranged into a draft pseudomolecule order using Hi-C and optical map data (provided by Hana Šimková, Olomouc) (Figure 6b). This draft order was manually adjusted using these repetitive sequences themselves as relative positional indicators, as described by (Macas et al. 2023): eight families of sequence features with known distributions on the rye B (Klemme et al. 2013) were identified on the contigs (Bilby, CL11, Sc55c1, Sc63c34, D1100, Sc26c38, E3900, and Sc9c130 repeats; mitochondrial and chloroplastic DNA fragments), Figure 6c), and the order adjusted to accord with both the sequence feature distribution and the Hi-C/Optical Map-based draft order. Thirty-eight contigs were thus arranged into a ~430 Mb large pseudomolecule (Figure 6b,d; Table 10) representing ~77% of the rye B size as determined by flow cytometry. We confirmed that the missing portion of the assembly is accounted for by the collapsing of long runs of extremely repetitive sequences, as described by (Navrátilová et al. 2022). Aligning the B-associated optical reads to the B pseudomolecule revealed the expected presence of repetitive regions with elevated coverage (data provided by Hana Šimková, Olomouc), and the assembled size of E3900, CL11, and Sc26c38 repeats is only 67%, 84% and 87% of the actual size estimated from unassembled short reads (Figure 6d).

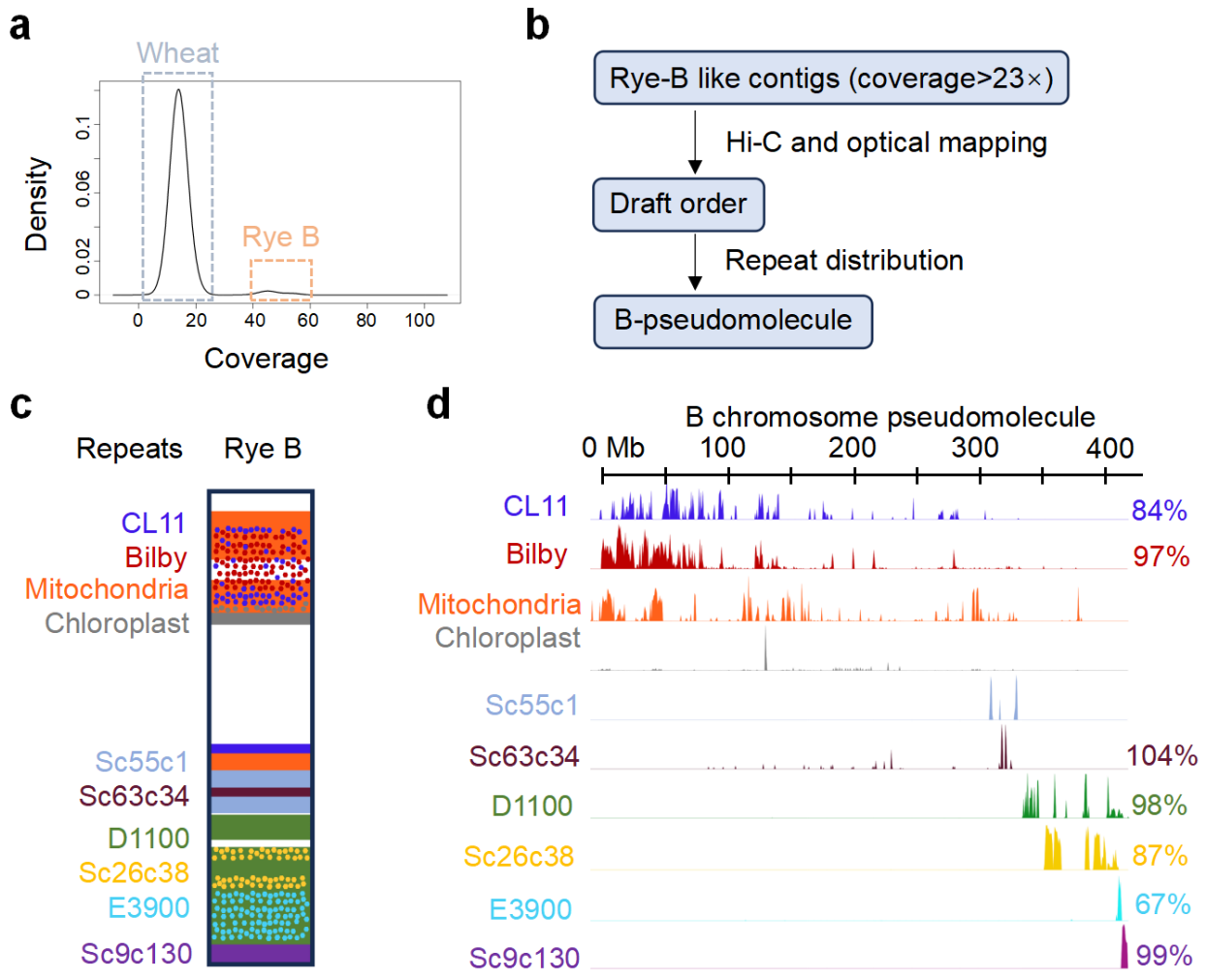


Figure 6 Whole-genome assembly of wheat with the rye B chromosomes and scaffolding the rye B-like contigs into a B chromosome pseudomolecule. (**a**) The density plot of HiFi reads coverage across the whole genome. The higher peak~14× represents sequences from the wheat genome. The lower peak ~44× represents rye B sequences. x-axis: HiFi reads coverage on the assembled contigs, y-axis: density; (**b**) The schemata of the scaffolding strategy; (**c**) A model of repeat distribution on the rye B chromosome; (**d**) Distribution of 8 repeats and organellar DNA on the B chromosome pseudomolecule (chrB) in a 1-Mb window, visualized by pyGenomeTracks. Each track represents the abundance of a repeat from minimum to maximum on chrB. x-axis:0 to 430 Mb on B-pseudomolecule. On the right are the proportions of the assembled size of repeat/actual size estimated from unassembled reads. Organellar DNA was not able to be compared as they also exist in cytoplasm. Sc55c1 was not able to compare as it has similar sequences in the wheat genome.

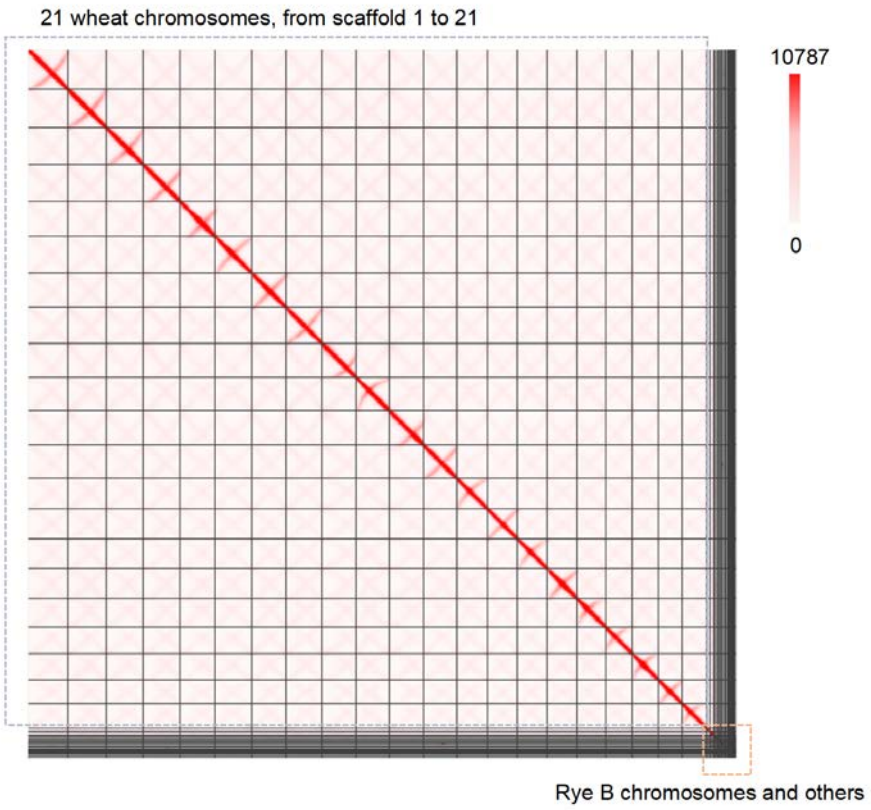


Figure 7 Hi-C scaffolds the 21 wheat chromosomes but fails to scaffold the rye B chromosome. Hi-C interaction heatmap of the scaffolds of wheat with the rye B chromosomes. The color bar on the right represents the density of Hi-C interactions, which are indicated by the number of links at the 5-Mb resolution. The 21 large scaffolds that show Rabl configuration come from the wheat genome, and the remaining small scaffolds come from the rye B chromosome and others.

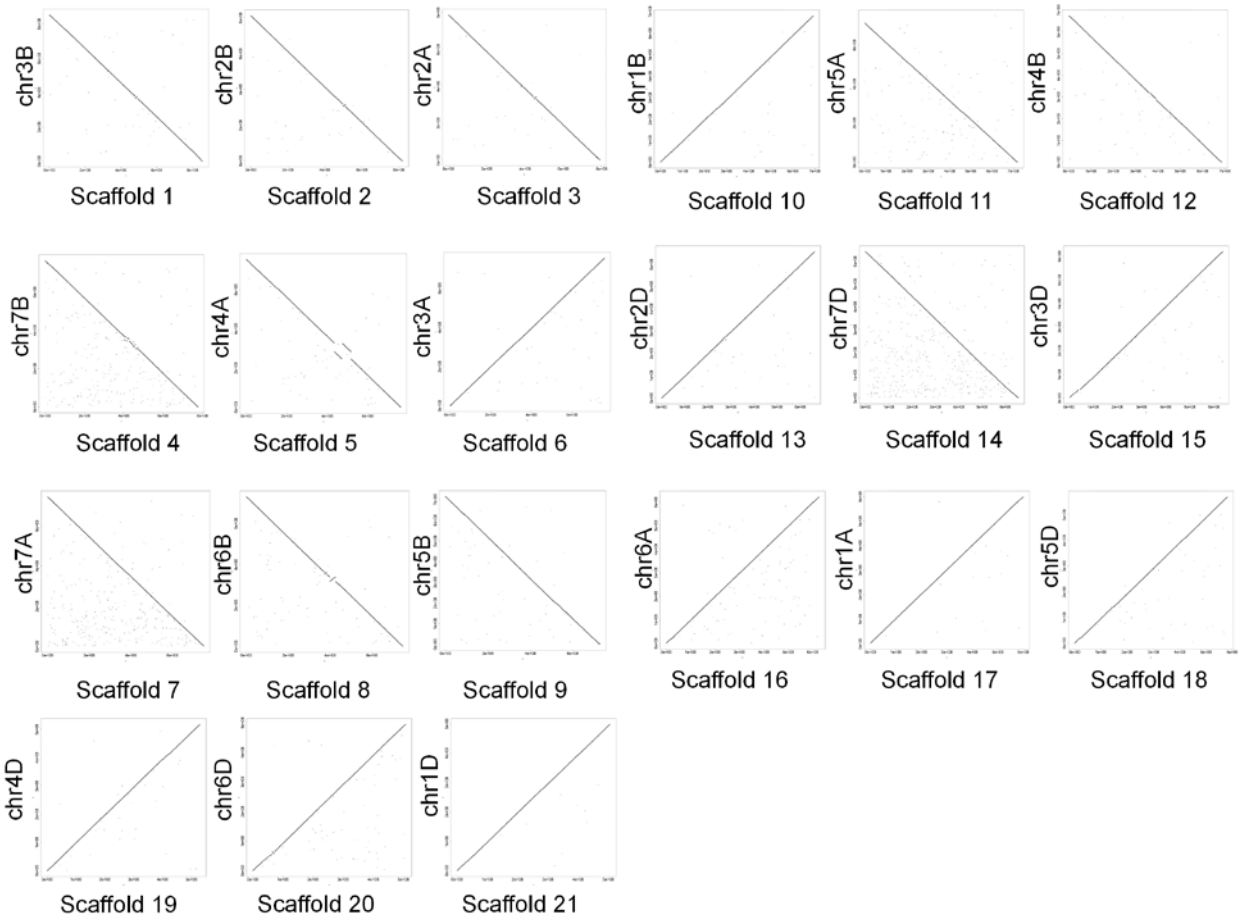


Figure 8 Alignment of the 21 large scaffolds to the wheat genome reveals their corresponding chromosomes. Sequence alignment between Scaffold (x-axis) and chromosome of wheat (y-axis)

Annotation of the B chromosome genic sequences was performed based upon ~159 Gbp of Illumina short-read RNA-seq data collected from seven tissues (root meristems, anthers at both the PMI and PMII pollen mitotic stages, leaves, spikes undergoing meiosis, young shoots, and immature seeds) of wheat with $2B^S$ (Table 3). A total of 1,292 transcriptionally-active rye B-encoded sequences were predicted, including 799 encoding predicted proteins longer than 100 residues (Table 10, Supplementary Table 2). This is likely an underestimate of the total gene number as it does not account for lowly expressed or silenced genes. In addition, the annotation of B-encoded genes confirmed the by Martis

et al. (2012) suggested mosaic origin of the rye B. Because the B is composed of sequences derived from all seven rye A chromosomes as well as plastid and mitochondria DNA (Figure 9).

Table 10 The characteristics of the rye B-like contigs, B chromosomal pseudomolecule and genes on the rye B chromosome

| | | |
|---|---|---|
| **Rye B chromosome-like contigs** | Total number of rye B-like contigs | 160 |
| | Largest contig | 93,027,977 bp |
| | Total length of all rye B-like contigs | 452,394,662 bp |
| | N50 | 60,109,561 bp |
| | L50 | 3 |
| **B Assembled chromosome pseudomolecule** | Length of the B chromosomal pseudomolecule | 429,632,691 bp |
| | Number of assigned B-like contigs | 38 |
| | Size of largest assigned contig | 93,027,977 bp |
| **B Rye chromosome encoded genes** | Number of transcriptionally active genes | 1292 |
| | Max, median length of transcripts (nt) | 44051, 1279 nt |
| | Number of protein-coding genes (ORF> 100 aa) | 799 |
| | Max and median length of peptides | 1879 and 199 aa |

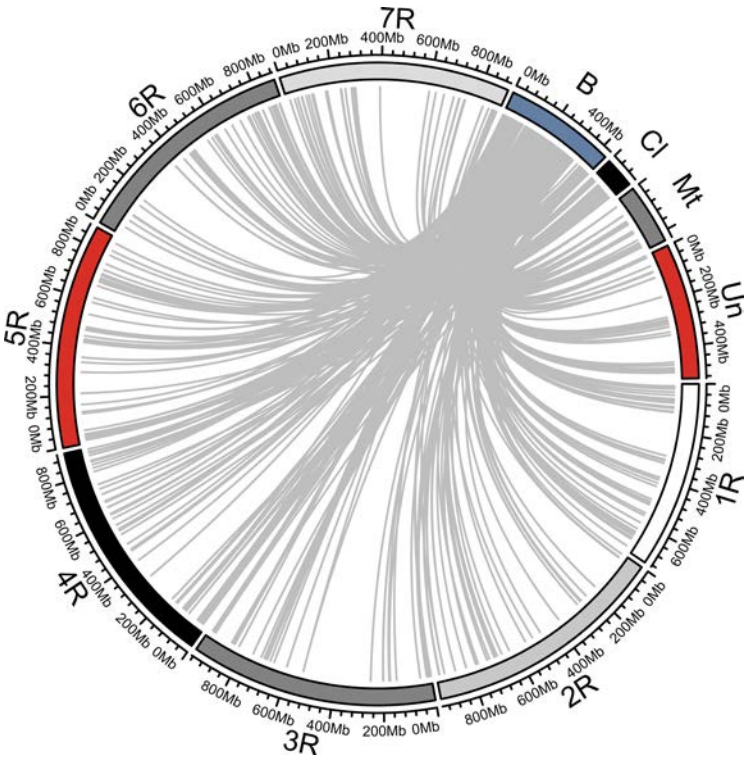


Figure 9 Circos plot shows the relationship between rye B-encoded transcripts and the high-confidence genes on rye A chromosomes (1R – 7R) and organellar genomes (Mt: mitochondria; Cl: chloroplast). B: the rye B chromosome, 1R-7R: rye A chromosomes. Un: the unassigned scaffold of the A chromosomes. Cl: Choloplast DNA, was enlarged 200 times. Mt: Mitochondrial DNA, was enlarged 100 times.

## *3.3 Identification of candidate genes that control the drive process of the rye B chromosome during the first pollen mitosis*

The pseudomolecule coordinates of the DCR were established based on the comparative mapping depth of sequence reads derived from drive-positive ($B^k$-2, $B^s$) and drive-negative ($B^k$-3) B-containing wheat lines. Approximately 36 Gb (~2x coverage) of short-read genome sequencing data were mapped to the B pseudomolecule and unplaced B contigs, constraining the drive control region to a ~40 Mb chromosome segment between 383.9 and 423.8 Mb on the rye B pseudomolecule (Figure 10), and 16 unplaced B contigs (totalling 3.7 Mb) (Table 11). The location of this segment on our B chromosomal

assembly closely corresponded to the results of FISH-mapping. In total, 88 genes (representing 31 single-copy genes and 11 gene families) are located in the drive control region of the B pseudomolecule, 66 of which contain open reading frames (Supplementary Table 2). No active genes were annotated on the 16 unplaced contigs.

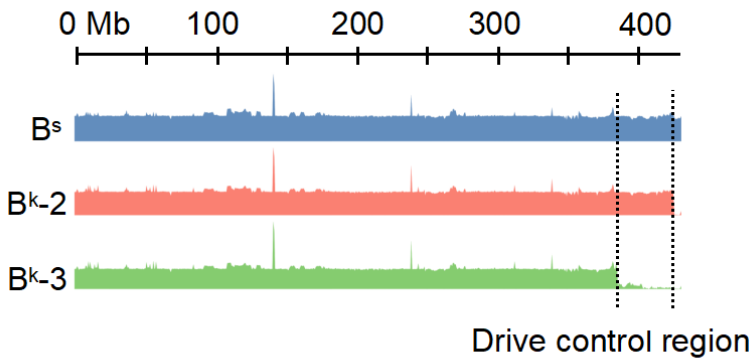


Figure 10 Determination of the rye B drive control region using the short reads data from wheat with $B^k$-2 and wheat with $B^k$-3. The data of wheat with $B^s$ is used as a control. The data mapping was visualized by pyGenomeTracks. The double dash lines indicate the drive control region (383,864,014 to 423,790,502 bp);

Table 11 Contigs belonging to the drive control region

| contigs | length (bp) |
|---|---|
| ptg000157l | 360262 |
| ptg000534l | 503097 |
| ptg000844l | 689855 |
| ptg000867l | 182053 |
| ptg000879l | 68258 |
| ptg000921l | 490121 |
| ptg000922l | 535399 |
| ptg000937l | 160138 |
| ptg000947l | 144940 |
| ptg000965l | 164745 |
| ptg001057l | 89161 |
| ptg001142l | 100942 |
| ptg001158l | 59870 |
| ptg001501l | 53728 |
| ptg002084l | 45252 |
| ptg002112l | 48517 |
| Total | 3.696338 (Mb) |

To identify genes that might control the drive of the rye B, we aimed for a tissue-specific, comparative transcriptome analysis of B containing rye and wheat plants with and without the ability of B drive. We generated RNA-seq reads from anthers undergoing the first pollen mitosis (PMI) of wheat and rye with and without B chromosomes (Table 3). The data included 18 RNA-seq sets from wheat with different numbers of standard Bs (0B, $2B^s$, and $4B^s$) and of 0B and 2B rye (Boudichevskaia et al. 2022). 15 RNA-seq data derived from wheat possessing B variants with ($1B^k$-2) or without the ability to drive ($1B^s$-8, $1B^k$-1) and from rye carrying a drive negative B (1defB). For wheat, four replicates and for rye, three replicates were generated in each group.

Next, we performed a differential expression analysis between plants (wheat and rye) with and without B drive to find commonly drive up-regulated genes (fold change > 2, p-adjusted value < 0.01). A subtractive approach was used; first, we pair-wise compared the drive-positive genes of wheat carrying the B variants ($2B^s$, $4B^s$, and $1B^k$-2) with 0B, respectively (Figure 11). 533 commonly up-regulated differentially expressed genes (DEs) were identified in three comparisons. Next, the genes of wheat with $2B^s$, $4B^s$, and $1B^k$-2

were compared to the genes of the drive-negative wheat+ $1B^s$-8, and 305 up-regulated DEs remained. Afterward, we compared the genes of wheat with $2B^s$, $4B^s$, and $1B^k$-2 with the data of the drive-negative wheat+$1B^k$-1, and 29 commonly up-regulated DEs were found. Finally, after comparing the data of rye with 2B to the data of 0B rye and rye+1defB, respectively, a total of 23 commonly up-regulated DEs were found across the 11 comparisons. CD-HIT clustering revealed that the 23 DEs belong to 7 single-copy genes and 2 gene families with multiple members (Table 12).

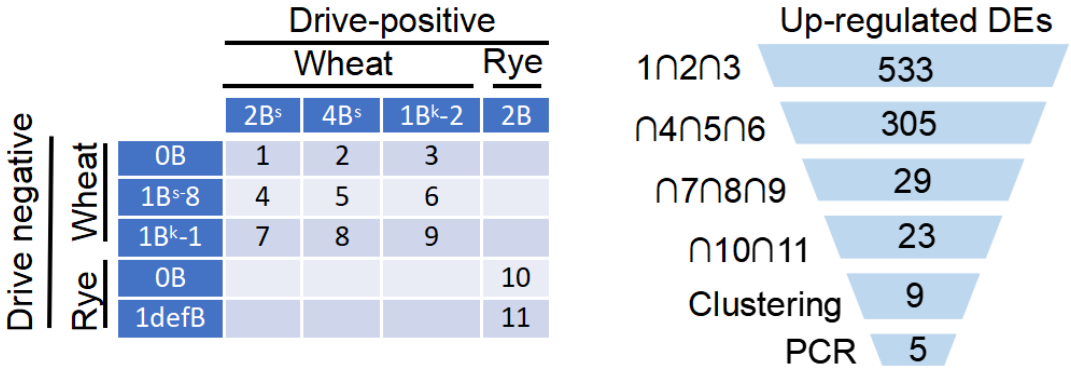


Figure 11 Comparative RNA-seq analysis to identify candidates in charge of the drive. The left table indicates four drive-positive data (horizontal) were compared with five drive-negative data (lateral). The results in 11 comparisons and different numbers indicate different comparisons between drive-positive data and drive-negative data. On the right, '∩' indicates intersection. '1∩2∩3' indicates the intersection among comparisons 1, 2, and 3, which results in 533 differentially expressing candidates;

Table 12 A subtractive approach reveals common DEs and their PCR results

| Transcript | Gene | primer | $B^s$-8 | $B^k$-1 | $B^k$-3 | $B^s$ | $B^k$ | $B^k$-2 |
|---|---|---|---|---|---|---|---|---|
| pseudoScB.83899 | DCR83 | DCR83-3 | ✗ | ✗ | ✗ | ✓ | ✓ | ✓ |
| pseudoScB.83910 | DCR260 | DCR260-1 | ✗ | ✗ | ✗ | ✓ | ✓ | ✓ |
| pseudoScB.83912 | DCR145 | DCR145-1 | ✓ | ✓ | ✓ | ✓ | ✓ | ✓ |
| pseudoScB.83913 | DCR154 | DCR154-1 | ✓ | ✓ | ✓ | ✓ | ✓ | ✓ |
| pseudoScB.83921 | DCR398 | DCR398-1 | ✓ | ✓ | ✓ | ✓ | ✓ | ✓ |
| pseudoScB.83925 | DCR399 | DCR399-1 | ✗ | ✓ | ✓ | ✓ | ✓ | ✓ |
| pseudoScB.83928 | DCR400 | DCR400-1 | ✗ | ✗ | ✗ | ✓ | ✓ | ✓ |
| pseudoScB.83929 | DCR28 | DCR28-2 | ✗ | ✗ | ✗ | ✓ | ✓ | ✓ |
| pseudoScB.83931 | | | | | | | | |
| pseudoScB.83932 | | | | | | | | |
| pseudoScB.83934 | | | | | | | | |
| pseudoScB.83936 | | | | | | | | |
| pseudoScB.83937 | | | | | | | | |
| pseudoScB.83940 | | | | | | | | |
| pseudoScB.83941 | | | | | | | | |
| pseudoScB.83942 | | | | | | | | |
| pseudoScB.83945 | | | | | | | | |
| pseudoScB.83947 | | | | | | | | |
| pseudoScB.84363 | DCR169 | DCR169-1 | ✗ | ✗ | ✗ | ✓ | ✓ | ✓ |
| pseudoScB.84469 | | | | | | | | |
| pseudoScB.84472 | | | | | | | | |
| pseudoScB.84508 | | | | | | | | |
| pseudoScB.84471 | | | | | | | | |

Summary of the genomic PCR (see Supplementary Figure 2) to test the rye B drive control region-specific location of preselected candidate sequences. Genomic DNA of wheat with B variants possessing either a drive-functional drive control region ($2B^s$, $2B^k$, $1B^k$-2) or nonfunctional drive control region ($1B^s$-8, $1B^k$-1, $2B^k$-3) was used as a PCR template. "✓": Expected PCR amplification is present; "✗" Expected PCR amplification isn't present.

To confirm the results of the *in silico* analysis and whether the drive control region encodes these candidates specifically, we designed primers for each candidate and performed genomic PCR. Genomic DNA of wheat with B variants possessing either a drive-functional ($B^s$, $B^k$, $B^k$-2) or nonfunctional regions ($B^s$-8, $B^k$-1, $B^k$-3) was used as a PCR template. According to our PCR result, we divided the 9 genes into two categories. Class I includes

5 drive control region (DCR)-located genes (*DCR260*, *DCR169*, *DCR83*, *DCR400*, and *DCR28)* that showed specific amplicons in only wheat with drive-positive B variants ($B^s$, $B^k$, $B^k$-2) (Table 12, Supplementary Figure 2), indicating that they are only located in the drive control region. Class II consists of 4 genes (*DCR398*, *DCR399*, *DCR145,* and *DCR154*) that are located not only in the drive control region but also in other regions on the rye B chromosome (Table 12, Supplementary Figure 2). Because $B^s$-8, $B^k$-1, and $B^k$-3 lost the drive completely, we speculate that the *trans*-acting element(s), governing the drive of the B chromosome is (are) probably among the class I candidates.

For these five candidates, their activities were compared in 7 different tissues (young shoots, root apical meristem, spikes undergoing meiosis, immature seeds, leaves, anthers undergoing the second pollen mitosis (PMII) and the first pollen mitosis (PMI) of wheat with $2B^s$ since we assumed that drive-control region-encoded genes are mainly active during PMI (Figure 12). Only *DCR28* and *DCR83* showed increased activity during PMI, and *DCR28* is the highest expressing candidate among all the candidates (Figure 12). Reverse transcription polymerase chain reaction (RT-PCR) confirmed the PMI-specific expression pattern of *DCR28* (Supplementary Figure 3). To better understand their function, the PANTHER (Protein Analysis Through Evolutionary Relationships) Classification System (http://www.pantherdb.org) was used. DCR28 was classified as the TPX2 domain-containing protein subfamily, belonging to the microtubule-associated Futsch-like protein family (PTHR34468). The Futsch-like family is unknown in plants, but TPX2-like proteins are key mitotic spindle assembly factors important for chromosome segregation (Evrard et al. 2009). Thus, DCR28 might be one of the genes that control the drive of the B chromosome.

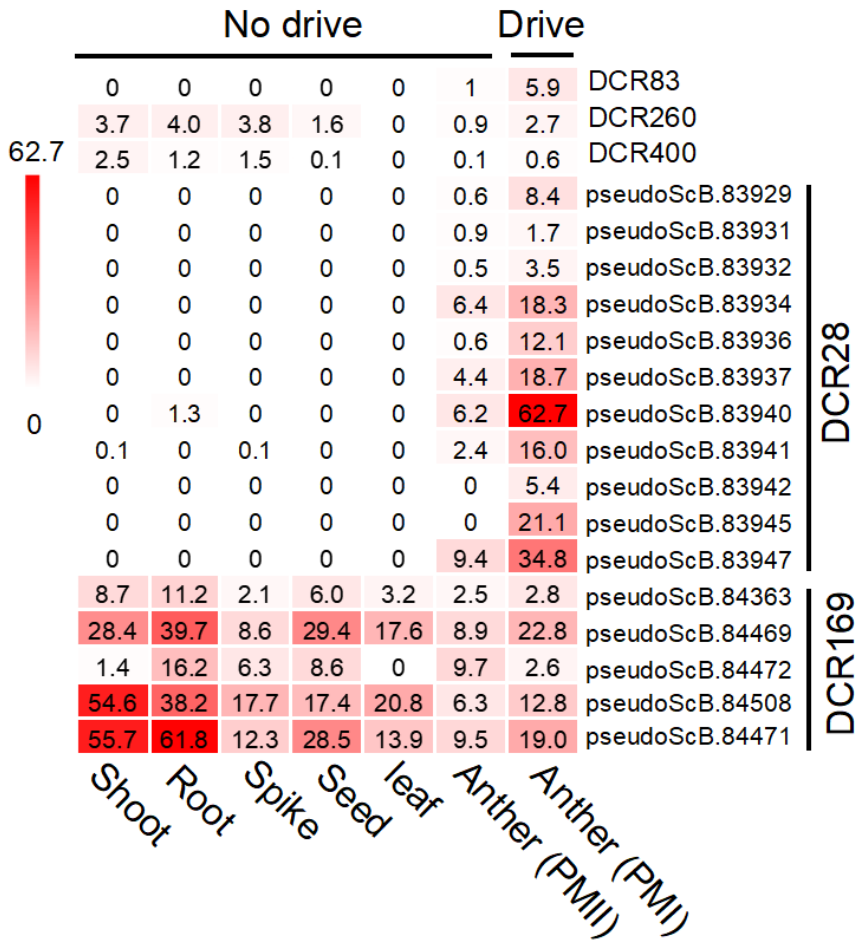


Figure 12 Relative expression activity of the five drive candidates (DCRs) in different tissues. Expression calculation method: transcripts per million (TPM). Different tissues of wheat+2Bs: Shoot-shoot apical meristem, Root-root apical meristem, Spike-young spikes undergoing meiosis, Seed-seeds (7 days after pollination), leaf-young and old leaves, and Anther-anthers undergoing second pollen mitosis (PMII) and the first pollen mitosis (PMI);

DCR400 is possibly also related to the nondisjunction of the B chromosome since it belongs to the ATP-dependent DNA helicase DDX11-related family (PTHR11472:SF41), which is related to DNA duplex unwinding and sister chromatid cohesion (van Schie et al. 2020). However, it not only shows stronger expression in shoot apical meristem (TPM=2.5) than in the anthers during PMI (TPM=0.6) but also expresses in roots and spikes (Fig. 4b). It indicates that if DCR400 is likely involved in the drive of the B

chromosome, it works together with a second factor like DCR28 which doesn't express at roots, shoots, and spikes. The other three candidates are less likely related to chromosome segregation: DCR83 encodes a 288-aa protein belonging to the family glycine-rich cell wall structural protein 1.8-like (PTHR31286). DCR260 encodes 670-aa protein similar to 2-isopropylmalate synthase (PTHR36786). All 5 transcript variants of *DCR169* share similarities with long non-coding RNA-producing B-specific satellite E3900 (Supplementary Figure 4).

## *3.4 B-specific DCR28 family arose from an A chromosome located paralog that underwent repeat-mediated tandem duplication and neofunctionalization*

Given the known monophyletic origin of the rye B chromosome (Marques et al. 2013), and the necessity of a reliable drive mechanism for its persistence over evolutionary time, we reason that the drive mechanism is most likely common across ryes and, thus, that a plausible candidate drive gene must have homologs in all +B ryes. To establish this for DCR28, we analyzed a panel of diverse weedy ryes (*Secale cereale* subsp. *segetale*), which also carry drive-positive B chromosomes (Niwa and Sakamoto 1995; Marques et al. 2013). The presence of *DCR28* was confirmed by genomic PCR in all +B rye genotypes (Figure 13).

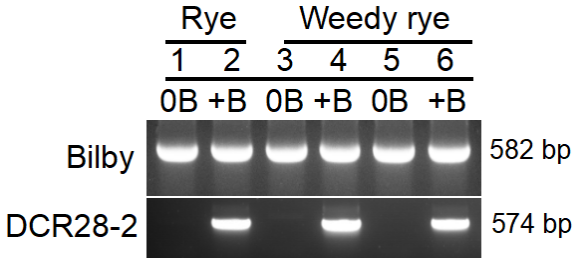


Figure 13 B-specific PCR amplicon demonstrates that *DCR28* are B chromosome-specific in cultivated rye (1, 2) and weedy rye from Afghanistan (3, 4) and Pakistan (5, 6). Bilby-specific primers were used as rye-specific control.

The B location of *DCR28* within the DCR of these weedy ryes and cultivated reference variety was cytogenetically verified by FISH using mitotic metaphase chromosomes of cultivated and weedy rye with standard B chromosomes and pachytene chromosomes of wheat with $B^S$ (Figure 14a, b; Supplementary Figure 5). Strong overlap of hybridization signals between *DCR28* and Sc26C38/D1100 suggested the presence of clustered *DCR28* copies in the DCR of both species (Figure 14b; Supplementary Figure 5). Application of FISH to naturally extended pachytene chromosomes confirmed overlapping *DCR28* and Sc26c38 signals and demonstrated the distal position of E3900 arrays (Figure 14b, Supplementary Figure 5b).

The multiplicity of *DCR28* in the DCR is consistent with diversification as an evolutionary means of competing in an arms race. Local gene clusters are suggestive of duplication events mediated by local microhomologies via (e.g.) repeat arrays that lead to strand slippage during replication (Hastings et al. 2009; Muirhead and Presgraves 2021). In the assembled B genotype, members of the *DCR28* family cluster in a 2.3 Mb-long subregion intermingled with Sc26c38 repeat arrays. Several other genes intermingle with the *DCR28* cluster (Figure 14c). Three of them show close homology to the rye gene SECCE4Rv1G0278580 on chromosome 4R, suggesting, in common with *DCR28*, a copying event followed by local duplication (Supplementary Table 2). Moderate sequence variation exists between *DCR28* members, with predicted proteins varying in length from 122 to 303 residues (Figure 15). *DCR400,* by contrast, is present in a single copy located ~7 Mb away from *DCR28*.

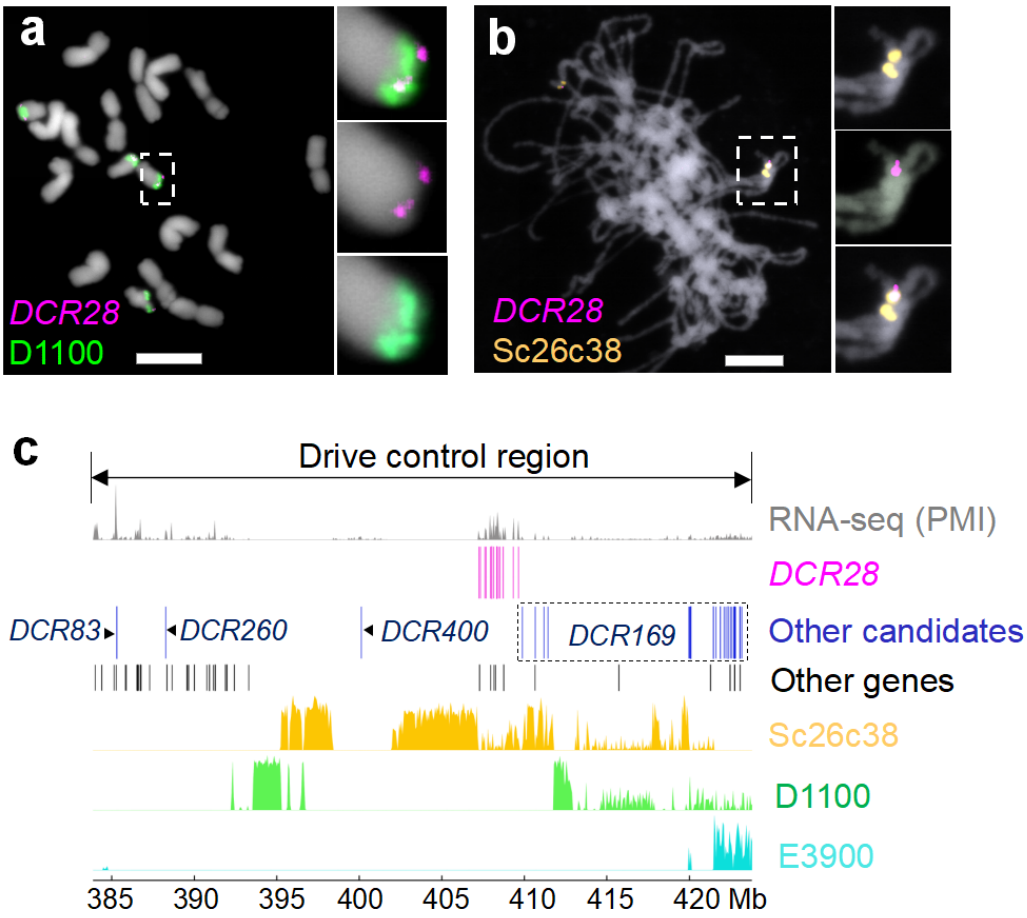


Figure 14 *DCR28* genes intermingle with Sc26c38 repeats within the rye B chromosome drive control region. (**a**) Mitotic metaphase of cultivated rye with 4 standard B chromosomes showing *DCR28*-specific (magenta) and D1100-specific (green) FISH signals. (**b**) Pachytene chromosomes of wheat with 3 rye $B^S$ chromosomes showing *DCR28*-specific (magenta) and Sc26c38-specific (orange) FISH signals. Inlets are showing further enlarged B chromosome regions after FISH. Bar = 10 µm. (**c**) Schematic rye B chromosome depicting the localization of *DCR28* and Sc26c38. (d) Multiple copies of *DCR28* form a cluster in a 2.3-Mb region. The drive control region (383.9 to 423.8 Mb) on the chrB was visualized by pyGenomeTracks. The first track (grey) indicates the expression of the RNA-seq data of anthers undergoing the first pollen mitosis (PMI) of wheat with $2B^s$. The second track (magenta) represents the *DCR28* gene cluster, from 407,247,670 to 409,643,611 bp on chrB. The third track (blue) represents other candidate genes in this region, including three single-copy genes *DCR83*, *DCR260*, *DCR400,* and the *DCR169* gene family (dashed box). The fourth track represents other genes in this region that do not belong to the differentially expressing candidate list. The fifth track (orange) represents the distribution of the repeat Sc26c38, and the sixth track (green) represents the distribution of the repeat D1100. The last track (sky blue) represents the distribution of the repeat E3900.

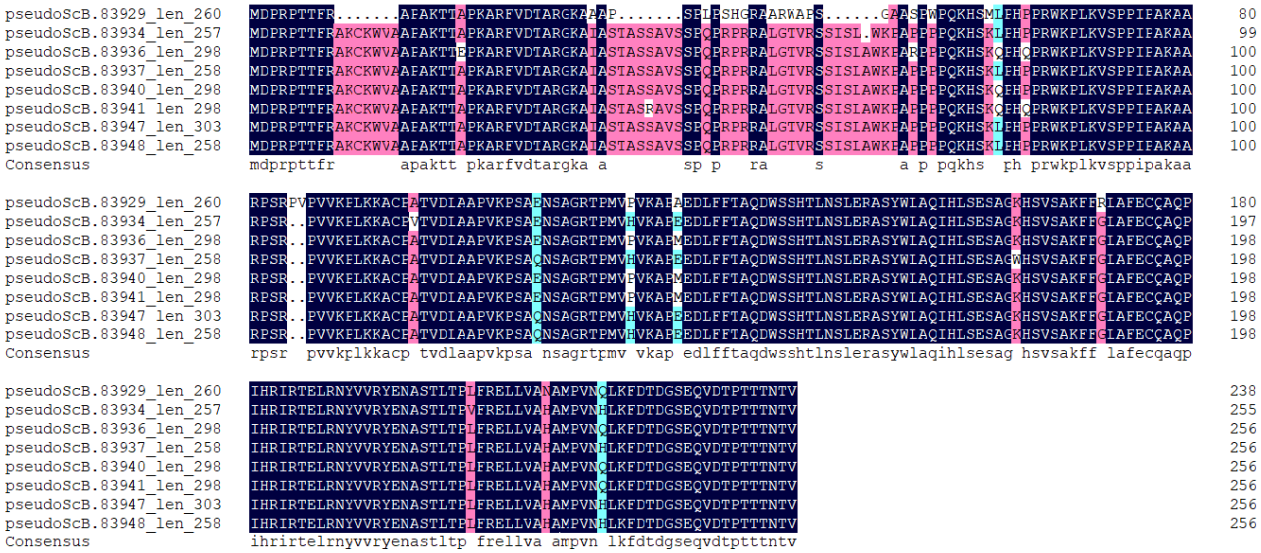


Figure 15 Multiple amino acid sequence alignment of eight DCR28 copies reveals they encode a conserved 256-aa protein.

Homology search using BLASTp showed *DCR28* and *DCR400* share recent common ancestry with rye A chromosome-located paralogs; *DCR28* is most closely related to the single-copy gene SECCE7Rv1G047916 (called *DCR28-like rye)* on rye chromosome 7R, though DCR28 encodes a protein 71 residues shorter than its A chromosome counterpart (Supplementary Figure 6a). *DCR400* shows exceptionally high amino acid identity to the rye paralog gene SECCE1Rv1G0060580 (called *DCR400-like rye*) on A chromosome 1R (Supplementary Figure 7e), suggesting a more recent copying event. *DCR28*-like genes and *DCR400*-like genes also possess homologs in all three wheat genomes. *DCR28* shares closest homology with TraesCS4A03G0224100 (*DCR28-like wheat A*), TraesCS4B03G0550000 (*DCR28-like wheat B*), TraesCS4D03G0484200 (*DCR28-like wheat D*), and *DCR400*-like shares closest homology with TraesCS1D03G0983600 (*DCR400-like wheat D*), TraesCS1B03G1206100 (*DCR400-like wheat B*), and TraesCS1A03G1024600 (*DCR400-like wheat A*) (Supplementary Figure 6b-d, Supplementary Figure 7f-h).

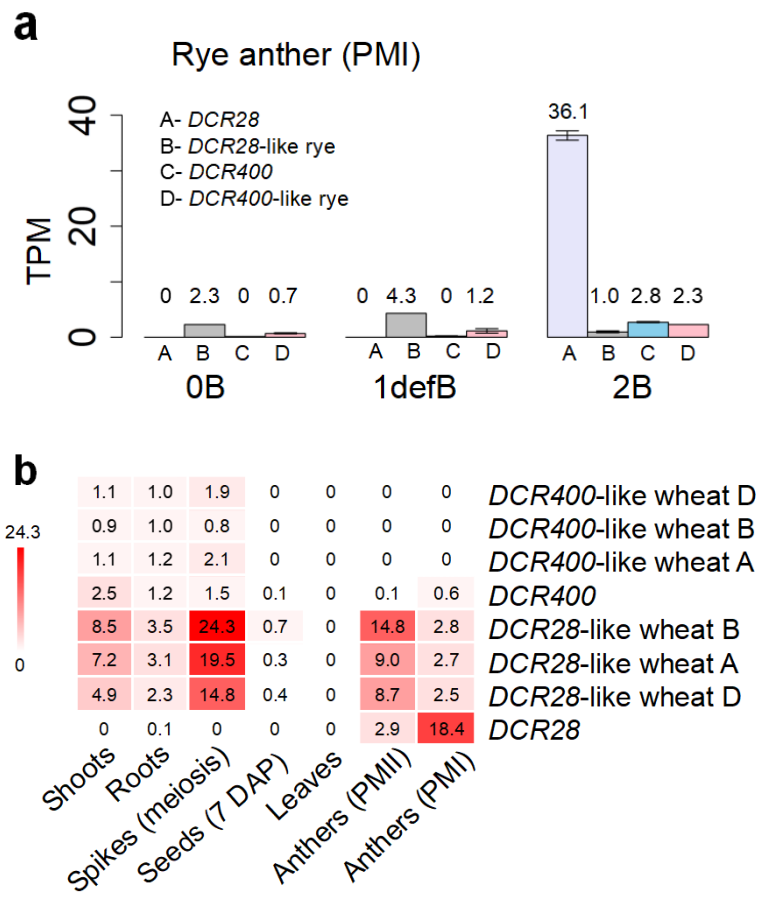


Figure 16 The transcriptional activity of *DCR28* and its paralogous genes differs, while the transcriptional activity of *DCR400* and its paralogous genes are similar**.** (**a**) The expression of *DCR28* (A) and its rye A paralog (*DCR28-like rye*, SECCE7Rv1G0479160) (B), *DCR400* (C) and its rye A-paralog (*DCR400-like rye*, SECCE1Rv1G0060580) (D) in rye with 0B, 1 deficient B (defB), and 2B chromosomes during the first pollen mitosis (PMI). Expression calculation method: transcripts per million (TPM); (**b**) The mean expression of *DCR28*, and the expression *DCR400* and their paralogous genes in wheat in different tissues of wheat+2B$^{s}$: Shoot-shoot apical meristem, root-root apical meristem, spike-young spikes undergoing meiosis, seed-seeds (7 days after pollination), leaf-young and old leaves, and anthers undergoing PMII and PMI. Expression calculation method: TPM. *DCR400*-like wheat D: TraesCS1D03G0983600, *DCR400-like wheat B*: TraesCS1B03G1206100, *DCR400-like wheat A*: TraesCS1A03G1024600. *DCR28-like wheat D*: TraesCS4D03G0484200, *DCR28-like wheat B*: TraesCS4B03G0550000, *DCR28-like wheat A*: TraesCS4A03G0224100.

Compared with the *DCR28* family, the *DCR28-like rye* expressed at a much lower level during the first pollen mitosis (PMI) (Figure 16a), while *DCR400* and *DCR400-like rye* both express at a very low level (TPM: 2~3) during PMI (Figure 16a). The expression patterns of the three A-paralogs of *DCR28* in wheat (*DCR28-like wheat A, B, D*) are similar: They showed high expression in young meiotic spikelets and lower expression in other tissues including PMI and PMII anthers (Figure 16b). Thus, expression dynamics definitively differ between *DCR28* and the A chromosome-encoded *DCR28*-like genes of rye and wheat. In contrast, no significant DGE is evident between *DCR400* and *DCR400-like wheat A, B, D* (Figure 16b).

## *3.5 The phylogeny of DCR28*

DCR28 is classified as a member of the microtubule-associated Futsch-like protein family (PTHR34468) by PANTHER. To better understand its evolution, a phylogenetic tree of DCR28-like genes was built based on 434 protein sequences of 325 species obtained from the NCBI database. Members of this gene family were detected throughout the major plant groups, from algae to angiosperms. The unrooted phylogenetic tree revealed three clusters (Figure 17a). Rooting the tree with *Chara brownii*, an alga representing the phylogenetically earliest branch in our dataset, we found early DCR28-related gene duplication in angiosperms, which resulted in two major groups (type 1 and type 2) (Figure 17b). This duplication must have happened at or after the origin of the angiosperms, as in algae, sporophytes, and gymnosperms, we found only one type of the genes (Figure 17a,b). Not all angiosperm species in our dataset carry both types of DCR28-related proteins (Figure 17c), and it seems that type 2 sequences were particularly lost in many branches of angiosperms. The DCR28 sequence groups with *Triticum*- and *Triticeae*-derived genes within the grass clade of type 2, placing its origin within this group.

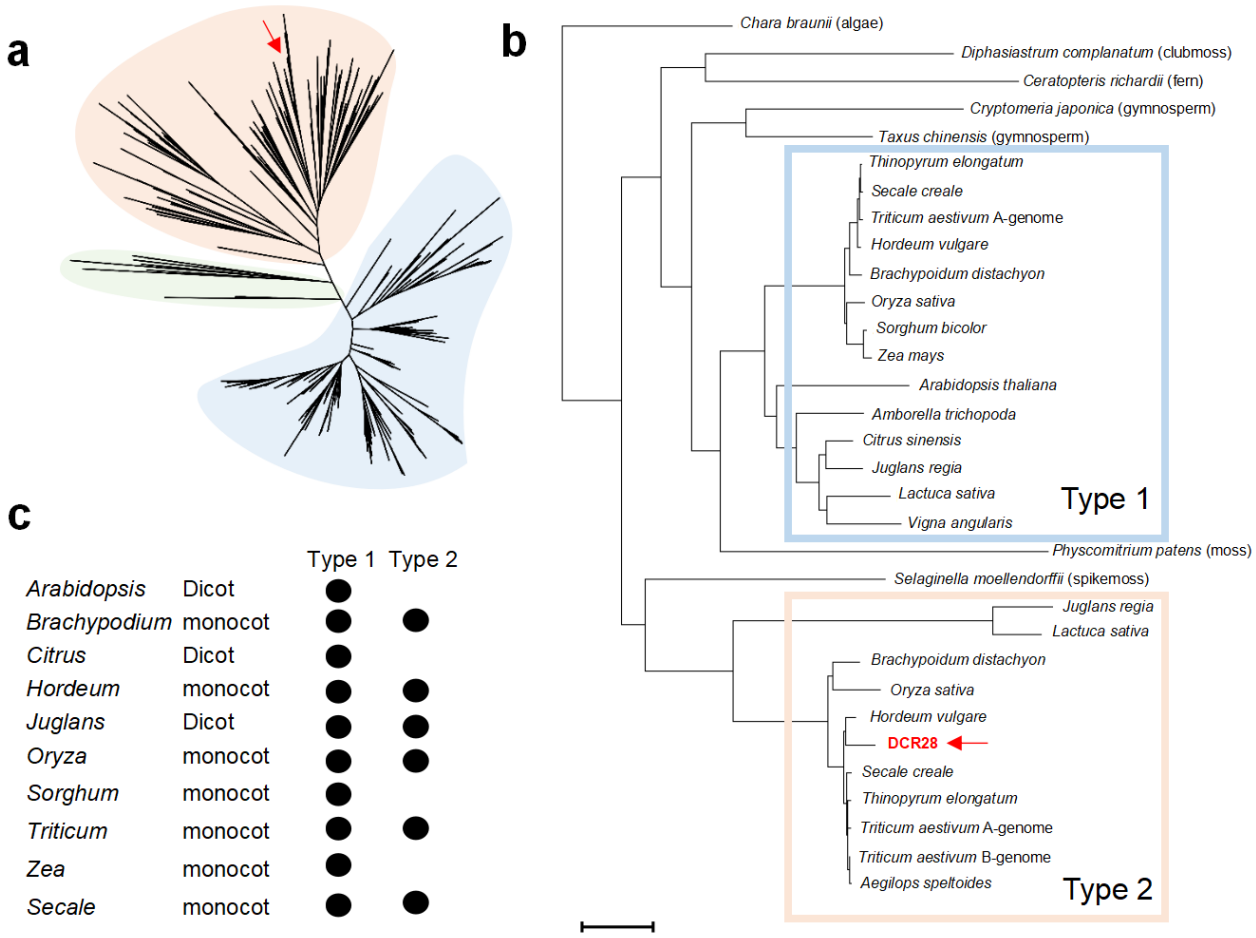


Figure 17 Gene tree indicating phylogenetic relationships of the DCR28-like Futsch-like proteins. (**a**) Maximum-likelihood phylogenetic unrooted tree of DCR28 (red arrow) and 434 DCR28-like genes from 325 species. (**b**) A smaller phylogenetic tree represents examples from different plant species rooted with *Chara brownii*. Distance scale=0.5; (**c**) The distribution of genes from type 1 and type 2 in 10 angiosperm species; Black dot indicates gene exists, no dot indicates no gene exists. The light green cluster indicates plant species with earlier evolutionary history (e.g. algae, mosses, gymnosperms). The light blue cluster indicates type 1 sequences, and the light orange cluster indicates type 2 sequences.

## *3.6 DCR28 is a microtubule-associated protein*

To determine whether DCR28 and its rye A chromosome paralog DCR28-like are related to chromosome segregation, we fused the Enhanced Yellow Fluorescent Protein (EYFP) to their N-termini and analyzed their transient expression under the control of the

CaMV35S promoter in *Nicotiana benthamiana* leaves. Both showed fiber-like signals on the cytoskeleton compared to the EYFP control (Figure 18a). Independent co-infiltration with mCherry-Microtubule Binding Domain (mCherry-MBD) (Marc et al. 1998) and mCherry-Actin Binding Domain 2 (mCherry-ABD2) (Sheahan et al. 2004) revealed that DCR28 and DCR28-like rye are associated with microtubules rather than actin (Supplementary Figure 8). However, among cells that showed microtubule-like signals, DCR28 alone appeared to encourage the formation of bundled fibers, which were observed in 28% (94/336) of cells expressing EYFP-DCR28, but in no cells expressing EYFP-DCR28-like rye (Figure 18a).

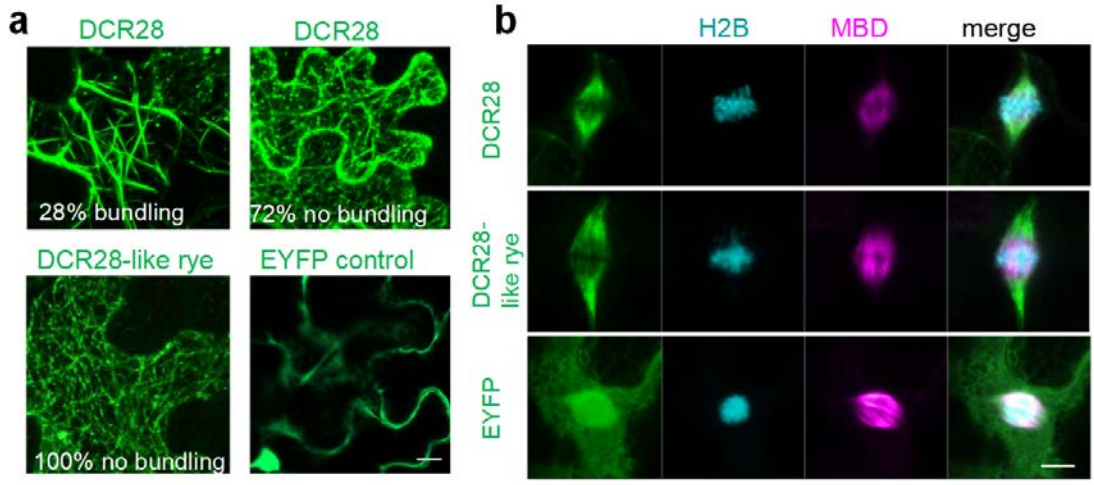


Figure 18 DCR28 is a microtubule-associated protein. (**a**) Transient co-overexpression of EYFP-DCR28 or EYFP-DCR28-like rye (in green) and mCherry-MBD (in magenta) in *N. benthamiana* stably expressing histone H2B-CFP (in blue). Overexpression of EYFP-DCR28 results in 28% tubulin fiber bundling at interphase (n=336). Overexpression of DCR28-like rye results in no bundling of fibers (n=411). (**b**) Note spindle localization of EYFP-DCR28 and EYFP-DCR28-like rye during metaphase. Bars = 10 µm.

To ascertain whether DCR28 and DCR28-like rye relate to cell division, we employed the cell division-enabled leaf system (Xu et al. 2020) in a stably transformed histone CFP-H2B reporter line of *N.* benthamiana (Martin et al. 2009). DCR28 and DCR28-like rye localize to the spindle during cell division, and their signals are identical to the microtubule during cell division (Figure 18b, Supplementary Figure 9). To find differences between

DCR28 and DCR28-like rye during the cell division, we fused the fluorescent protein mCherry to the N-termini of DCR28 and DCR28-like rye and co-infiltrated EYFP-DCR28-like rye and EYFP-DCR28, respectively. No difference was observed between DCR28 and DCR28-like rye during prophase to telophase (Supplementary Figure 10). We conclude that DCR28 and DCR28-like rye are microtubule-associated proteins and only DCR28 promotes microtubule-bundling. Both participate in cell division and are likely involved in chromosome segregation.

## *3.7 Targeted size reduction of the rye B chromosome via CRISPR*

Although our characterization of six B chromosome variants resulted in the identification of a small region that controls drive, this region is still larger than 40 Mb. In addition, our comparative RNA-seq analysis only focused on protein-coding genes and polyadenylated RNA. Therefore, we can’t exclude the possibility that other long non-coding RNAs are involved in addition in the drive control of the rye B chromosome. Thus, further reduction of the drive control region's size is necessary. However, the non-Mendelian segregation of the rye B chromosome prevented the application of a recombination-based method for gene mapping and identification.

To address this issue, we assumed that CRISPR-based targeting of a B-specific repeat could cause the deletion of repeat arrays and even chromosome deletions. By targeting a B-specific repeat in the drive control region, we might generate additional B variants instrumental to the map drive-controlling factor.

To test this idea, we designed a sgRNA (gE3900-6) targeting the drive control region-specific repeat E3900. We utilized the newly developed virus-induced genome editing (VIGE) system in wheat (Wang et al. 2022) to deliver the gE3900-6 into a Cas9-positive wheat line carrying a single rye $B^S$ via the barley stripe mosaic virus (BSMV). In total, we infected five plants, and two plants showed symptoms of virus infection. To identify the presence of the rye B chromosomes, we used primers targeting the rye B-specific variant of the kinetochore protein nuf2 (321,949,858-321,954,295 on chrB, Table 7, Table 13,

Supplementary Table 2). 179 seeds from the two virus-positive plants were germinated, and PCR genotyping revealed that 82 of them carry B chromosomes.

Next, we searched for a genotype with a deletion in the E3900-containing chromosome region. Since E3900- and Sc9c130-positive regions are adjacent to each other, and Sc9c130 is closer to the B chromosome end of the long arm (Figure 5), deletion of the E3900-region should result in the complete loss of Sc9c130. Therefore, we used PCR to detect the subtelomeric repeat Sc9c130 (Table 1) in the VIGE progenies. Eight Sc9c130-negative plants likely lost the end of the B chromosome (Table 13). To further confirm the B chromosome deletion, six plants were selected from these plants, and FISH was applied to detect the FISH signals of Sc9c130 and E3900 (Table 13). All of them showed loss of Sc9c130 (e.g. plant 1-A10 in Figure 19b), and five of these six plants lost E3900 completely (e.g. plant 3-D8 in Figure 19d) (Table 13).

Table 13 B chromosome deletions detected by PCR and FISH

| Plant | Number of B | Bnuf2-1/PCR | Sc9c130/PCR | Sc9c130/FISH | E3900/FISH |
|---|---|---|---|---|---|
| 3-D8 | 2 | ✓ | ✗ | ✗ | ✗ |
| 1-A10 | 1 | ✓ | ✗ | ✗ | ✓ |
| 3-B9 | 2 | ✓ | ✗ | ✗ | ✗ |
| 1-H11 | 1 | ✓ | ✗ | ✗ | ✗ |
| 3-A4 | 2 | ✓ | ✗ | ✗ | ✗ |
| 3-B3 | 1 | ✓ | ✗ | ✗ | ✗ |
| 3-C10 | ? | ✓ | ✗ | ? | ? |
| 3-H12 | ? | ✓ | ✗ | ? | ? |

"✓": Expected PCR amplification or FISH signal is present; "✗" Expected PCR amplification or FISH signal isn't present; "?", unknown result; B-specific primer pair Bnuf2-1 (targeting kinetochore protein nuf2 on the B chromosome, Table 7) was used to detect the presence of the B chromosome.

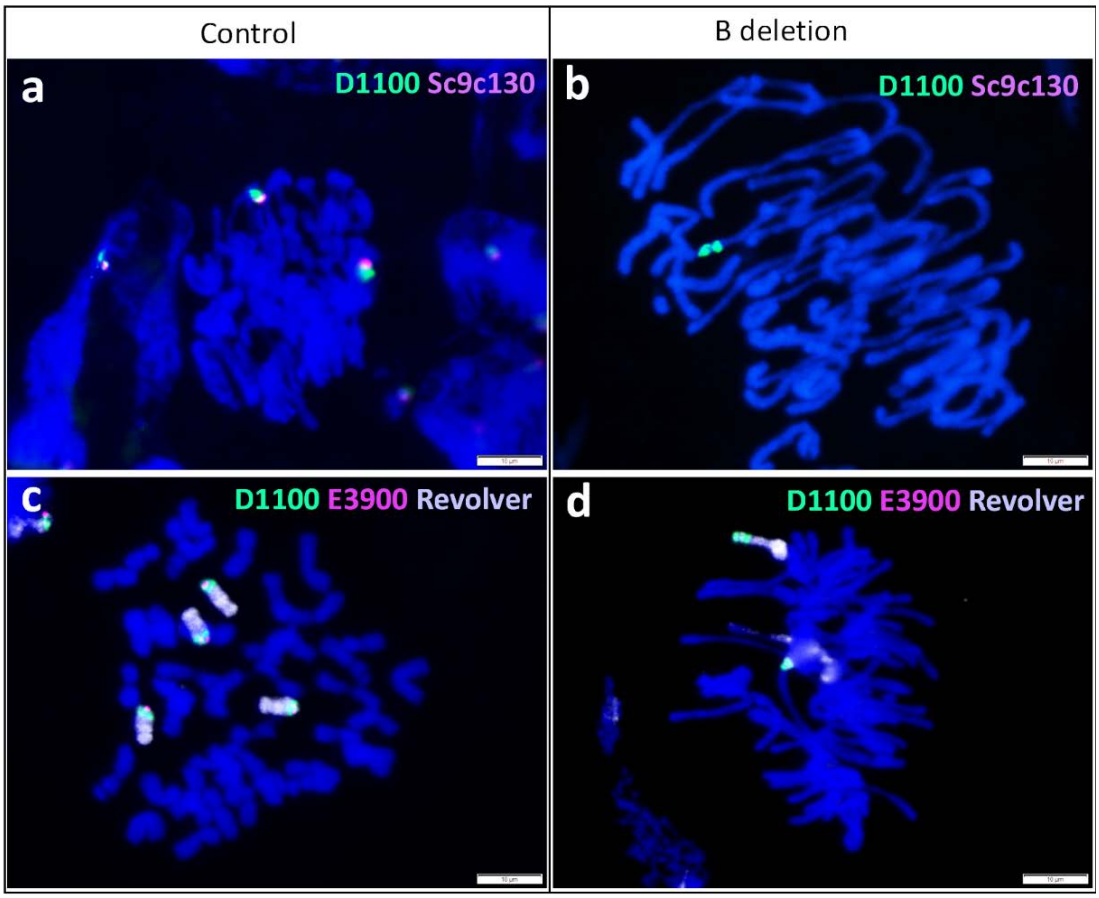


Figure 19 Identification of CRISPR-generated B chromosome deletion using FISH. (**a**) Wheat+2B$^{s}$ (control) was analyzed by FISH using B-specific repeats D1100 (green) and Sc9c130 (magenta). (**b**) plant 1-A10 (wheat with a B chromosome deletion) was analyzed by FISH using B-specific repeats D1100 (green) and Sc9c130 (magenta). (**c**) Wheat+4B$^{s}$ (control) was analyzed by FISH using the rye genome-specific repeat Revolver (white), and the B-specific repeats D1100 (green), and E3900 (magenta). (**d**) plant 3-D8 (wheat with two B chromosome deletions) was analyzed by FISH using the rye genome-specific repeat Revolver (white), and the B-specific repeats D1100 (green), E3900 (magenta). Note in plant 1-A10 (**b**); that the Sc9c130-signals are lost. In plant 3-D8 (**d**), the E3900-signals are lost. Bars = 10 µm.

# 4 Discussion and outlook

In this study, I report the identification of rye B chromosome drive-controlling candidate genes. Although the post-meiotic irregular segregation of the rye B chromosome was reported nearly a century ago (Hasegawa 1934), and the B repeat-enriched chromosome region was identified as a *trans*-active region controlling the drive of the B chromosome (Endo et al. 2008; Müntzing 1945, 1948; Lima-de-Faria 1963; Banaei-Moghaddam et al. 2012), the identification of candidate genes controlling this process was lagging behind.

To identify the drive-controlling, *trans*-acting factor(s) of the rye B chromosome first, we narrowed down the size of the drive control region by characterizing different drive-positive and drive-negative B variants by applying a set of B-specific FISH probes. Next, the assembly of PacBio highly accurate long reads and Nanopore ultra-long reads of a wheat-rye B chromosome addition line, together with Hi-C, optical, and repeat mapping, resulted in a ~430 Mb-long B chromosome pseudomolecule. Finally, a tissue-specific, comparative RNA-seq analysis using B chromosome variants with or without the ability to drive revealed five B chromosome drive-controlling candidate genes embedded in the B repeat-enriched drive control region. The PMI-specific, transcriptionally highly active, multicopy candidate DCR28 encodes a protein that belongs to the TPX2 domain-containing Futsch-like protein subfamily. Compared with its A chromosome paralog, the DCR28 underwent partial deletion but remained mitotic microtubule association and showed stronger microtubule-bundling ability. The next promising gene candidate, DCR400, was classified as an ATP-dependent DNA helicase DDX11-related family related to DNA duplex unwinding and sister chromatid cohesion.

## *4.1 DCR28 shows features of a driver gene*

Although, according to gene annotation, DCR400 is likely involved in the extended cohesion of the B sister chromatids, the high similarity (98%) of protein sequences between DCR400 and its paralog on the A chromosome suggests that *DCR400* is a young gene which the B chromosome “gained” more recently, in contrast to its long evolution

(more than 1 million years (Martis et al. 2012)). Moreover, it is expressed in different tissues where there is no drive of the B chromosomes. On the other hand, the *DCR28* is mainly expressed during the drive stage and shows the features of a driver gene. It mainly expresses during the drive stage and presents on the B chromosome of weedy rye.

The most interesting thing is that *DCR28* has many copies. Drivers always occur in multiple copies in plants, animals, and fungi like, *Kindr* (8 copies) *in Z. mays* (Dawe et al. 2018), *R2d2* (0~ >30 copies) in mice (Didion et al. 2015), Dxl (5 ~12 copies) in *Drosophila*, and wtf (0 ~42 copies) in *Schizosaccharomyces* (De Carvalho et al. 2022). De Carvalho et al. (2022) proposed that this multiple-copy feature enables a driver to perpetually reborn a new via gene duplication and evade extinction. Although the B chromosome of rye drives in a post-meiotic way, the likely lack of recombination of the rye B chromosome raises a question: how does the gene control the drive of the rye B chromosome cope with deleterious mutation and the suppression from the host plant? Therefore, the characteristic of the gene cluster of *DCR28*, rather than of a single locus, might favor its evolution over long timescales.

## *4.2 Neofunctionalization of DCR28 might lead to its specific interaction with the unknown cis-element on the rye B chromosome*

The drive of maize abnormal chromosome 10 (Ab10) depends on the interaction between the heterochromatic regions called knobs and kinesin-14 motor *Kindr* (Dawe et al. 2018). To unravel the puzzle of B chromosome drive, the other critical question is: how does the DCR28 identify the B chromosome specifically?

The B-pericentromere is different from the A-pericentromere, which contains many B-specific DNA, such as repeat CL11 and mitochondrial and chloroplast DNA. We suspect the B-specific DNA or their binding proteins could be the unknown *cis*-elements of nondisjunction. In *D. melanogaster*, the expansion of a 359-base satellite on the X chromosome can trigger the adaptive evolution of its interacting proteins (Brand and Levine 2022). We speculated that the *trans*- and *cis*-elements that control the drive of the

rye B chromosome should coevolve to increase the drive frequency to over 90% gradually. Thus, there should be a big difference in protein structure between the B-located *trans*-element and its paralog on the A chromosome. We have proved that the mutation and partial deletions on the DCR28 result in its neofunctionalization compared to its paralog on the A chromosome e.g. stronger microtubule-bundling ability.

*R2d2*, which is a repetitive DNA of a 127 kb long monomer located on mouse chromosome 2, has a transmission rate of more than 95% from heterozygous female mice. Recently Clark et al. (2024) showed that *R2d2*-containing chromosomes show lagging during anaphase of female meiosis to preferentially remain in the egg. They suspected that *R2d2* must interact with some structures, like the spindle to slow its poleward movement during anaphase. The lagging chromosome behavior in asymmetrical cell division is similar between the rye B chromosome and *R2d2*. Therefore, we propose a simple model of how DCR28 controls the drive of the rye B chromosome (Figure 20):

1. DCR28 could either bind to B chromosome-specific DNA (e.g. CL11, mitochondrial, and chloroplast DNA) or their binding proteins on the B-pericentromere.
2. Since DCR28 is a microtubule-binding protein that could interact with the spindle, we suspect that these interactions will lead to erroneous microtubule attachment on the B-pericentromere from different orientations kind of like merotelic attachment (Gregan et al. 2011).
3. A lot of microtubules are enriched on the B sister chromatids that antagonize the pulling force of kinetochore-microtubules from both spindle poles and finally cause the nondisjunction of the B chromosome.

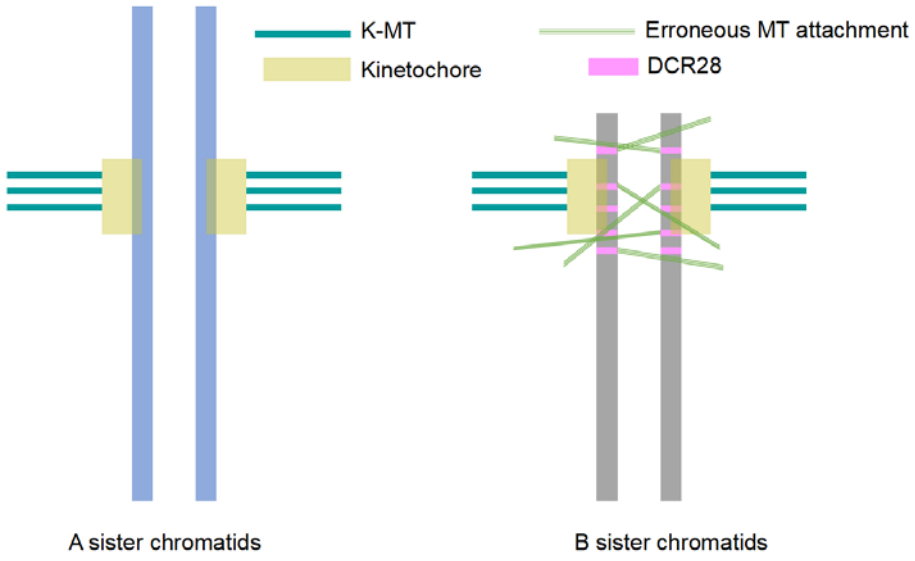


Figure 20 A proposed model of how DCR28 controls the nondisjunction of the rye B chromosome during first pollen mitosis. DCR28 first binds to B chromosome-specific DNA/proteins on the B-pericentromere. Meanwhile, it interacts with the microtubules of the spindle, causing erroneous microtubule attachment to the B-pericentromere like merotelic attachment. MT: microtubules. K-MT: kinetochore-microtubules.

## *4.3 The VIGE system enables the functional analysis of the rye B chromosome*

In total, we identified five candidates that might control the drive of the rye B chromosome. Unlike *DCR28* and *DCR169*, the other three candidates, *DCR83*, *DCR260*, and *DCR400*, are single-copy genes. Therefore, there is a higher chance of knocking out these single-copy genes using the standard CRISPR approach. Recently, a virus-based CRISPR delivery system was developed for wheat using barley stripe mosaic virus (BSMV) (Hu et al. 2019; Wang et al. 2022). This method can skip the time- and resource-consuming plant transformation because a wheat line with stably expressing Cas9 already exists. Additionally, the virus can be modified to deliver different sgRNAs to target different genes. Wang et al. (2022) revealed that the efficiency of BSMV-based CRISPR editing depends on the Cas9 expression levels, and they identified two high-expressing wheat Cas9 lines

C413 and 707, after measuring the relative levels of Cas9 expression in multiple transgenic wheat Bobwhite lines. We obtained the transgenic wheat line 707 with high-expressing Cas9 from this study via Prof. Dr. Thorsten Schnurbusch (IPK, Germany). Wheat with rye B chromosomes was crossed with this line, resulting in wheat with high-expressing Cas9 and rye B chromosomes. This material will be useful for future gene function studies of *DCR83*, *DCR260*, and *DCR400*, or other genes of interest on the rye B chromosome. It is, however, not necessarily impossible, given the rapid pace of development of CRISPR technology. For example, adding 13 introns into the Cas9 coding sequence dramatically improved the editing efficiency in *Arabidopsis thaliana* (70%~90% of primary transformants showed mutant phenotypes) (Grützner et al. 2021). It is therefore anticipated that the use of Cas9 with greater efficiency will enable the generation of a fully DCR28 knock-out mutant in the future. Should this not be achieved in a single generation, the plants can be grown for several generations until the desired mutant is obtained.

RNA interference (RNAi) could be the alternative approach to knock down the expression of DCR28. RNAi is a post-transcriptional gene silencing (PTGS) mechanism that down-regulates target genes regardless of their copy number (Matthew 2004). Uiltizing RNAi, Dawe et al. (2018) successfully knocked down the expression from 8 copies of kinesin-14 motor (*Kindr*), and it resulted in the loss of meiotic drive of the maize abnormal A chromosome 10 (Ab10). A similar approach could be used to reduce the expression of *DCR28* during the first pollen mitosis to see if the drive frequency of the rye B chromosome is affected.

## *4.4 Overexpression of DCR28 in wheat with drive-negative B-variant*

However, the transformation in rye is still very difficult to achieve. Therefore, we propose the genetic manipulation of DCR28 in wheat carrying rye B chromosomes. The ability of the rye B chromosome to drive in the background of wheat, similarly to that of rye (Endo et al. 2008; Lindström 1965a), was essential to study the genes on the rye B chromosome. Recently, a significant improvement in *Agrobacterium tumefaciens*-mediated wheat transformation achieved efficiency as high as 50-90% in the wheat genotype ‘Fielder’

(Ishida et al. 2015). *DCR28* contains 15 active copies and is located in a heterochromatin-enriched region, making it a significant challenge to completely knock it out using CRISPR, as mentioned above. However, it is possible to approach this from a different angle. One option is to transform a copy of DCR28 driven by the ubiquitin promoter into wheat cv. 'Fielder' and then cross the offspring with wheat that carries the drive-negative B-variant, such as $B^k$-3. If DCR28 is the *trans*-factor controlling the drive of the rye B chromosome, its overexpression could rescue the drive of $B^k$-3 or cause the nondisjunction of $B^k$-3 during embryogenesis. However, there is a risk that if there is more than one *trans*-factors in the drive control region, overexpression of DCR28 driven by ubiquitin promoter could not be enough to rescue the drive of the B variant $B^k$-3.

## *4.5 Subcellular localization of DCR28 during the first pollen mitosis*

To test the functional model of DCR28 as mentioned above, a DCR28 antibody would be instrumental in determining the distribution and dynamics of DCR28 during the first pollen mitosis. Unfortunately, we failed to generate a DCR28 peptide-based antibody. To address this issue, recombinant DCR28 protein could be produced in *E. coli* and purified to generate a new antibody, even if it had a reduced specificity. In addition, a GFP-DCR28 fluorescence reporter construct could be transformed into wheat cv. 'Fielder' and subsequently crossed with wheat-containing standard rye B chromosomes. This work will allow us to perform live imaging to determine the distribution and dynamics of DCR28 during the first pollen mitosis. Immunostaining could also be performed in the fixed anthers using a GFP antibody to check the localization of GFP-DCR28. In combination with super-resolution microscopy, GFP-DCR28 immunostaining could allow a comprehensive analysis of the spatial relationships between DCR28 and other cellular components (e.g. microtubules, kinetochores, chromatids).

## *4.6 Targeted chromosome deletion induced by CRISPR*

A limitation of our comparative RNA-seq analysis is that this method was only based on polyadenylated RNA. However, it is possible that non-polyadenylated transcripts like small

RNAs or some long non-coding RNAs (lncRNAs) also act as *trans*-elements controlling the drive. Furthermore, we still don't know how many elements control the drive, so it's necessary to reduce the size of the B drive control region further. To overcome this problem, there are three options: the gametocidal chromosome system [reviewed by Endo (2007)], radiation-induced chromosome mutations (Larik 1975), and wheat homeologous pairing suppressor mutants (e.g. *Ph1* locus) (Sears 1977). Unfortunately, wheat homeologous pairing suppressor mutants only allow pairing between homoeologous chromosomes like wheat chromosome 2B and rye chromosome 2R (Lukaszewski et al. 2004). Therefore, this system is unsuitable for generating wheat-rye B chromosome translocation, as the rye B chromosome is not homoeologous to wheat chromosomes.

The other two options can work. For example, in this study, B-variants $B^s$-8, $B^k$-1, and $B^k$-2 were created by a gametocidal chromosome system derived from *Ae. cylindrica* (2C) by (Endo et al. 2008). The mechanisms behind the size reduction of the B chromosome by radiation and the application of gametocidal chromosomes are largely different, but the outcome is similar: causing random chromosome breakage. Although these two methods have achieved much success over the last few decades [reviewed by Gill (2022); Said et al. (2024)], their drawbacks are obvious, e.g. random chromosome rearrangements, genome instability, and time-consuming and labor-intensive analysis of mutants. In this study, we developed a CRISPR-based chromosome down-sizing system using VIGE. By targeting a B-specific repeat, we reduced the size of the drive control region.

Compared to radiation and the gametocidal chromosome system, our chromosome “chopping” system will not cause trouble in the genome because the off-target of the sgRNA is predictable, and the virus itself cannot cause any heritable change in the wheat genome. In addition, ~10% +B plants containing B chromosome deletion were found in the experiment by chopping off the E3900 region, suggesting that our method is efficient. In the future, this chromosome “chopping” system could be applied to create more mutations by targeting the drive control region-located repeats D1100 and Sc26c38. It sheds light on studying the *cis*-acting elements in the B (peri)centromere and the generation of the mini-chromosome. One disadvantage of this technique is that it requires a Biosafety Level 2 laboratory, as plant viruses are used to deliver the sgRNA.

## *4.7 Are similar mechanisms controlling the drive of the B chromosomes in closely related species?*

The B chromosome behavior during the first pollen mitosis is highly similar in the rye and *Ae. speltoides* (Banaei-Moghaddam et al. 2012; Wu et al. 2019). Given the close phylogenetic relationship between *Secale* and *Aegilops*, a similar mechanism may control the drive of B chromosomes in both species. Strikingly, we identified an orthologous gene of *DCR28* on the B chromosome of *Ae. speltoides* (Chen, Kim, et al. unpublished). To our surprise, the B-located DCR28 of rye and *Ae. speltoides* show a closer relationship than their corresponding A chromosome-located paralogs (Chen, Kim, et al. unpublished). Together with *Ae. mutica*, B chromosomes of all three species share the B-specific tandem-repeat AesTR-183 (Wu et al. 2019). In addition, the high accumulation frequency of organelle-derived DNA in the B chromosomes of rye, *Ae. speltoides* and *Ae. mutica* may indicate a common way of the B evolution in these species (Martis et al. 2012; Ruban et al. 2014). These observations trigger the question of whether the B chromosomes of rye, *Ae. speltoides* and *Ae. mutica* originated in a common ancestor? Does the same gene control the drive? Since the assembled rye B and *Ae. speltoides* B chromosomes (Chen, Kim et al. unpublished) are available. We could also assemble the *Ae. mutica* B chromosomes and annotate its genes. To uncover the similarity between the B chromosomes of rye, *Ae. speltoides* and *Ae. mutica*, the degree of synteny among the three B chromosomes could be analyzed. It will be interesting to identify active B-encoded genes that are shared in all three species and might be crucial to the function of B chromosomes (chromosome drive).

## *4.8 A proposed B chromosome-enabled wheat hybrid system*

In crop breeding, heterosis is typically observed in the yield advantage of F1 hybrids over both inbred parents. Nevertheless, hybrid varieties in selfing crops (except for hybrid rice) have not been particularly successful [reviewed by Gupta et al. (2019)]. Here, I proposed a hybrid wheat system induced by the rye B chromosome.

Ruban et al. (2020) demonstrated that the programmed elimination of *Ae. speltoides* B chromosomes during embryo differentiation is due to B-chromatid nondisjunction and anaphase lagging, which leads to micronucleation. This highly efficient process is strictly controlled by genetic elements encoded by the *Ae. speltoides* B chromosome (Ruban et al. 2020). It is conceivable that the overexpression of the *trans*-acting factor that controls the nondisjunction of the rye B chromosome during embryogenesis may also result in B chromosome elimination in closely related species, like rye. The rye B chromosome could become an ideal vector to convey the male sterility (*Ms*) gene of wheat, as the *Ms* gene could be excised from the F1 hybrid by eliminating the rye B chromosome.

Wheat lines carrying the dominant male-sterile gene *Ms2* are 100% male sterile (Ni et al. 2017). This gene encodes for an orphan protein that confers male sterility in grass species (Ni et al. 2017). *Ms2* could be transformed into wheat carrying four rye B chromosomes. Given the random nature of transgene insertion, there is a ~6% chance that *Ms2* will insert into the rye B chromosome. Wheat with a *Ms2*-positive rye B chromosome is male-sterile and could be used as the female parent (Figure 21). Any elite wheat line could become the female parent by crossing the *Ms2*-positive rye B chromosome to them. Next, the *trans*-acting gene that controls the nondisjunction of the rye B chromosome will be transformed into another elite wheat line to create the male parent (Figure 21). After crossing, the *Ms2*-positive rye B chromosome will be eliminated during embryogenesis in F1 hybrids under the control of the *trans*-acting gene (Figure 21). Finally, the fertility of the F1 hybrid is recovered (Figure 21). The male-sterile female parent could be easily maintained by pollination from the same genotype without the *Ms2*-positive rye B chromosome (Figure 21).

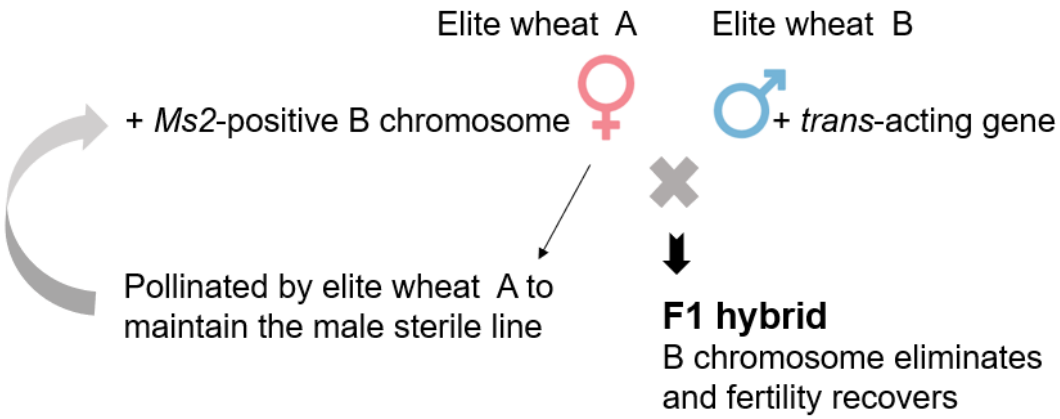


Figure 21 A proposed hybrid wheat system enabled by a rye B chromosome. In the female parent (elite wheat A), a dominant male-sterile gene *Ms2* is located on the rye B chromosome. The male parent (elite wheat B) carries the *trans*-acting gene that controls the nondisjunction of the rye B chromosome, which should cause the elimination of the rye B chromosome. The female parent is maintained by pollination from elite wheat A without the *Ms2*-positive rye B chromosome.

It should be noted that there are some challenges to this system. Firstly, the F1 offspring will be subjected to restrictions on genetically modified organisms (GMOs), given that both parents are transgenic. The molecular mechanism of the nondisjunction of the rye B chromosome remains unclear. Whether the overexpression of DCR28 or other candidates during embryogenesis leads to the nondisjunction and complete elimination of the rye B chromosome is unknown. These key questions must be addressed before applying the B chromosome in plant breeding in the future.

# 5 Summary

The following results were obtained:

1. The size of the rye B chromosome drive control region was determined using six rye B chromosome variants in the background of wheat;
2. A ~430 Mb large pseudomolecule of the rye B chromosome representing ~77% of its actual size was assembled. The rye B drive control region was mapped to a ~40 Mb region of the B pseudomolecule (383.9 to 423.8 Mb);
3. Using comparative RNA-seq analysis and PCR-mapping, five candidates were identified that might control the drive process of the rye B chromosome during the first pollen mitosis;
4. Candidate *DCR28* arose from a single-copy, rye A chromosome located paralog that underwent tandem duplication and sequence changes;
5. DCR28 is highly active during the first pollen mitosis only and also exists in the B chromosome of weedy rye;
6. DCR28 is a microtubule-associated protein which evolved microtubule-bundling ability;
7. Using Virus-Induced Genome Editing (VIGE), I demonstrated that the further size reduction of the drive control region is possible by employing B-repeat-specific gRNAs.

# 6 Literature


Akera T, Chmatal L, Trimm E, Yang K, Aonbangkhen C, Chenoweth DM, Janke C, Schultz RM, Lampson MA (2017) Spindle asymmetry drives non-Mendelian chromosome segregation. Science 358 (6363):668-672. doi:10.1126/science.aan0092

Aldrich JC, Leibholz A, Cheema MS, Ausió J, Ferree PM (2017) A 'selfish'B chromosome induces genome elimination by disrupting the histone code in the jewel wasp Nasonia vitripennis. Scientific Reports 7 (1):42551

Alfenito MR, Birchler JA (1993) Molecular characterization of a maize B chromosome centric sequence. Genetics 135 (2):589-597

Aliyeva-Schnorr L, Beier S, Karafiátová M, Schmutzer T, Scholz U, Doležel J, Stein N, Houben A (2015) Cytogenetic mapping with centromeric bacterial artificial chromosomes contigs shows that this recombination-poor region comprises more than half of barley chromosome 3 H. The Plant Journal 84 (2):385-394

Auger D, Birchler J (2002) Maize tertiary trisomic stocks derived from BA translocations. Journal of heredity 93 (1):42-47

Austin B, Trivers R, Burt A (2009) Genes in conflict: the biology of selfish genetic elements. Harvard University Press,

Banaei-Moghaddam AM, Schubert V, Kumke K, Weibeta O, Klemme S, Nagaki K, Macas J, Gonzalez-Sanchez M, Heredia V, Gomez-Revilla D, Gonzalez-Garcia M, Vega JM, Puertas MJ, Houben A (2012) Nondisjunction in favor of a chromosome: the mechanism of rye B chromosome drive during pollen mitosis. Plant Cell 24 (10):4124-4134. doi:10.1105/tpc.112.105270

Bauerly E, Hughes SE, Vietti DR, Miller DE, McDowell W, Hawley RS (2014) Discovery of supernumerary B chromosomes in Drosophila melanogaster. Genetics 196 (4):1007-1016

Bernardino ACS, Cabral-de-Mello DC, Machado CB, Palacios-Gimenez OM, Santos N, Loreto V (2017) B Chromosome Variants of the Grasshopper Xyleus discoideus angulatus Are Potentially Derived from Pericentromeric DNA. Cytogenet Genome Res. doi:10.1159/000480036

Beukeboom LW (1994) Bewildering Bs - an Impression of the 1st B-Chromosome Conference. Heredity 73:328-336. doi:Doi 10.1038/Hdy.1994.140

Blavet N, Yang H, Su H, Solanský P, Douglas RN, Karafiátová M, Šimková L, Zhang J, Liu Y, Hou J (2021) Sequence of the supernumerary B chromosome of maize provides insight into its drive mechanism and evolution. Proceedings of the National Academy of Sciences 118 (23):e2104254118

Blunden R, Wilkes TJ, Forster JW, Jimenez MM, Sandery MJ, Karp A, Jones RN (1993) Identification of the E3900 family, a second family of rye B chromosome-specific repeated sequences. Genome / National Research Council Canada = Genome / Conseil national de recherches Canada 36 (4):706-711

Bolger AM, Lohse M, Usadel B (2014) Trimmomatic: a flexible trimmer for Illumina sequence data. Bioinformatics 30 (15):2114-2120

Borg M, Brownfield L, Twell D (2009) Male gametophyte development: a molecular perspective. J Exp Bot 60 (5):1465-1478

Bosemark NO (1954) On Accessory Chromosomes In Festuca Pratensis: I. Cytological Investigations. Hereditas 40 (3-4):346-376

Bosemark NO (1956) Cytogenetics of accessory chromosomes in Phleum phleoides. Hereditas 42 (3-4):443-466

Bosemark NO (1957) Further studies on accessory chromosomes in grasses. Hereditas 43 (2):236-297
Boudichevskaia A, Fiebig A, Kumke K, Himmelbach A, Houben A (2022) Rye B chromosomes differently influence the expression of A chromosome–encoded genes depending on the host species. Chromosome Research:1-15
Brand CL, Levine MT (2022) Cross-species incompatibility between a DNA satellite and the Drosophila Spartan homolog poisons germline genome integrity. Current Biology 32 (13):2962-2971. e2964
Bravo Núñez MA, Nuckolls NL, Zanders SE (2018) Genetic villains: killer meiotic drivers. Trends in Genetics 34 (6):424-433
Burt A, Trivers R (2006) Genes in conflict : The biology of selfish genetic elements. The Belknap Press of Harvard University Press, Cambridge, Massachusetts, London, England:pp602
Camacho JPM, Sharbel TF, Beukeboom LW (2000) B-chromosome evolution. Philos T Roy Soc B 355 (1394):163-178
Carchilan M, Delgado M, Ribeiro T, Costa-Nunes P, Caperta A, Morais-Cecílio L, Jones RN, Viegas W, Houben A (2007) Transcriptionally active heterochromatin in rye B chromosomes. The Plant Cell 19 (6):1738-1749
Carlson WR (1969) A test of homology between the B chromosome of maize and abnormal chromosome 10, involving the control of nondisjunction in B's. Molecular and General Genetics MGG 104 (1):59-65
Chen J, Birchler JA, Houben A (2022) The non-Mendelian behavior of plant B chromosomes. Chromosome Res. doi:10.1007/s10577-022-09687-4
Chen J, Tang Y, Yao L, Wu H, Tu X, Zhuang L, Qi Z (2019) Cytological and molecular characterization of Thinopyrum bessarabicum chromosomes and structural rearrangements introgressed in wheat. Molecular Breeding 39 (10):1-14
Chen Q, Jahier J, Cauderon Y (1993) The B Chromosome System of Inner Mongolian Agropyron Gaertn. 3. Cytogenetical Evidence for B-A Pairing at Metaphase I. Hereditas 119 (1):53-58
Cheng H, Asri M, Lucas J, Koren S, Li H (2023) Scalable telomere-to-telomere assembly for diploid and polyploid genomes with double graph. arXiv preprint arXiv:230603399
Cheng H, Concepcion GT, Feng X, Zhang H, Li H (2021) Haplotype-resolved de novo assembly using phased assembly graphs with hifiasm. Nature methods 18 (2):170-175. doi:10.1038/s41592-020-01056-5
Chmátal L, Gabriel SI, Mitsainas GP, Martínez-Vargas J, Ventura J, Searle JB, Schultz RM, Lampson MA (2014) Centromere strength provides the cell biological basis for meiotic drive and karyotype evolution in mice. Current biology 24 (19):2295-2300
Clark FE, Greenberg NL, Silva DM, Trimm E, Skinner M, Walton RZ, Rosin LF, Lampson MA, Akera T (2024) An egg sabotaging mechanism drives non-Mendelian transmission in mice. bioRxiv:2024.2002. 2022.581453
Dalla Benetta E, Antoshechkin I, Yang T, Nguyen HQM, Ferree PM, Akbari OS (2020) Genome elimination mediated by gene expression from a selfish chromosome. Sci Adv 6 (14):eaaz9808. doi:10.1126/sciadv.aaz9808
Dawe RK, Lowry EG, Gent JI, Stitzer MC, Swentowsky KW, Higgins DM, Ross-Ibarra J, Wallace JG, Kanizay LB, Alabady M (2018) A kinesin-14 motor activates neocentromeres to promote meiotic drive in maize. Cell 173 (4):839-850. e818
De Carvalho M, Jia G-S, Srinivasa AN, Billmyre RB, Xu Y-H, Lange JJ, Sabbarini IM, Du L-L, Zanders SE (2022) The wtf meiotic driver gene family has unexpectedly persisted for over 100 million years. Elife 11:e81149

de Saint Phalle B, Oldenbourg R, Kubai DF, Salmon E, Gerbi SA (2021) Paternal chromosome elimination and X non-disjunction on asymmetric spindles in Sciara male meiosis. BioRxiv:2021.2005. 2013.444088
Didion JP, Morgan AP, Clayshulte AM-F, Mcmullan RC, Yadgary L, Petkov PM, Bell TA, Gatti DM, Crowley JJ, Hua K (2015) A multi-megabase copy number gain causes maternal transmission ratio distortion on mouse chromosome 2. PLoS genetics 11 (2):e1004850
Didion JP, Morgan AP, Yadgary L, Bell TA, McMullan RC, Ortiz de Solorzano L, Britton-Davidian J, Bult CJ, Campbell KJ, Castiglia R (2016) R2d2 drives selfish sweeps in the house mouse. Molecular biology and evolution 33 (6):1381-1395
Douglas RN, Birchler J (2017) B chromosomes. TA Bhat, AA Wani (eds), Chromosome Structure and Aberrations,© Springer India 2017 13 doi: 101007/978-81-322-3673-3_2:13-39
Ebrahimzadegan R, Fuchs J, Chen J, Schubert V, Meister A, Houben A, Mirzaghaderi G (2023) Meiotic segregation and post-meiotic drive of the Festuca pratensis B chromosome. Chromosome Research 31 (3):26
Ebrahimzadegan R, Houben A, Mirzaghaderi G (2019) Repetitive DNA landscape in essential A and supernumerary B chromosomes of Festuca pratensis Huds. Sci Rep 9 (1):19989. doi:10.1038/s41598-019-56383-1
Endo T (2007) The gametocidal chromosome as a tool for chromosome manipulation in wheat. Chromosome Research 15:67-75
Endo TR, Nasuda S, Jones N, Dou Q, Akahori A, Wakimoto M, Tanaka H, Niwa K, Tsujimoto H (2008) Dissection of rye B chromosomes, and nondisjunction properties of the dissected segments in a common wheat background. Genes & genetic systems 83 (1):23-30
Engler C, Kandzia R, Marillonnet S (2008) A one pot, one step, precision cloning method with high throughput capability. PloS one 3 (11):e3647
Escribá MC, Giardini MC, Goday C (2011) Histone H3 phosphorylation and non-disjunction of the maternal X chromosome during male meiosis in sciarid flies. Journal of cell science 124 (10):1715-1725
Escribá MC, Goday C (2013) Histone H3 phosphorylation and elimination of paternal X chromosomes at early cleavages in sciarid flies. Journal of cell science 126 (14):3214-3222
Esteban M, Campos M, Perondini ALP, Goday C (1997) Role of microtubules and microtubule organizing centers on meiotic chromosome elimination in Sciara ocellaris. Journal of Cell Science 110 (6):721-730
Evrard J-L, Pieuchot L, Vos JW, Vernos I, Schmit A-C (2009) Plant TPX2 and related proteins. Plant signaling & behavior 4 (1):69-72
Ferree PM, Blagojević J, Houben A, Martins C, Trifonov VA, Vujošević M (2024) What is a B chromosome? Early definitions revisited. G3: Genes, Genomes, Genetics:jkae068
Fishman L, Kelly AJ, Morgan E, Willis JH (2001) A genetic map in the Mimulus guttatus species complex reveals transmission ratio distortion due to heterospecific interactions. Genetics 159 (4):1701-1716
Fishman L, Saunders A (2008) Centromere-associated female meiotic drive entails male fitness costs in monkeyflowers. Science 322 (5907):1559-1562
Fröst S (1959) The cytological behaviour and mode of transmission of accessory chromosomes in Plantago serraria. Hereditas 45 (2-3):191-210
Fröst S (1964) Further studies of accessory chromosomes in Crepis conyzaefolia. Hereditas 52 (2):237-239
Fröst S (1969) The inheritance of accessory chromosomes in plants, especially in Ranunculus acris and Phleum nodosum. Hereditas 61 (3):317-326

Fröst S, Östergren G (1959) Crepis Pannonica And Crepis Conyzaefolia-Two More Species Having Accessory Chromosomes. Hereditas 45 (2-3):211-214
Fu L, Niu B, Zhu Z, Wu S, Li W (2012) CD-HIT: accelerated for clustering the next-generation sequencing data. Bioinformatics 28 (23):3150-3152
Garcia S, Nualart N (2023) Plant Genomic and Cytogenetic Databases. Springer,
Gerbi SA (2022) Non-random chromosome segregation and chromosome eliminations in the fly Bradysia (Sciara). Chromosome Research 30 (2):273-288
Gill BS (2022) A century of cytogenetic and genome analysis: impact on wheat crop improvement. In: Wheat Improvement: Food Security in a Changing Climate. Springer International Publishing Cham, pp 277-297
González-Sánchez M, González-García M, Vega J, Rosato M, Cuacos M, Puertas M (2007) Meiotic loss of the B chromosomes of maize is influenced by the B univalent co-orientation and the TR-1 knob constitution of the A chromosomes. Cytogenetic and genome research 119 (3-4):282-290
Gregan J, Polakova S, Zhang L, Tolić-Nørrelykke IM, Cimini D (2011) Merotelic kinetochore attachment: causes and effects. Trends in cell biology 21 (6):374-381
Grützner R, Martin P, Horn C, Mortensen S, Cram EJ, Lee-Parsons CW, Stuttmann J, Marillonnet S (2021) High-efficiency genome editing in plants mediated by a Cas9 gene containing multiple introns. Plant communications 2 (2)
Gupta PK, Balyan HS, Gahlaut V, Saripalli G, Pal B, Basnet BR, Joshi AK (2019) Hybrid wheat: past, present and future. Theoretical and Applied Genetics 132:2463-2483
Gurevich A, Saveliev V, Vyahhi N, Tesler G (2013) QUAST: quality assessment tool for genome assemblies. Bioinformatics 29 (8):1072-1075. doi:10.1093/bioinformatics/btt086
Habig M, Quade J, Stukenbrock EH (2017) Forward Genetics Approach Reveals Host Genotype-Dependent Importance of Accessory Chromosomes in the Fungal Wheat Pathogen Zymoseptoria tritici. Mbio 8 (6). doi:ARTN e01919-17 10.1128/mBio.01919-17
Håkansson A (1948) Behaviour of accessory rye chromosomes in the embryo-sac. Hereditas 34 (1-2):35-59
Hanlon SL, Hawley RS (2023) B chromosomes reveal a female meiotic drive suppression system in Drosophila melanogaster. Current Biology 33 (11):2300-2306. e2305
Hastings PJ, Lupski JR, Rosenberg SM, Ira G (2009) Mechanisms of change in gene copy number. Nature Reviews Genetics 10 (8):551-564
Houben A, Banaei Moghaddam AM, Klemme S (2013) Biology and evolution of B chromosomes. Plant Genome Diversity, Physical structure, behavour and evolutio of plant genomes Edited: I K Leich, Springer Press:149-166
Hsu F, Wang C, Chen C, Hu H, Chen C (2003) Molecular characterization of a family of tandemly repeated DNA sequences, TR-1, in heterochromatic knobs of maize and its relatives. Genetics 164 (3):1087-1097
Hu J, Li S, Li Z, Li H, Song W, Zhao H, Lai J, Xia L, Li D, Zhang Y (2019) A barley stripe mosaic virus-based guide RNA delivery system for targeted mutagenesis in wheat and maize. Molecular Plant Pathology 20 (10):1463-1474
Ishida Y, Tsunashima M, Hiei Y, Komari T (2015) Wheat (Triticum aestivum L.) transformation using immature embryos. Agrobacterium Protocols: Volume 1:189-198
IWGSC (2018) Shifting the limits in wheat research and breeding using a fully annotated reference genome. Science 361 (6403):eaar7191
Jiménez MM, Romera F, González-Sánchez M, Puertas MJ (1997) Genetic control of the rate of transmission of rye B chromosomes. III. Male meiosis and gametogenesis. Heredity 78 (6):636-644
Jin W, Lamb JC, Vega JM, Dawe RK, Birchler JA, Jiang J (2005) Molecular and functional dissection of the maize B chromosome centromere. The Plant Cell 17 (5):1412-1423

Jones RN (1991) B-chromosome drive. American Naturalist 137:430-442
Jones RN (1995) Tansley Review No 85, B chromosomes in plants. New Phytol 131:411-434
Kamenz J, Hauf S (2017) Time To Split Up: Dynamics of Chromosome Separation. Trends Cell Biol 27 (1):42-54. doi:10.1016/j.tcb.2016.07.008
Kato A, Zheng Y-Z, Auger D, Phelps-Durr T, Bauer M, Lamb J, Birchler J (2005) Minichromosomes derived from the B chromosome of maize. Cytogenetic and genome research 109 (1-3):156-165
Kayano H (1957) Cytogenetic studies in Lilium callosum III. Preferential segregation of a supernumerary chromosome in EMCs. Proceedings of the Japan Academy 33 (9):553-558
Kim D, Paggi JM, Park C, Bennett C, Salzberg SL (2019) Graph-based genome alignment and genotyping with HISAT2 and HISAT-genotype. Nature biotechnology 37 (8):907-915
Kimura M, Kayano H (1961) The maintenance of supernumerary chromosomes in wild populations of Lillium callosum by preferential segregation. Genetics 46:1699-1712
Kishikawa H, Suzuki A (1982) Cytological study on hypo-pentaploid Triticale with four B chromosomes of rye. The Japanese Journal of Genetics 57 (1):17-24
Klemme S, Banaei-Moghaddam AM, Macas J, Wicker T, Novák P, Houben A (2013) High-copy sequences reveal distinct evolution of the rye B chromosome. New Phytologist 199 (2):550-558. doi:10.1111/nph.12289
Langmead B, Salzberg SL (2012) Fast gapped-read alignment with Bowtie 2. Nature methods 9 (4):357-359
Larik A (1975) Radiation-induced chromosome breakages in bread wheat (Triticum aestivum L.). Genetica Polonica 16 (3-4)
Leach CR, Donald TM, Franks TK, Spiniello SS, Hanrahan CF, Timmis JN (1995) Organization and origin of a B chromosome centromeric sequence from Brachycome dichromosomatica. Chromosoma 103 (10):708-714
Lee H, Seo P, Teklay S, Yuguchi E, Benetta ED, Werren JH, Ferree PM (2023) Ability of a selfish B chromosome to evade genome elimination in the jewel wasp, Nasonia vitripennis. Heredity 131 (3):230-237
Li H, Handsaker B, Wysoker A, Fennell T, Ruan J, Homer N, Marth G, Abecasis G, Durbin R, Subgroup GPDP (2009) The sequence alignment/map format and SAMtools. bioinformatics 25 (16):2078-2079
Lima-de-Faria A (1962) Genetic interaction in rye expressed at the chromosome phenotype. Genetics 47 (10):1455
Lima-de-Faria A (1963) The evolution of the structural pattern in a rye B chromosome. Evolution:289-295
Lin B-Y (1978) Regional control of nondisjunction of the B chromosome in maize. Genetics 90 (3):613-627
Lindström J (1965) Transfer to wheat of accessory chromosomes from rye. Hereditas 54 (2):149-155
Longley AE (1945) Abnormal segregation during megasporogenesis in maize. Genetics 30 (1):100-113. doi:10.1093/genetics/30.1.100
Lopez-Delisle L, Rabbani L, Wolff J, Bhardwaj V, Backofen R, Grüning B, Ramírez F, Manke T (2021) pyGenomeTracks: reproducible plots for multivariate genomic datasets. Bioinformatics 37 (3):422-423
Love M, Anders S, Huber W (2014) Differential analysis of count data–the DESeq2 package. Genome Biol 15 (550):10-1186
Lukaszewski A, Rybka K, Korzun V, Malyshev S, Lapinski B, Whitkus R (2004) Genetic and physical mapping of homoeologous recombination points involving wheat chromosome 2B and rye chromosome 2R. Genome 47 (1):36-45

Ma S, Wang M, Wu J, Guo W, Chen Y, Li G, Wang Y, Shi W, Xia G, Fu D (2021) WheatOmics: A platform combining multiple omics data to accelerate functional genomics studies in wheat. Molecular Plant 14 (12):1965-1968
Macas J, Ávila Robledillo L, Kreplak J, Novák P, Koblížková A, Vrbová I, Burstin J, Neumann P (2023) Assembly of the 81.6 Mb centromere of pea chromosome 6 elucidates the structure and evolution of metapolycentric chromosomes. PLoS Genetics 19 (2):e1010633
Marc J, Granger CL, Brincat J, Fisher DD, Kao T-h, McCubbin AG, Cyr RJ (1998) A GFP–MAP4 reporter gene for visualizing cortical microtubule rearrangements in living epidermal cells. The Plant Cell 10 (11):1927-1939
Marques A, Banaei-Moghaddam AM, Klemme S, Blattner FR, Niwa K, Guerra M, Houben A (2013) B chromosomes of rye are highly conserved and accompanied the development of early agriculture. Ann Bot 112 (3):527-534. doi:10.1093/aob/mct121
Martin K, Kopperud K, Chakrabarty R, Banerjee R, Brooks R, Goodin MM (2009) Transient expression in Nicotiana benthamiana fluorescent marker lines provides enhanced definition of protein localization, movement and interactions in planta. The Plant Journal 59 (1):150-162
Martis MM, Klemme S, Banaei-Moghaddam AM, Blattner FR, Macas J, Schmutzer T, Scholz U, Gundlach H, Wicker T, Šimková H (2012) Selfish supernumerary chromosome reveals its origin as a mosaic of host genome and organellar sequences. Proceedings of the National Academy of Sciences 109 (33):13343-13346
Mascher M, Richmond TA, Gerhardt DJ, Himmelbach A, Clissold L, Sampath D, Ayling S, Steuernagel B, Pfeifer M, D'Ascenzo M, Akhunov ED, Hedley PE, Gonzales AM, Morrell PL, Kilian B, Blattner FR, Scholz U, Mayer KF, Flavell AJ, Muehlbauer GJ, Waugh R, Jeddeloh JA, Stein N (2013) Barley whole exome capture: a tool for genomic research in the genus Hordeum and beyond. Plant J 76 (3):494-505. doi:10.1111/tpj.12294
Matthew L (2004) RNAi for plant functional genomics. Comparative and Functional Genomics 5 (3):240-244
Matthews R, Jones R (1983) Dynamics of the B chromosome polymorphism in rye II. Estimates of parameters. Heredity 50 (2):119-137
Mendelson D, Zohary D (1972) Behaviour and transmission of supernumerary chromosomes in Aegilops speltoides. Heredity
Metz C (1925) Chromosome behavior in Sciara (Diptera). Anat Rec 31:346-347
Modahl CM, Brahma RK, Koh CY, Shioi N, Kini RM (2020) Annual Review of Animal Biosciences. Annu Rev Anim Biosci 8:91-116
Muirhead CA, Presgraves DC (2021) Satellite DNA-mediated diversification of a sex-ratio meiotic drive gene family in Drosophila. Nature Ecology & Evolution 5 (12):1604-1612
Müntzing A (1945) Cytological studies of extra fragment chromosomes in rye II. Transmission and multiplication of standard fragments and iso-fragments. Hereditas 31 (3-4):457-477
Müntzing A (1948) Cytological Studies Of Extra Fragment Chromosomes In Rye: V. A New Fragment Type Arisen By Deletion. Hereditas 34 (4):435-442
Müntzing A (1970) Chromosomal variation in the Lindström strain of wheat carrying accessory chromosomes of rye. Hereditas 66 (2):279-285
Navrátilová P, Toegelová H, Tulpová Z, Kuo YT, Stein N, Doležel J, Houben A, Šimková H, Mascher M (2022) Prospects of telomere-to-telomere assembly in barley: Analysis of sequence gaps in the MorexV3 reference genome. Plant biotechnology journal 20 (7):1373-1386
Ni F, Qi J, Hao Q, Lyu B, Luo M-C, Wang Y, Chen F, Wang S, Zhang C, Epstein L (2017) Wheat Ms2 encodes for an orphan protein that confers male sterility in grass species. Nature Communications 8 (1):15121

Niwa K, Horiuchi G, Hirai Y (1997) Production and characterization of common wheat with B chromosomes of rye from Korea. Hereditas 126 (2):139-146
Niwa K, Sakamoto S (1995) Origin of B chromosomes in cultivated rye. Genome / National Research Council Canada = Genome / Conseil national de recherches Canada 38 (2):307-312
Niwa K, Sakamoto S (1996) Detection of B chromosomes in rye collected from Pakistan and China. Hereditas 124 (3):211-215
Östergren G (1947) Heterochromatic B-chromosomes in Anthoxanthum. Hereditas 33 (1-2):261-296
Padmarasu S, Himmelbach A, Mascher M, Stein N (2019) In situ Hi-C for plants: an improved method to detect long-range chromatin interactions. Plant Long Non-Coding RNAs: Methods and Protocols:441-472
Parker J, Jones G, Edgar L, Whitehouse C (1989) The population cytogenetics of Crepis capillaris. II. The stability and inheritance of B-chromosomes. Heredity 63 (1):19-27
Patro R, Duggal G, Love MI, Irizarry RA, Kingsford C (2017) Salmon provides fast and bias-aware quantification of transcript expression. Nature methods 14 (4):417-419
Pereira HS, Delgado M, Viegas W, Rato JM, Barão A, Caperta AD (2017) Rye (Secale cereale) supernumerary (B) chromosomes associated with heat tolerance during early stages of male sporogenesis. Annals of botany 119 (3):325-337
Pertea G, Pertea M (2020) GFF utilities: GffRead and GffCompare. F1000Research 9
Pertea M, Pertea GM, Antonescu CM, Chang T-C, Mendell JT, Salzberg SL (2015) StringTie enables improved reconstruction of a transcriptome from RNA-seq reads. Nature biotechnology 33 (3):290-295
Plowman AB, Bougourd SM (1994) Selectively advantageous effects of B-chromosomes on germination behavior in Allium schoenoprasum L. Heredity 72:587-593
Puertas M, Romera F, De La Peña A (1985) Comparison of B chromosome effects on Secale cereale and Secale vavilovii. Heredity 55 (2):229-234
Puertas MJ, González-Sánchez M, Manzanero S, Romera F, Jiménez MM (1998) Genetic control of the rate of transmission of rye B chromosomes. IV. Localization of the genes controlling B transmission rate. Heredity 80 (2):209-213
Rabanus-Wallace MT, Hackauf B, Mascher M, Lux T, Wicker T, Gundlach H, Baez M, Houben A, Mayer KF, Guo L (2021) Chromosome-scale genome assembly provides insights into rye biology, evolution and agronomic potential. Nature genetics 53 (4):564-573
Rhoades M, Dempsey E (1972) On the mechanism of chromatin loss induced by the B chromosome of maize. Genetics 71 (1):73-96
Rhoades M, Dempsey E, Ghidoni A (1967) Chromosome elimination in maize induced by supernumerary B chromosomes. Proceedings of the National Academy of Sciences 57 (6):1626-1632
Ribeiro T, Pires B, Delgado M, Viegas W, Jones N, Morais-Cecilio L (2004) Evidence for 'cross-talk' between A and B chromosomes of rye. Proc Biol Sci 271 Suppl 6:S482-484
Robinson PM, Hewitt GM (1976) Annual cycles in the incidence of b chromosomes in the grasshopper Myrmeleotettix maculatus (acrididae: orthoptera). Heredity 36 (3):399-412
Roman H (1947) Mitotic nondisjunction in the case of interchanges involving the B-type chromosome in maize. Genetics 32 (4):391
Roman H (1948) Directed fertilization in maize. Proceedings of the National Academy of Sciences 34 (2):36-42
Romera F, Jimenez M, Puertas M (1991) Genetic control of the rate of transmission of rye B chromosomes. I. Effects in 2B× 0B crosses. Heredity 66 (1):61-65

Ruban A, Fuchs J, Marques A, Schubert V, Soloviev A, Raskina O, Badaeva E, Houben A (2014) B chromosomes of Aegilops speltoides are enriched in organelle genome-derived sequences. PLoS One 9 (2):e90214
Ruban A, Schmutzer T, Wu DD, Fuchs J, Boudichevskaia A, Rubtsova M, Pistrick K, Melzer M, Himmelbach A, Schubert V, Scholz U, Houben A (2020) Supernumerary B chromosomes of Aegilops speltoides undergo precise elimination in roots early in embryo development. Nat Commun 11 (1):2764. doi:10.1038/s41467-020-16594-x
Rusche ML, Mogensen HL, Shi L, Keim P, Rougier M, Chaboud A, Dumas C (1997) B chromosome behavior in maize pollen as determined by a molecular probe. Genetics 147 (4):1915-1921
Rutishauser A (1956) Genetics of fragment chromosome in Trillium grandiflorum.
Rutishauser A, Rothlisberger E (1966) Boosting mechanism of B chromosomes in Crepis capillaris. Chromosomes today 1:28-30
Said M, Gaál E, Farkas A, Molnár I, Bartoš J, Doležel J, Cabrera A, Endo TR (2024) Gametocidal genes: from a discovery to the application in wheat breeding. Frontiers in Plant Science 15:1396553
Sandery MJ, Forster JW, Blunden R, Jones RN (1990) Identification of a family of repeated sequences on the rye B chromosome. Genome 33 (6):908-913
Schindele P, Wolter F, Puchta H (2020) CRISPR guide RNA design guidelines for efficient genome editing. RNA Tagging: methods and protocols:331-342
Sears ER (1977) Genetics society of canada award of excellence lecture an induced mutant with homoeologous pairing in common wheat. Canadian Journal of Genetics and Cytology 19 (4):585-593
Sheahan MB, Staiger CJ, Rose RJ, McCurdy DW (2004) A green fluorescent protein fusion to actin-binding domain 2 of Arabidopsis fimbrin highlights new features of a dynamic actin cytoskeleton in live plant cells. Plant physiology 136 (4):3968-3978
Simão FA, Waterhouse RM, Ioannidis P, Kriventseva EV, Zdobnov EM (2015) BUSCO: assessing genome assembly and annotation completeness with single-copy orthologs. Bioinformatics 31 (19):3210-3212. doi:10.1093/bioinformatics/btv351
Swentowsky KW, Gent JI, Lowry EG, Schubert V, Ran X, Tseng K-F, Harkess AE, Qiu W, Dawe RK (2020) Distinct kinesin motors drive two types of maize neocentromeres. Genes & Development 34 (17-18):1239-1251
Tamilselvan-Nattar-Amutha S, Dreissig S, Kumlehn J, Heckmann S (2023) Barley stripe mosaic virus-mediated somatic and heritable gene editing in barley (Hordeum vulgare L.). Frontiers in Plant Science 14:1201446
Timoshevskiy VA, Herdy JR, Keinath MC, Smith JJ (2016) Cellular and molecular features of developmentally programmed genome rearrangement in a vertebrate (sea lamprey: Petromyzon marinus). PLoS genetics 12 (6):e1006103
Tomita M, Shinohara K, Morimoto M (2008) Revolver is a new class of transposon-like gene composing the Triticeae genome. DNA research 15 (1):49-62
van Schie JJ, Faramarz A, Balk JA, Stewart GS, Cantelli E, Oostra AB, Rooimans MA, Parish JL, de Almeida Estéves C, Dumic K (2020) Warsaw Breakage Syndrome associated DDX11 helicase resolves G-quadruplex structures to support sister chromatid cohesion. Nature Communications 11 (1):4287
Wang W, Yu Z, He F, Bai G, Trick HN, Akhunova A, Akhunov E (2022) Multiplexed promoter and gene editing in wheat using a virus-based guide RNA delivery system. Plant Biotechnology Journal 20 (12):2332-2341
Ward EJ (1973) Nondisjunction: localization of the controlling site in the maize B chromosome. Genetics 73 (3):387-391

Werren JH (1991) The paternal-sex-ratio chromosome of Nasonia. The American Naturalist 137 (3):392-402
Wu D, Ruban A, Fuchs J, Macas J, Novak P, Vaio M, Zhou Y, Houben A (2019) Nondisjunction and unequal spindle organization accompany the drive of Aegilops speltoides B chromosomes. New Phytol 223 (3):1340-1352. doi:10.1111/nph.15875
Xu J, Lee YRJ, Liu B (2020) Establishment of a mitotic model system by transient expression of the D-type cyclin in differentiated leaf cells of tobacco (Nicotiana benthamiana). New Phytol 226 (4):1213-1220
Zhang X, Ferree PM PSRs: Selfish chromosomes that manipulate reproductive development. In: Seminars in Cell & Developmental Biology, 2024. Elsevier, pp 66-73
Zhou C, McCarthy SA, Durbin R (2023) YaHS: yet another Hi-C scaffolding tool. Bioinformatics 39 (1):btac808
Zhu T, Liang C, Meng Z, Li Y, Wu Y, Guo S, Zhang R (2017) PrimerServer: a high-throughput primer design and specificity-checking platform. bioRxiv:181941

# 7 Supplementary Figures

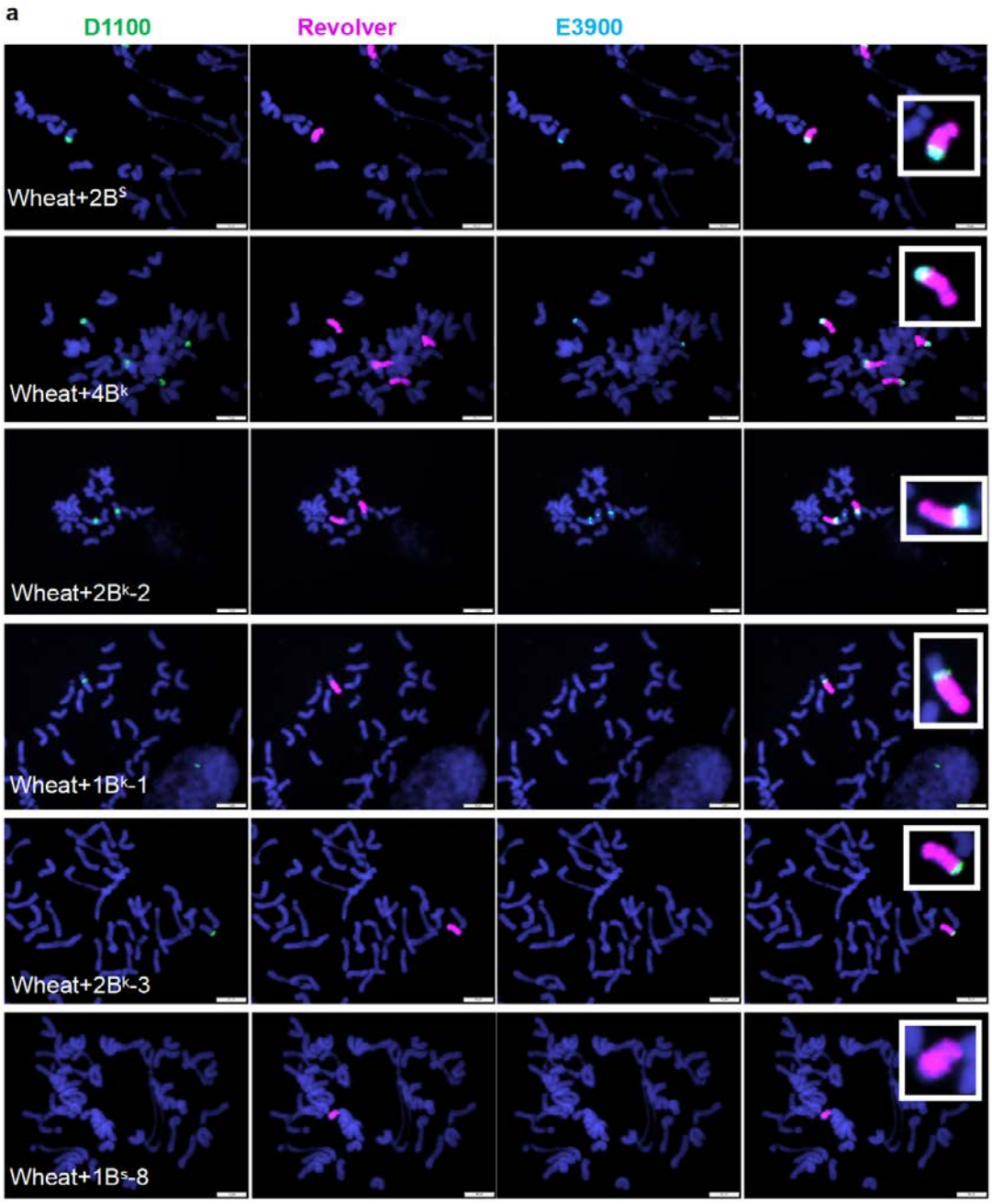


Supplementary Figure 1 Characterization of rye B chromosome variants ($B^{s}$-8, $B^{s}$,$B^{k}$,$B^{k}$-1,$B^{k}$-2,$B^{k}$-3) in the background of wheat by FISH. Mitotic metaphase chromosomes were labelled with (**a**) D1100 (green), Revolver (magenta) and E3900 (sky blue); (**b**) D1100 (green), Sc26c38 (orange) and E3900 (sky blue) and (**c**) Sc9c130 (violet), Sc26c38 (orange), E3900 (sky blue). Chromosomes were counterstained with DAPI (blue). Inlets showing selected, further enlarged B variants. Bar =10 µm.

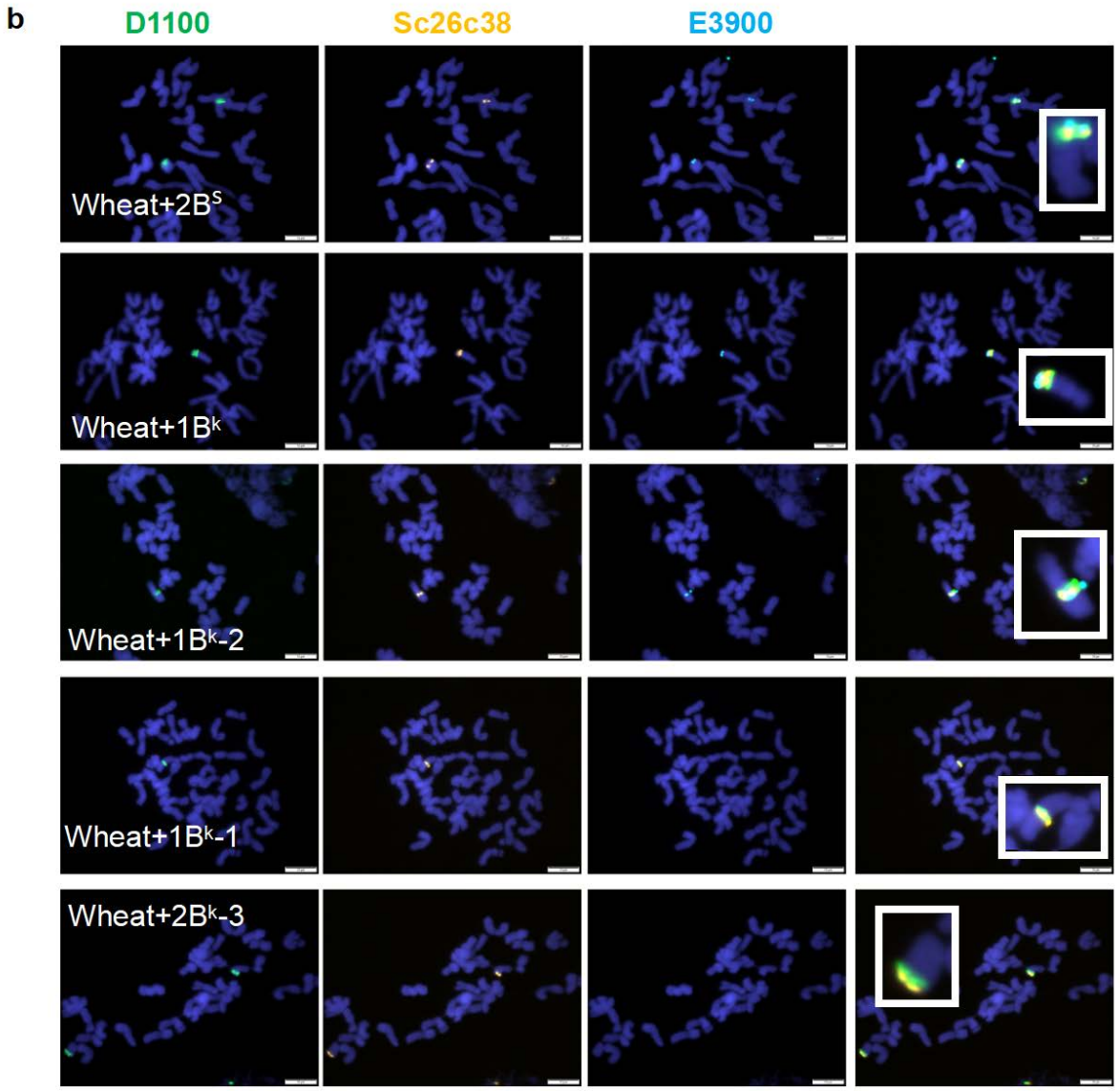


Supplementary Figure 1 Characterization of rye B chromosome variants ($B^{s}$-8, $B^{s}$,$B^{k}$,$B^{k}$-1,$B^{k}$-2,$B^{k}$-3) in the background of wheat by FISH (continued). Mitotic metaphase chromosomes were labelled with (**a**) D1100 (green), Revolver (magenta) and E3900 (sky blue); (**b**) D1100 (green), Sc26c38 (orange) and E3900 (sky blue) and (**c**) Sc9c130 (violet), Sc26c38 (orange), E3900 (sky blue). Chromosomes were counterstained with DAPI (blue). Inlets showing selected, further enlarged B variants. Bar =10 µm.

**c**

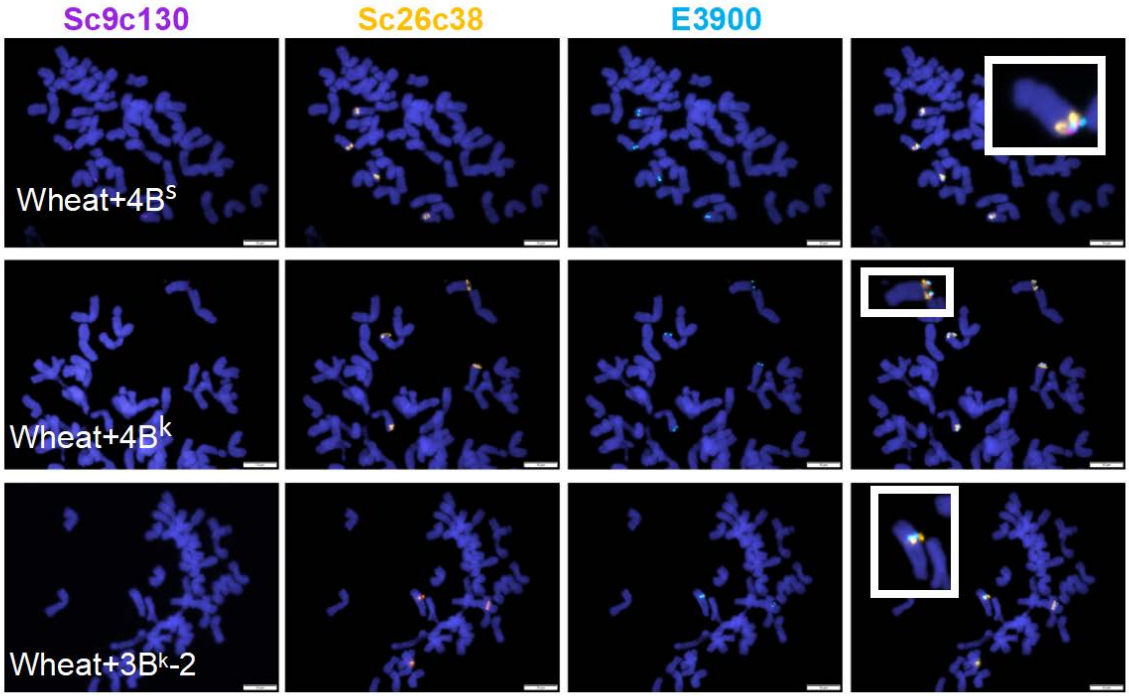


Supplementary Figure 1 Characterization of rye B chromosome variants ($B^{s}$-8, $B^{s}$,$B^{k}$,$B^{k}$-1,$B^{k}$-2,$B^{k}$-3) in the background of wheat by FISH (continued). Mitotic metaphase chromosomes were labelled with (**a**) D1100 (green), Revolver (magenta) and E3900 (sky blue); (**b**) D1100 (green), Sc26c38 (orange) and E3900 (sky blue) and (**c**) Sc9c130 (violet), Sc26c38 (orange), E3900 (sky blue). Chromosomes were counterstained with DAPI (blue). Inlets showing selected, further enlarged B variants. Bar =10 µm.

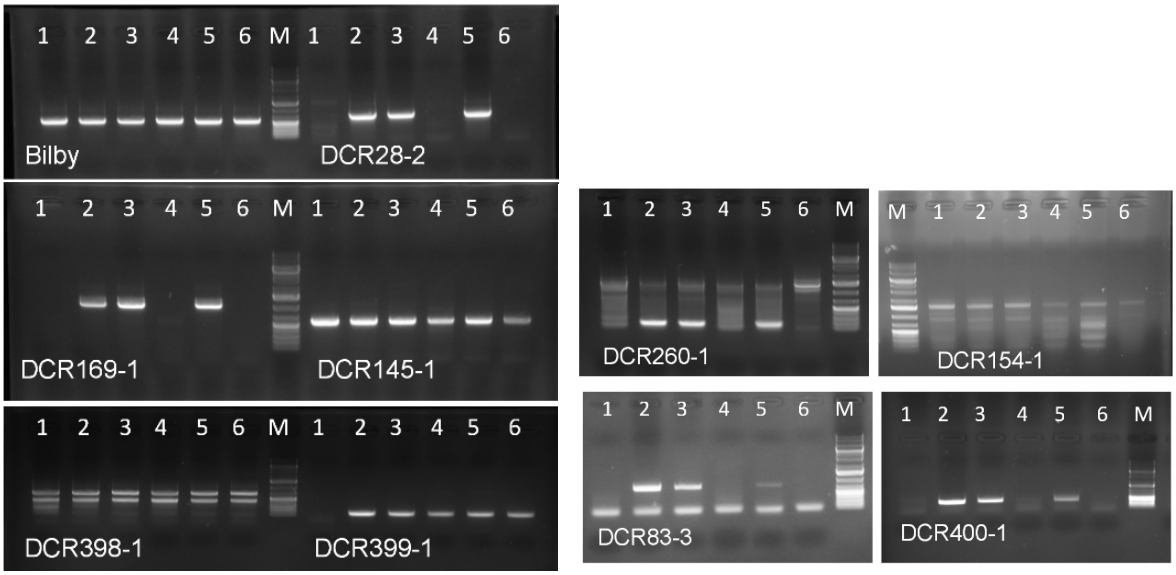


Supplementary Figure 2 Genomic PCR to test the rye B drive control region-specific location of preselected candidates. Genomic DNA of wheat with B variants possessing either a drive-functional drive control region ($2B^s$, $2B^k$, $1B^k$-2) or nonfunctional drive control region ($1B^s$-8, $1B^k$-1, $2B^k$-3) was used as a PCR template in combination with DCR-specific primers. Lane: Wheat cv. Chinese Spring (1) $+B^s$-8; (2) $+2B^s$; (3) $+2B^k$; (4) $+1B^k$-1; (5) $+1B^k$-2; (6) $+2B^k$-3, (7) Marker (M): 1kb plus DNA marker.

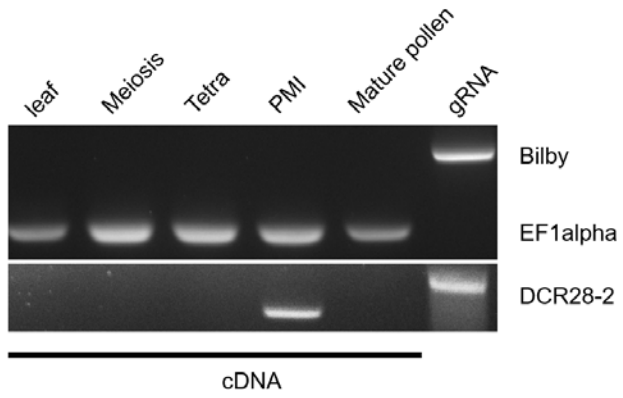


Supplementary Figure 3 Reverse transcription polymerase chain reaction (RT-PCR) confirmed *DCR28* expresses in a tissue-specific way. cDNAs of wheat with $2B^s$ include leaf tissues, spikes undergoing meiosis, spikes undergoing the tetrad stage, anthers undergoing the first pollen mitosis (PMI), and mature pollen. The quality of the cDNA was tested via control primer EF1 α. In addition, the quality of gDNA of wheat with $2B^s$ was tested by control primer Bilby. Primer DCR28-2 amplified a smaller product in the cDNA than gDNA, indicating that there was no gDNA contamination in the cDNA templates.

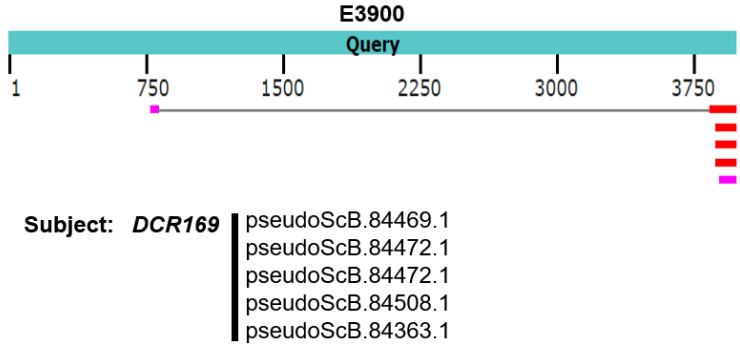


Supplementary Figure 4 Blast alignment reveals that *DCR169* shares similiarities with the end of E3900. Query: E3900, subject: 5 genes of *DCR169* (pseudoScB.84469.1,pseudoScB.84472.1, pseudoScB.84472.1, pseudoScB.84508.1, pseudoScB.84363.1)

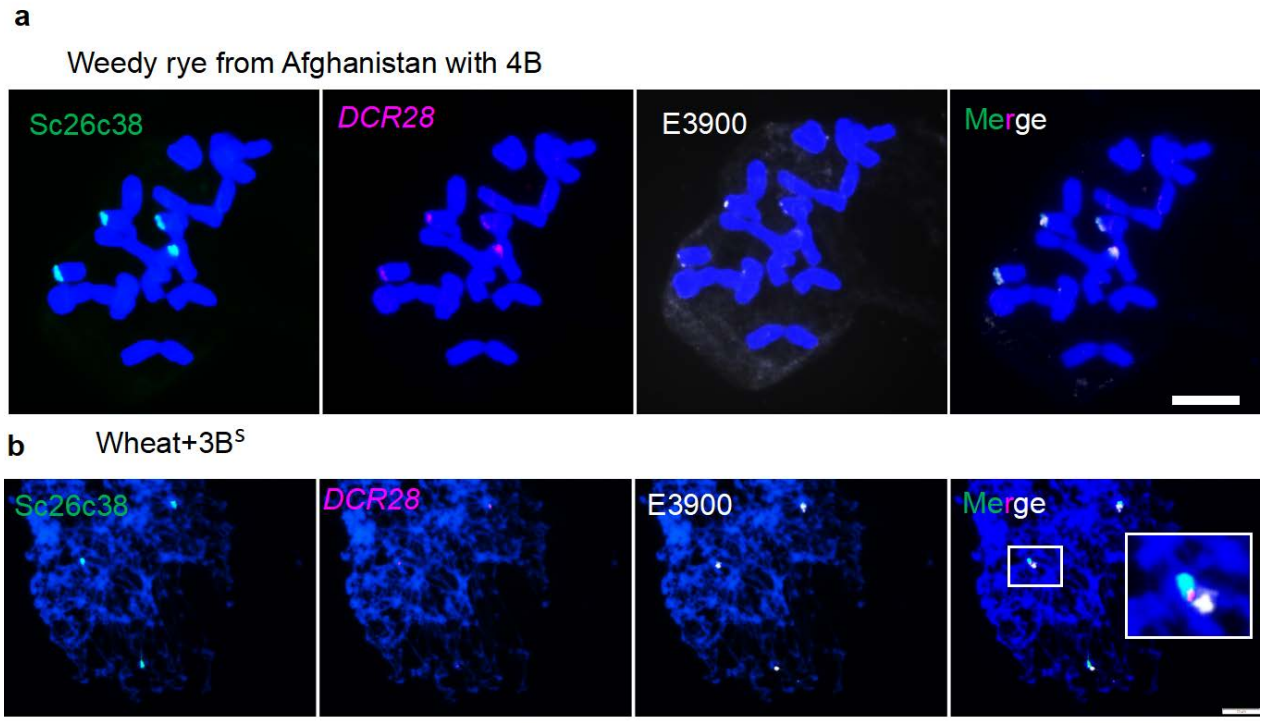


Supplementary Figure 5 Rye B drive control region-specific position of DCR28 confirmed by FISH. (a) Mitotic metaphase of weedy rye from Afghanistan with 4B after FISH using Sc26c38 (green), *DCR28* (magenta) and E3900 (white) specific probes, bar = 200 pixel. (b) Pachytene chromosomes of wheat with $3B^s$ after FISH using Sc26c38 (green), *DCR28* (magenta) and E3900 (white) specific probes. DAPI was used to counterstain the chromosomes (blue), The inlet shows selected, further enlarged Sc26c38-, *DCR28*- and E3900- signals. Bar = 10 µm.

a Query: DCR28
*vs* Subject: DCR28-like rye

**Sequence ID:** SECCE7Rv1G0479160.1 **Length:** 557 **Number of Matches:** 1

**Range 1: 1 to 328** Gene details (IWGSC gene id only) DownloadSequence

| Score | Expect | Identities | Gaps | Strand |
|---|---|---|---|---|
| 313.9 bits(803) | 0.0 | 192/328(59%) | 71/328(22%) | None/None |

```
Query          1  MDPRPTTFRAKCKWVAAPAKTTAPKARFVDTARGKAIASTASSAVSS---PQPRPRRALG  60
                  MDP PT FRAK K VAAPAKT APK + V TARGK   S  +SAVS+   PQPR RRA G
Subject        1  MDPHPTPFRAKRKSVAAPAKTPAPKPKSVTTARGKMTTSATTSAVSAGAAPQPRLRRAFG  60

Query         61  TVRSSISLAWKPAPPPPQKHSKQPHPPRWKPLKV--------------------------  120
                  TVRSS  LA KPAPPPPQKHSK   PP  KPLKV
Subject       61  TVRSSNPLAEKPAPPPPQKHSKLSPPPPQKPLKVSPPKLQKPAAKVSSPPPQKPAKVSPP  120

Query        121  --------SPPIPAKAARPSRPVVKP-LKKACPA------------------TVDLAAP  180
                         SPPIPAKAARPSRP  KP LKKACP                      LAAP
Subject      121  PQQKPSKLSPPIPAKAARPSRPAEKPLLKKACPGPDLAAKAKKKSQRVSFQDDVAALAAP  180

Query        181  -----VKPSAENSAGRTPMVPVKA---------PMEDLFFTAQDWSSHTLNSLERASYWL  240
                       VK S E SAGRTP+VPVKA           E  FF+AQ+ SS TL+ LE ASYWL
Subject      181  RSGEKVKASIEESAGRTPLVPVKALEKKPAKVVAAETPFFSAQNCSSCTLDQLESASYWL  240

Query        241  AQIHLSESAGKHSVSAKFFGLAFECQAQPIHRIRTELRNYVVRYENASTLTPLFRELLVA  300
                  AQIHL+ES GKH+VSA FF LAFECQAQP HRIR+ELRNYVVR+E+ASTLTPLF ELLV+
Subject      241  AQIHLAESVGKHNVSAAFFRLAFECQAQPFHRIRSELRNYVVRHESASTLTPLFHELLVS  300

Query        301  HAMPVNQLKFDTDGSEQVDTPTTTNTVD  328
                  HAM VNQLKFDTDGSE+VDT   T TV+
Subject      301  HAMAVNQLKFDTDGSEKVDTLAATTTVN  328
```

b Query: DCR28
*vs* Subject: DCR28-like wheat A

**Sequence ID:** TraesCS4A03G0224100.1 **Length:** 561 **Number of Matches:** 1

**Range 1: 1 to 330** Gene details (IWGSC gene id only) DownloadSequence

| Score | Expect | Identities | Gaps | Strand |
|---|---|---|---|---|
| 332.0 bits(850) | 0.0 | 198/331(60%) | 75/331(23%) | None/None |

```
Query          1  MDPRPTTFRAKCKWVAAPAKTTAPKARFV--DTARGKAIASTASSAVSS---PQPRPRRA  60
                  MDP PT FRAK K VAAPAKT APK + V   TARG+   S  +SAVS+   PQPRPRRA
Subject        1  MDPHPTPFRAKRKSVAAPAKTPAPKPKSVANGTARGRMTTSATTSAVSAGAAPQPRPRRA  60

Query         61  LGTVRSSISLAWKPAPPPPQKHSKQPHPPRWKPLKVSPP---------------------  120
                   GTVRSS SLA KPAPPPPQKHSK   PP  KPLKVSPP
Subject       61  FGTVRSSNSLAEKPAPPPPQKHSKLSPPPPQKPLKVSPPKLQKPAAKVSPPPPQKPAKVS  120

Query        121  -------------IPAKAARPSRPVVKPLKKACPATVDLAAP-----------------  180
                              +PAKAARPSRP  KPLKKACPA  DLAA
Subject      121  PPPQQKLSRLSPPVPAKAARPSRPAEKPLKKACPAPPDLAAKAKKKSQRVSFQDDVAALA  180

Query        181  -------VKPSAENSAGRTPMVPVKAPMEDL----------FFTAQDWSSHTLNSLERAS  240
                        VK S E+SAGRTPMVPVK P+E             FF+AQ+ SS TL+ LE AS
Subject      181  PSGSGEKVKASTEDSAGRTPMVPVK-PLEKKPAKVVAAETPFFSAQNCSSCTLDQLESAS  240

Query        241  YWLAQIHLSESAGKHSVSAKFFGLAFECQAQPIHRIRTELRNYVVRYENASTLTPLFREL  300
                  YWLAQIHL+ES GKH+VSA FF LAFECQAQP HRIR+ELRNYV R+E+ASTLTPLF EL
Subject      241  YWLAQIHLAESVGKHNVSAAFFRLAFECQAQPFHRIRSELRNYVARHESASTLTPLFHEL  300

Query        301  LVAHAMPVNQLKFDTDGSEQVDTPTTTNTVD  331
                  LVAHAM VNQLKFDTDGSE+VDTP TTNTVD
Subject      301  LVAHAMAVNQLKFDTDGSEKVDTPATTNTVD  331
```

c Query: DCR28
*vs* Subject: DCR28-like wheat B

**Sequence ID:** TraesCS4B03G0550000.1 **Length:** 557 **Number of Matches:** 1

**Range 1: 1 to 328** Gene details (IWGSC gene id only) DownloadSequence

| Score | Expect | Identities | Gaps | Strand |
|---|---|---|---|---|
| 339.3 bits(869) | 0.0 | 200/328(61%) | 71/328(22%) | None/None |

```
Query          1  MDPRPTTFRAKCKWVAAPAKTTAPKARFVDTARGKAIASTASSAVSS---PQPRPRRALG  60
                  MDP PT FRAK K VAAPAKT APK + V TARGK   S  +SAVS+   PQPRPRRA G
Subject        1  MDPHPTPFRAKRKSVAAPAKTPAPKPKSVATARGKMTTSATTSAVSAGAAPQPRPRRAFG  60

Query         61  TVRSSISLAWKPAPPPPQKHSKQPHPPRWKPLKVSPP---------------------  120
                  TVRSS SLA KPAPPPPQKHSK   PP  KPLKVSPP
Subject       61  TVRSSNSLAEKPAPPPPQKHSKLSPPPPQKPLKVSPPKLQKPAAKVSPPPPQKPAKVSPP  120

Query        121  -----------IPAKAARPSRPVVKPLKKACPATVDLAAP----------------------  180
                            IPAKAARPSRP  KPLKKACPA  DLAA
Subject      121  PQQKPSKLSPPIPAKAARPSRPAEKPLKKACPAPPDLAAKAKKKSQRVSFQDDVAAVAAS  180

Query        181  -----VKPSAENSAGRTPMVPVKA---------PMEDLFFTAQDWSSHTLNSLERASYWL  240
                       VK S E+SAGRTPMVPVKA           E  FF+AQ+ SS TL+ LE ASYWL
Subject      181  GSGEKVKASTEDSAGRTPMVPVKALEKKPAKVVVAETPFFSAQNCSSCTLDQLESASYWL  240

Query        241  AQIHLSESAGKHSVSAKFFGLAFECQAQPIHRIRTELRNYVVRYENASTLTPLFRELLVA  300
                  AQIHL+ES GKH+VSA FF LAFECQAQP HRIR+ELRNYVVR+E+ASTLTPLF ELLVA
Subject      241  AQIHLAESVGKHNVSAAFFRLAFECQAQPFHRIRSELRNYVVRHESASTLTPLFHELLVA  300

Query        301  HAMPVNQLKFDTDGSEQVDTPTTTNTVD  328
                  HAM  NQLKFDTDGSE+VDTP TTNTVD
Subject      301  HAMAANQLKFDTDGSEKVDTPATTNTVD  328
```

d Query: DCR28
*vs* Subject: DCR28-like wheat D

**Sequence ID:** TraesCS4D03G0484200.1 **Length:** 566 **Number of Matches:** 1

**Range 1: 1 to 327** Gene details (IWGSC gene id only) DownloadSequence

| Score | Expect | Identities | Gaps | Strand |
|---|---|---|---|---|
| 335.1 bits(858) | 0.0 | 198/327(61%) | 70/327(21%) | None/None |

```
Query          1  MDPRPTTFRAKCKWVAAPAKTTAPKARFVDTARGKAIASTASSAVS---SPQPRPRRALG  60
                  MDP PT FRAK K VAAPAKT APK + V TARGK   S  +SAVS   +PQPRPRRA G
Subject        1  MDPHPTPFRAKRKSVAAPAKTPAPKPKSVTTARGKMTTSATTSAVSGGAAPQPRPRRAFG  60

Query         61  TVRSSISLAWKPAPPPPQKHSKQPHPPRWKPLKV-------------------------  120
                  TVRSS  LA KPAPPPPQKHSK   PP  KPLKV
Subject       61  TVRSSNPLAEKPAPPPPQKHSKLSPPPPQKPLKVSPPKLQKPAAKLSPPPPQKPAKVSPP  120

Query        121  --------SPPIPAKAARPSRPVVKPLKKACPATVDLAAPVKPSA---------------  180
                         SPPIPAKAARPSRP  KPLKKACPA  DLAA  K  +
Subject      121  PQQKPSKLSPPIPAKAARPSRPAEKPLKKACPAPPDLAAKAKKKSQRVSFQDDVAALAVP  180

Query        181  ---------ENSAGRTPMVPVKA---------PMEDLFFTAQDWSSHTLNSLERASYWLA  240
                           E+SAGRTPMVPVKA           E  FF+AQ+ SS TL+ LE ASYWLA
Subject      181  GSGEKVKATEDSAGRTPMVPVKALEKKPAKVVAAETPFFSAQNCSSCTLDQLESASYWLA  240

Query        241  QIHLSESAGKHSVSAKFFGLAFECQAQPIHRIRTELRNYVVRYENASTLTPLFRELLVAH  300
                  QIHL+ES GKH+VSA FF LAFECQAQP HRIR+ELRNYVVR+E+ASTLTPLF ELLVAH
Subject      241  QIHLAESVGKHNVSAAFFRLAFECQAQPFHRIRSELRNYVVRHESASTLTPLFHELLVAH  300

Query        301  AMPVNQLKFDTDGSEQVDTPTTTNTVD  327
                  AM VNQLKFDTDGSE+VDTP TTNTVD
Subject      301  AMAVNQLKFDTDGSERVDTPATTNTVD  327
```

Supplementary Figure 6 Amino acid alignment between DCR28 and it's A chromosome-paralogs of (a) rye and (b-d) wheat

e Query: DCR400
*vs* Subject: DCR400-like rye

f Query: DCR400
*vs* Subject: DCR400-like wheat D

g Query: DCR400
*vs* Subject: DCR400-like wheat B

h Query: DCR400
*vs* Subject: DCR400-like wheat A

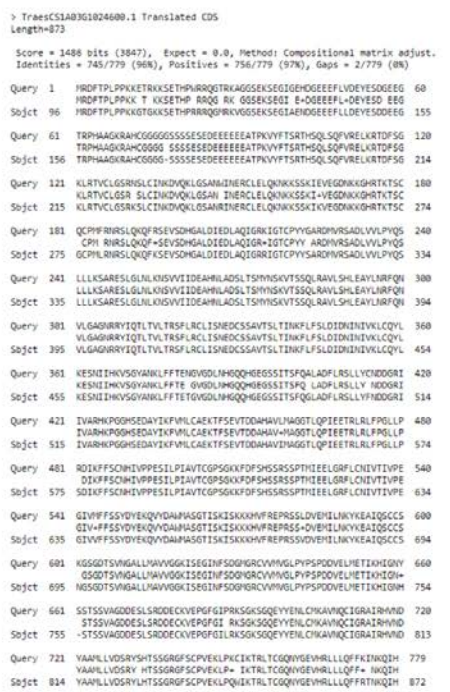

Supplementary Figure 7 Amino acid alignment between between DCR400 and it's A chromosome-paralogs of (e) rye and (f-h) wheat.

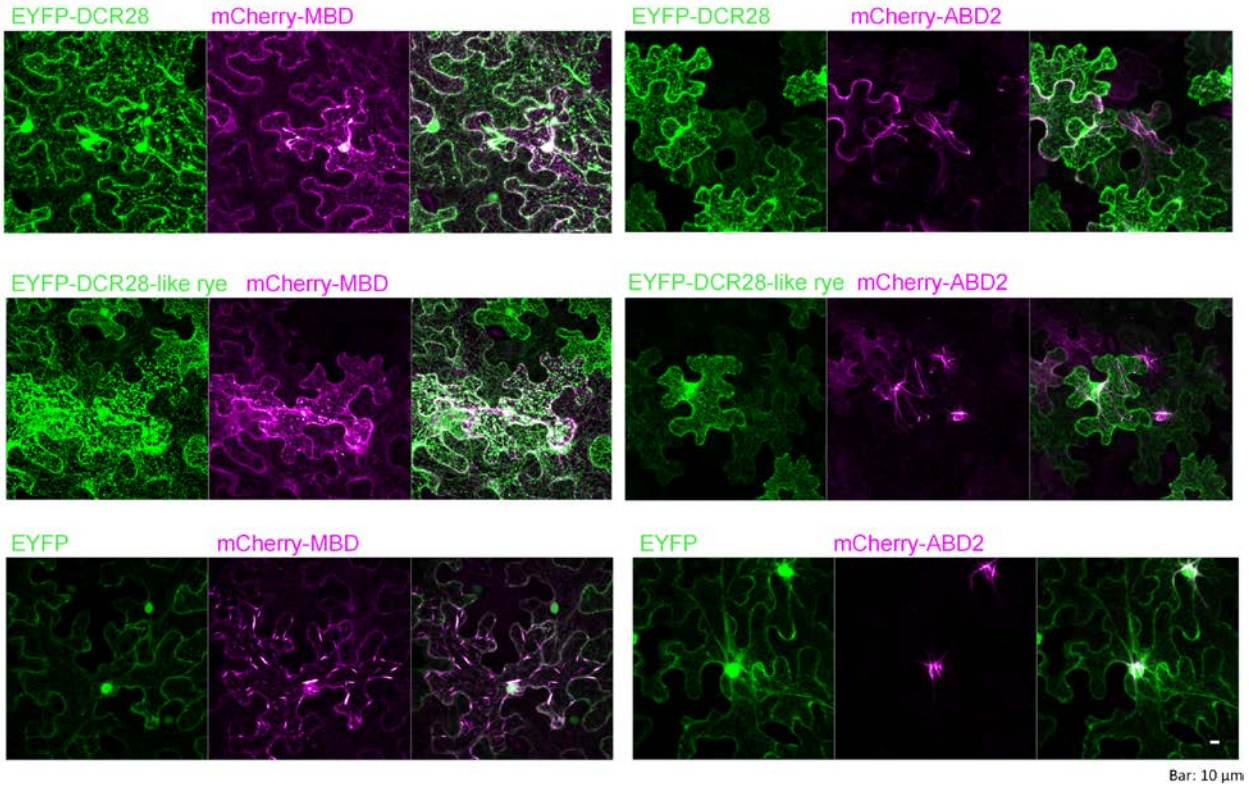


Supplementary Figure 8 Transient overexpression of EYFP-DCR28, EYFP-DCR28-like rye, and EYFP (all green) together with mCherry-MBD (magenta) and mCherry-ABD2 (magenta), respectively in *N. benthamiana.* Note: colocalization of EYFP-DCR28 and EYFP:DCR28-like rye with the tubulin marker mCherry:MBD. No colocalization exists between EYFP:DCR28 and EYFP:DCR28-like rye with the actin marker mCherry:ABD2.

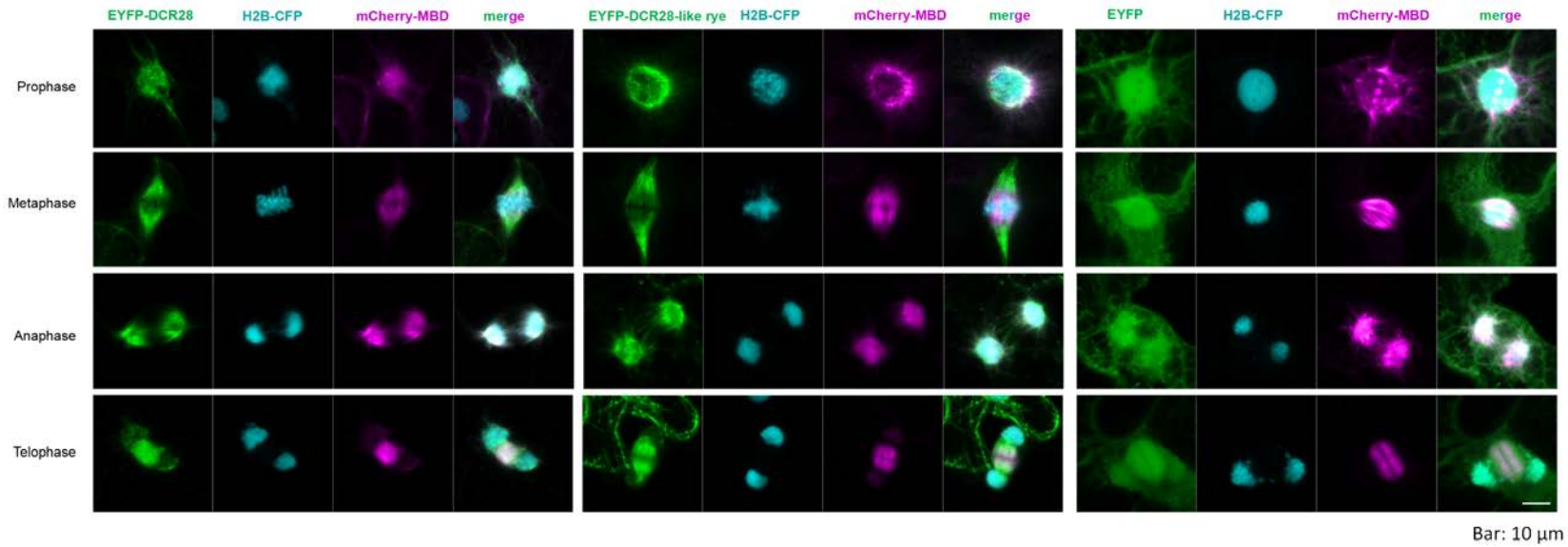


Supplementary Figure 9 Mitotic cell cycle dynamic of EYFB-DCR28 and EYFP-DCR28-like rye. Transient overexpression of EYFP-DCR28, EYFP-DCR28-like rye, and EYFP (all green) using the cell division-enabled leaf system in the *N. benthamiana* with stable expression of histone H2B-CFP (blue). Transient coexpression mCherry-MBD (magenta) was used as tubulin-specific marker. Note the spindle-specific distribution of EYFB-DCR28 and EYFP-DCR28-like rye.

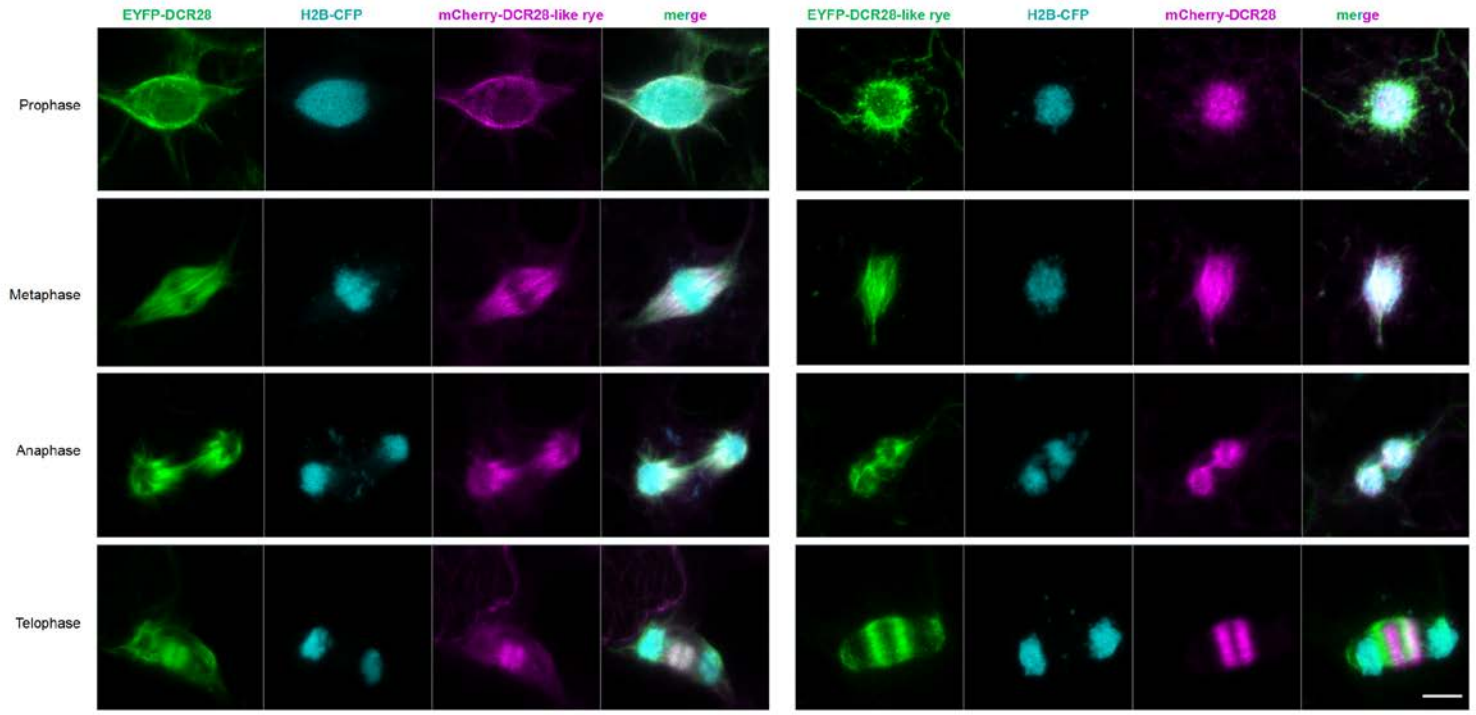


Supplementary Figure 10 Mitotic cell cycle dynamic and colocaliztion of EYFB-DCR28 and EYFP-DCR28-like rye. Transient co-overexpression of EYFP-DCR28 (green or magenta) and EYFP-DCR28-like rye (magenta or green) using the cell division-enabled leaf system in the *N. benthamiana* with stable expression of histone H2B-CFP (blue). Note the spindle-specific distribution of EYFB-DCR28 and EYFP-DCR28-like rye.

# 8 Supplementary Tables

Supplementary Table 1 (attached)

Mechanisms of B chromosome accumulation in plants.

Supplementary Table 2 (attached)

Annotation of the genes on the rye B chromosome

(1) The location, coding ability, homologous gene on the A chromosomes of the genes on the rye B chromosome

(2) The genes locate in the drive control region (DCR)

# 9 Curriculum Vitae

**Name** Jianyong Chen

https://orcid.org/0000-0002-6996-1032

**Academic Qualifications**

2017-2020

**M.Sc. in Crop Genetics and Breeding,** Nanjing Agricultural University, China

2013-2017

**B.Sc. in Agronomy**, Nanjing Agricultural University, China

**Research Experiences**

2020 September - now

PhD student, “Chromosome Structure and Function” Research Group, Department of Breeding Research, Leibniz-Institute of Plant Genetics and Crop Plant Research (IPK), Germany, Supervisor: Prof. Dr. Andreas Houben

2017 - 2020

Master student, Nanjing Agricultural University, China. Supervisor: Prof. Dr. Zengjun Qi, Research Topic: “Tandem repeat analysis of *Thinopyrum bessarabicum* and development of oligonucleotide probes for *in situ* hybridization”

**Awards and fellowships**

- China Scholarship Council (2020-2023, no. CSC202006850005)
- The best poster in Plant Chromosome Biology, Cytogenetics meeting 2023, September 11-13, 2023, Brno. Topic: “Identification of the trans-acting factors that control the non-Mendelian drive of the rye B chromosome”

**Publications**

- **Chen, J.**, Bartos, J., Boudichevskaia, A., Voigt, A., Rabanus-Wallace, M. T., Tulpová, Z., Šimková, H., Macas, J., Buhl, J., Bürstenbinder, K., Blattner, F.R., Fuchs, J., Schmutzer, T., Himmelbach, A., Schubert, V., & Houben, A. (2024). The genetic mechanism of B chromosome drive in rye illuminated by chromosome-scale assembly. Nature Communications, 15(1), p.9686. doi:10.1038/s41467-024-53799-w
- **Chen, J.**, Birchler, J. A., & Houben, A. (2022). The non-Mendelian behavior of plant B chromosomes. Chromosome Research, 30(2-3), 229-239. doi: 10.1007/s10577-022-09687-4
- **Chen, J.**, Tang, Y., Yao, L., Wu, H., Tu, X., Zhuang, L., & Qi, Z. (2019) Cytological and molecular characterization of *Thinopyrum bessarabicum* chromosomes and structural rearrangements introgressed in wheat. Molecular Breeding.39:146. doi:10.1007/s11032-019-1054-8
- Ebrahimzadegan, R., Fuchs, J., **Chen, J.**, Schubert, V., Meister, A., Houben, A., & Mirzaghaderi, G. (2023). Meiotic segregation and post-meiotic drive of the *Festuca pratensis* B chromosome. Chromosome Research, 31(3), 26. doi:10.1007/s10577-023-09728-6
- Kuo, Y. T., Câmara, A. S., Schubert, V., Neumann, P., Macas, J., Melzer, M., **Chen, J.** ... & Houben, A. (2023). Holocentromeres can consist of merely a few megabase-sized satellite arrays. Nature Communications, 14(1), 3502. doi:10.1101/2022.11.23.516916
- Karafiatova, M., Bojdová, T., Stejskalová, M., Harnádková, N., Kumar, V., Houben, A., **Chen, J.**, Dolezalova, A., Honys, D., & Bartos, J. (2024). Unravelling the unusual: Chromosome elimination, nondisjunction, and extra pollen mitosis characterize the B chromosome in wild sorghum. New Phytologist.

**Lectures and posters**

Lectures:

- Cytogenetics 2021 Meeting, Görlitz, Germany, September 27. – 28., 2021. Topic: “Identification of the *trans*-acting factors that cause the non-Mendelian drive of the rye B chromosome”.
- EUCARPIA, European Association for Research on Plant Breeding, Cereals Section, International Symposium on Rye Breeding & Genetics Online Meeting, 21-22 June 2021, Topic: “Identification of factors that make the B chromosome of rye deviate from the Mendelian law of equal segregation”.
- Plant Science Student Conference (PSSC), Gatersleben, Germany, July 3-4, 2023. Topic: “Identification of *trans*-acting factors that controls the post-meiotic drive of the rye B chromosome”.
- 5$^{th}$ B Chromosome Conference, Petnica, Serbia, October 14-17, 2023. Topic: “Identification of the *trans*-acting element that controls the non-disjunction of the rye B chromosome”.

Posters:

- EMBO Workshop, Chromosome segregation and aneuploidy, May 1-4, 2022, Vienna, Austria. Topic: “Identification of the factors that control non-disjunction of the rye B chromosome”.
- Plant Chromosome Biology, Cytogenetics meeting 2023, September 11-13, 2023, Brno. Topic: “Identification of the *trans*-acting factors that control the non-Mendelian drive of the rye B chromosome”.

# 10 Eidesstattliche Erklärung/Declaration on oath

Hiermit versichere, dass ich die vorliegende Arbeit selbstständig verfasst habe, dass ich keine anderen Quellen und Hilfsmittel als die angegebenen benutzt habe und dass ich die Stellen der Arbeit, dich ich anderen Werken – auch elektronischen Medien – dem Wortlaut oder Sinn nach entnommen habe, in jedem Fall unter Angabe der Quelle als Entlehnung kenntlich gemacht habe. Die Arbeit wurde bisher in gleicher oder ähnlicher Form keiner anderen Institution oder Prüfungsbehörde vorgelegt.

I hereby declare that I have written the submitted thesis independently and without illicit assistance of third parties. I have not used any other reference and sources than those listed in the thesis or engaged any plagiarism. All references and sources used in the presented work are properly cited and acknowledged. Further, I declare that the presented work has not been previously submitted for the purpose of academic examination, either in its original or similar form, anywhere else.

_____ _____

Gatersleben, 24.03.2025 Unterschrift/Signature